DEUTSCHES ELEKTRONEN-SYNCHROTRON
in der HELMHOLTZ-GEMEINSCHAFT

DESY-THESIS-2006-018
July 2006

QCD-Instantons and Conformal Inversion Symmetry

by

D. Klammer

ISSN 1435-8085

NOTKESTRASSE 85 - 22607 HAMBURG

To be sure that your reports and preprints are promptly included in the HEP literature database
send them to (if possible by air mail):

DESY Zentralbibliothek Notkestraße 85 22607 Hamburg Germany	DESY Bibliothek Platanenallee 6 15738 Zeuthen Germany

QCD-INSTANTONS AND CONFORMAL INVERSION SYMMETRY

Diplomarbeit zur Erlangung des akademischen Grades
Magistra der Naturwissenschaften

durchgeführt unter der Betreuung von
Dr. Fridger Schrempp
am Deutschen Elektronen Synchrotron, Hamburg

eingereicht von
Daniela Klammer

an der Fakultät für Physik
der Universität Wien

April 2006

Abstract

Instantons are an essential and non-perturbative part of Quantum Chromodynamics, the theory of strong interactions. One of the most relevant quantities in the instanton calculus is the instanton-size distribution, which can be described on the one hand within the framework of instanton perturbation theory and on the other hand investigated numerically by means of lattice computations.
A rapid onset of a drastic discrepancy between these respective results indicates that the underlying physics is not yet well understood. In this work we investigate the appealing possibility of a symmetry under conformal inversion of space-time leading to this deviation. The motivation being that the lattice data seem to be invariant under an inversion of the instanton size.
Since the instanton solution of a given size turns into an anti-instanton solution having an inverted size under conformal inversion of space-time, we ask in a first investigation, whether this property is transfered to the quantum level.
In order to introduce a new scale, which is indicated by the lattice data and corresponds to the average instanton size as inversion radius, we project the instanton calculus onto the four-dimensional surface of a five-dimensional sphere via stereographic projection. The radius of this sphere is associated with the average instanton size. The result for the instanton size-distribution projected onto the sphere agrees surprisingly well with the lattice data at qualitative level. The resulting symmetry under an inversion of the instanton size is almost perfect.

Zusammenfassung

Instantonen sind ein essentieller und nicht-perturbativer Aspekt der Quantenchromodynamik, der Theorie der starken Wechselwirkung. Eine der wichtigsten Größen innerhalb der Theorie der Instantonen ist die Instanton-Größenverteilung, welche einerseits im Rahmen der Instanton-Störungstheorie beschrieben und andererseits durch numerische Simulationen mittels Berechnungen auf dem Gitter bestimmt werden kann.
Ein rapide entstehende Diskrepanz zwischen den Ergebnissen dieser beiden Methoden, welche vor einigen Jahren festgestellt wurde, deutet auf eine noch nicht völlig verstandene, physikalische Ursache hin. Diese Arbeit untersucht die ansprechende Möglichkeit einer Symmetrie unter konformer Inversion der Raumzeit, welche zu dieser Abweichung führt. Die Motivation für diesen Ansatz findet sich in der Invarianz der Gitterdaten unter einer Inversion der Instantongröße.
Das Instanton-Eichfeld mit einer bestimmten Ausdehnung wird unter einer konformen Inversion der Koordinaten zu einem Antiinstanton mit invertierter Ausdehnung. In einer ersten Untersuchung fragen wir, ob sich diese Eigenschaft auch auf Quantenniveau finden lässt.
Weiters zeigen die Gitterdaten eine neue Skala auf, die der durchschnittlichen Größe eines Instantons als Inversionsradius entspricht. Um diese neue Skala in die Theorie einzuführen, projektieren wir den Instanton-Kalkül auf die vier-dimensionale Oberfläche einer fünf-dimensionalen Kugel mittels stereographischer Projektion. Die neue Skala erscheint in dieser Beschreibung als Radius der Kugel. Das Ergebnis für die projektierte Instanton-Größenverteilung auf der Kugel stimmt auf qualitativer Ebene überraschend gut mit den Gitterdaten überein. Die resultierende Symmetrie unter einer Inversion der Instantongröße, wie sie von den Gitterdaten nahe gelegt wird, ist beinahe perfekt.

Contents

Chapter 1

Introduction

Quantum Chromodynamics (QCD), the theory describing the nature of the strong force, is the basis for nuclear and hadron physics. Despite its appealing theoretical construction, which is even more self-contained than Quantum Electrodynamics (QED), it takes a long way starting from the Lagrangian to explain data from e.g. hadronic spectroscopy. The reason is that the world around us cannot be understood by the bare use of *perturbative* QCD (pQCD) only.

The QCD vacuum is a very complicated and dense state of matter, made of strongly interacting quarks and gluons. It is the *non-perturbative* aspects of QCD, which on the one hand play an essential role but on the other hand have proven to be a much more difficult task than pQCD. How should one understand the structure of hadrons without having a profound knowledge of the vacuum first?

One of the most exciting events in the development of analytical, non-perturbative QCD was the discovery of topological solutions of the Yang-Mills equations known as *instantons*. It is the rich vacuum structure of non-Abelian theories that induces topologically non-trivial fluctuations of the gauge fields. Due to these kinds of non-perturbative solutions, non-Abelian gauge theories like the electroweak theory and QCD seem to have an enormous capacity encoded in the vacuum structure. There are areas in physics, being completely inaccessible to perturbation theory, which can be explored with the help of topological methods.

Being the simplest example of such fluctuations, instantons have been discovered by Belavin *et al.* [1] in 1975. There exist other types of fluctuations too, such as merons, monopoles or vortices [2, 3, 4]. Instantons are the best studied effect, though. Moreover there are strong believes that they are the dominant fluctuations in the QCD vacuum. Physically they describe tunnelling processes between vacua with different topological structure, reflecting their non-perturbative nature.

They are believed to play a crucial role in various topics of both QCD and electroweak theory. Instantons lead to the formation of a gluon condensate [5], cure the $U(1)$ paradox [6, 7]

and provide a beautiful mechanism for chiral symmetry breaking [8, 9, 10, 11, 12, 13]. In the electroweak sector they are responsible for a violation of the baryon and lepton number $B + L$ [7, 6, 14], to mention just a few impacts of instantons.

Despite their undoubted importance for the theory of strong and electroweak interactions, experimental evidence for instanton-induced processes is still lacking today. It was shown [15, 16, 17, 18] that the instanton-induced cross-sections lie within measurable range. Thus a thorough analysis of new HERA data - and in the future also LHC data - might bring to the experimental confirmation of such processes.

Organisation of the work

Chapter 2 serves as a guideline through this thesis. The main subject of this work will be illustrated there. The chapter gives a detailed outlook on the ideas investigated in the course of this thesis and motivates the methods applied.

In Chapter 3 we present a short overview of the theory of instantons. The focus is on their role in QCD. We start with a brief description of the vacuum structure of non-Abelian gauge theories like QCD in Sect. 3.1. The instanton solution in Euclidean space will be introduced as well as their interpretation as a tunnelling process between topologically different vacua in Minkowski space. A detailed discussion of instanton perturbation theory follows in Sect. 3.3. The physical significance of instantons is the subject of the last section of this chapter, Sect. 3.4.

Thereafter, in Chapter 4, the preparations for the subsequent investigations on our symmetry approach are made. Sect. 4.1 starts with a discussion of the simulation of topological phenomena on the lattice. Moreover the properties of the instanton size distribution on the lattice and their comparison to instanton perturbation theory are addressed in that section. Then, in Sect. 4.2, we give a short overview of alternative approaches to the problem of the contradiction between lattice data and instanton perturbation theory. At the end of this chapter we introduce the conformal group and study the transformation laws for various fields in detail. These laws are used intensively throughout this work. The invariance of the instanton potential at the classical level is studied.

The invariance of the instanton calculus under conformal inversions at the quantum level is the main topic of Chapter 5. We investigate the behaviour of a major part of the instanton size distribution, which are the contributions from the zero modes, under conformal space-time inversion. For that purpose we introduce the method of collective coordinates in Sect. 5.1. After a derivation of the zero mode fraction for $SU(3)$- and $SU(N)$-instantons in Sect. 5.3, we study the properties of zero modes under conformal space-time inversions and give results in Sect. 5.4.

Finally, in Chapter 6, we deal with one of our main issues: The introduction of a new scale, which is indicated by the lattice data, into the instanton calculus. We begin with a discussion of the breaking of the dilatation in Sect. 6.1 which goes along with the introduction of a scale into

the theory. The rest of this section gives further motivations for our approach of projecting the instanton calculus onto the four-dimensional surface of a sphere in five-dimensional Euclidean space with a radius that corresponds to the average instanton size. In Sect. 6.2 we study the stereographic projection in detail and state the transformation rules for vector and tensor fields. The main results of this work are quoted in Sect. 6.3, where the zero modes are projected onto the sphere with a radius that equals the average instanton size. The following section provides consistency checks for our approach including a comparison with existing work in Sect. 6.4.1. We make contact between the results for the inverted zero modes on the sphere and in Euclidean space in the subsequent section. A rather lengthy excursus will be done in Sect. 6.4.3. The purpose of this deviation from the straight line of argumentation is to illustrate why our approach differs quite a lot from what has been done in the past.

The work finishes with concluding words and an outlook on topics that would be worthwhile to investigate in the future.

Chapter 2

Setting the Stage

This chapter serves as a guideline through this thesis. The question that will we will deal with during the main parts of this work will be posed. Moreover it gives an outlook on the ideas that have been investigated in the course of this work and provides motivations for the approach chosen. From now on instantons will be denoted as I, anti-instantons as $\bar{I}$.

One of the most relevant quantities in the I-sector is the so called *instanton-size distribution* $D(\rho)$, which gives the probability $n^{(I)}$ to find an instanton with a size of $(\rho \ldots \rho + \mathrm{d}\rho)$ in a volume element $\mathrm{d}^4 z$,

$$D(\rho) \simeq \frac{\mathrm{d}\, n^{(I)}}{\mathrm{d}^4 z\, \mathrm{d}\rho}. \tag{2.1}$$

The I-size distribution can be linked directly to the vacuum-to-vacuum transition amplitude of the tunnelling process as discussed in Eq. (3.32) of Sect. 3.3. In the context of so called *instanton perturbation theory* the quantum field theoretical probability for this vacuum transition to take place can be computed. This was first achieved in the seminal work by 't Hooft [6]. One expands the path integral for the generating functional of the Green's functions about the known, classical instanton solution, Eq. (3.16) in Sect. 3.1,

$$A_\mu(x) = A_\mu^{(I)}(x) + A_\mu^{\mathrm{qu}}(x), \tag{2.2}$$

instead of the trivial vacuum $A_\mu^{(0)}(x) = 0$. Not surprisingly, one finds the unphysical result of a divergent amplitude, see Eq. (3.41), in the infrared region, i.e. when the size of the instantons becomes too large.

However, this problem does not occur in lattice simulations of QCD. There the theory is probed numerically without any simplifying assumptions and thus includes all physics provided by the Lagrangian of the theory simulated. The topological structure of the vacuum in $SU(3)$

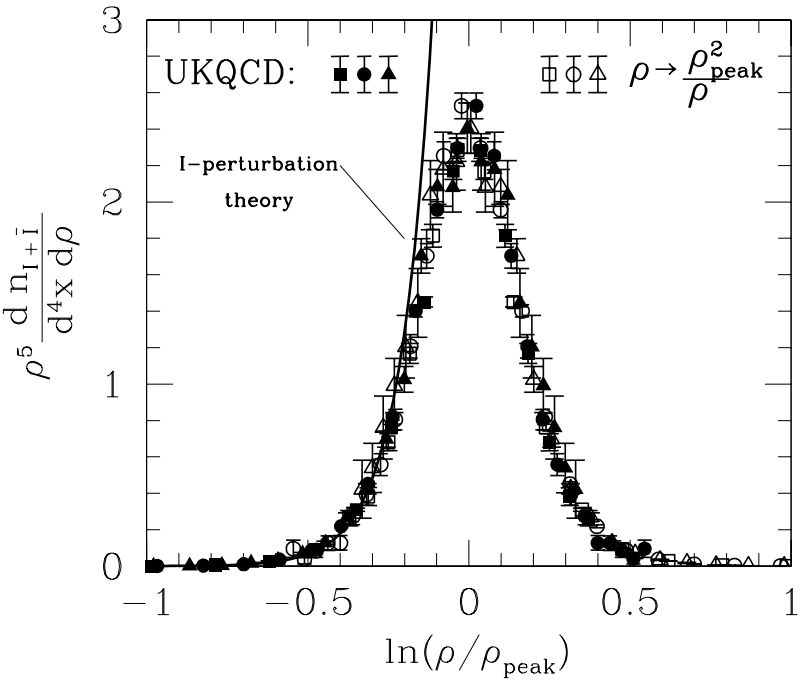

Figure 2.1: UKQCD lattice data [22, 23] (solid symbols) for the instanton-size distribution. The solid line refers to instanton-perturbation theory [23] using $\Lambda_{\overline{\rm MS}\, n_f=0} = (238 \pm 19)$ MeV from [24]. The open symbols display the according to $\rho \to \rho^2_{\rm peak}/\rho$ inverted data symbols. The data seem to be symmetric under an inversion of the instanton size.

and $SU(2)$ lattice gauge theory with zero flavours ($n_f = 0$) has been investigated by various groups [19, 20, 21], notably the UKQCD collaboration [22]. Their high-quality lattice data, analysed by Smith and Teper [22] and Ringwald and Schrempp [23], are depicted in Fig. 2.1. A comparison to I-perturbation theory has been done by [23]. One can see that I-perturbation theory (solid line) works perfectly, without any free parameter, until an I-size of 0.35 fm. Moreover the lattice data show a radical suppression of large instantons. The extremely surprising feature of the behaviour of the size distribution was the rapid breakdown of I-perturbation theory at an I-size of $\rho_{\rm peak} \cong 0.5$ fm. Furthermore the peak position, $\rho_{\rm peak}$, introduces a new, characteristic length scale in the I-sector, indicating the breakdown of I-perturbation theory.

So far the physical mechanism leading to such a rapid onset of a drastic discrepancy between lattice data and perturbation theory is not known. Clearly it would be of great importance to gain some understanding of that issue, since this would have crucial consequences for our insight to the vacuum structure of both the theory of electroweak and strong interaction.

This work is devoted to an investigation of exactly that question. Our approach will be the appealing possible explanation [25] of a *symmetry protecting instantons of becoming too large*. Near at hand is a potential symmetry under *conformal inversion of space-time*,

$$x_\mu \to x'_\mu = \frac{\rho^2_{\text{peak}}}{x^2}\, x_\mu. \tag{2.3}$$

The triggering motivation for this assumption is the fact, that the lattice data in Fig. 2.1 appear to be *invariant* under an *inversion* of the *I-size*,

$$\rho \Leftrightarrow \rho' = \frac{\rho^2_{\text{peak}}}{\rho}. \tag{2.4}$$

The size distribution in Fig. 2.1 is plotted against $\ln(\rho/\rho_{\text{peak}})$ to make the symmetry clearly visible. Both, the original data symbols (■, • and ▲) and the according to Eq. (2.4) inverted ones (open symbols) seem to fit onto one symmetric curve. The idea of such an inversion symmetry, regarded as a relict of the conformal invariance of the whole I-sector, relies on two observations:

- First of all the Euclidean equations of motions are covariant under the conformal group $O(5,1)$ and moreover the classical I-solution Eq. (3.16) is invariant under its subgroup $O(5)$ [26, 27], see Sect. 6.1.

- Secondly, as will be discussed out in detail in Sect. 4.3.3, at the classical level instantons of size ρ in regular gauge change under a conformal inversion of the coordinates, Eq. (2.3), to anti-instantons of inverted size ρ' in singular gauge,

  $$A'^{(I)_{\text{reg}}}_\mu (x,\rho)\,. = A^{(\bar{I})_{\text{sing}}}_\mu (x,\rho') \tag{2.5}$$

  That is to say that a transformation of the I-configuration under a space-time inversion of Eq. (2.3) effectively means an inversion of the I-size ρ. It is exactly this symmetry the lattice data is suggesting.

The first part of our investigation concentrates on the following question: Does the latter property survive at the quantum level?
For that purpose a thorough study of the behaviour of the one-loop I-size distribution under conformal inversion was made, it can be found in Chapter 5. Within this work we consider only one major part of the I-size distribution, the zero mode fraction, under space-time inversion. Zero modes correspond to the derivatives of the classical instanton potential with respect to collective coordinates, see Sect. 5.1. Since the instanton gauge field possesses the intriguing property under inversion, Eq. (2.5), this feature might be transfered to the zero modes. We assume that the remaining non-zero mode part is not affected by a conformal inversion.

According to our approach the typical size ρ_{peak} of an instanton equals the radius of inversion. Therefore one of the main aims of this work is to introduce this new scale into the I-calculus. It should be emphasised, that this scale does not exist at all in conventional I-perturbation theory.

This will be done in the central part of this work, Chapter 6. There we shall see, that the natural environment for studying the question of invariance under conformal space-time inversion seems to be the 4-dimensional surface of a 5-dimensional sphere with radius ρ_{peak}. In Chapter 6 the 4-dimensional Euclidean space is projected onto the surface of the sphere by means of a stereographic projection. In this description of the I-calculus the new physical scale ρ_{peak} appears as the radius of the sphere and is thus introduced in the whole I-sector.

There exists a simple relation between the stereographic projection and conformal inversion if the radius of inversion equals the radius of stereographic projection. On the one hand inversion corresponds on the one hand to a mapping of the points outside the sphere to points inside the sphere and vice versa in Euclidean space. On the other hand it represents a mapping from the northern hemisphere to southern hemisphere and vice versa after projection to the sphere, see Fig. 6.1 in Sect. 6.4.3.

In Sect. 6.3 we show that the computation of the *zero mode* part $J(\rho)$, an important fraction of the I-size distribution, on the sphere gives a result, that has indeed many of the features we are looking for. We find invariance of $J(\rho)$ under inversion of the coordinates. This leads to an almost perfect symmetry under $\rho \to \rho'$ and by that to a surprisingly good description of the lattice data at the qualitative level.

Chapter 3

Instantons in QCD - An Overview

The purpose of this chapter is to provide an introduction to instantons in non-Abelian gauge theories, especially in QCD. There exists a wide range of literature on that subject, see e.g. the following textbooks [28, 29, 30, 31] and reviews [32, 8]. Sects. 3.1 - 3.3 give a theoretical overview of the methods used in the I-calculus. Sect. 3.4 deals with the physical importance of instantons in gauge theories.

3.1 The vacuum structure of gauge field theories

Non-Abelian gauge theories such as QCD have a very rich vacuum structure. There is an infinite set of classical, degenerate vacua that are topologically different. In order to make that visible it is necessary to formulate the Yang-Mills theory, and by that also the theory of instantons, in 4-dimensional Euclidean space.

When studying gauge field theories, in particular pure Yang-Mills theories like we do for the moment, and their semiclassical approximations, one is interested in field configurations with finite action[1],

$$S_{\mathrm{E}} = \frac{1}{2} \int \mathrm{d}^4 x \, \mathrm{Tr} \left[F_{\mu\nu} F^{\mu\nu} \right], \tag{3.1}$$

since configurations with infinite action do not contribute to the functional integral. Hence the field strength tensor $F_{\mu\nu}$ must be of $\mathcal{O}\left(1/|x|^3\right)$, in order for the action to vanish at infinity,

$$F_{\mu\nu} \xrightarrow{|x| \to \infty} 0. \tag{3.2}$$

[1] For a definition of the Euclidean action see Appendix A.

This is trivially achieved by a gauge potential A_μ of $\mathcal{O}\left(1/|x|^2\right)$, but due to gauge invariance of the action this can also be accomplished by

$$A_\mu(x)\big|_{|x|\to\infty} = \tfrac{\mathrm{i}}{g}U^\dagger(x)\partial_\mu U(x) + \mathcal{O}\left(1/|x|^2\right), \tag{3.3}$$

where $U(x)$ is a function from four-space to the gauge group G. The field defined by Eq. (3.3) is often called *pure gauge*, since it arises from a gauge transformation

$$A'_\mu(x) = U^\dagger(x)A_\mu(x)U(x) + \frac{\mathrm{i}}{g}U(x)^\dagger\partial_\mu U(x) \tag{3.4}$$

of the trivial potential $A_\mu(x) = 0$.

It can be shown [30], that for every finite-action configuration there is actually a homotopy class of such mappings. Two continuous functions $f_0(x)$ and $f_1(x)$ of one topological space to another belong to one homotopy class if they can be continuously transformed into another by means of a continuous function $F(x,t)$, such that

$$F(x,t_0) = f_0(x) \quad \text{and} \quad F(x,t_1) = f_1(x). \tag{3.5}$$

The different homotopic classes are characterised by an integer *winding number* n_W, also called *Pontryagin index*.

It should be stressed that the gauge group $SU(2)$ plays an essential and also particular role in that context. This is due to the fact that the boundary of Euclidean space is the three-sphere $\mathcal{S}^3$. That means that topologically the group of space-time and the gauge group are equivalent. For mappings $f(x)$ from a three-sphere to $SU(2)$ the winding number is given by

$$n_W = \frac{1}{24\pi^2}\int \mathrm{d}^3x\, \epsilon_{ijk}\,\mathrm{Tr}\left[f^{-1}(x)\partial_i f(x)\, f^{-1}(x)\partial_j f(x)\, f^{-1}(x)\partial_k f(x)\right]. \tag{3.6}$$

Let us point out that in Eq. (3.3) the function $U(x)$ does indeed represent a mapping from three-spheres to $SU(2)$ space. Thus it is possible to associate a winding number to every field configuration in Euclidean space. It can be shown [30, 33], that this is true for every non-Abelian gauge theory with the gauge group $SU(N)$.

By defining a gauge-dependent current K_μ, the *Chern-Simons current*, we can express the winding number in terms of gauge fields,

$$K_\mu = \epsilon_{\mu\nu\kappa\lambda}\,\mathrm{Tr}\left[\frac{1}{2}A^\nu\partial^\kappa A^\lambda - \frac{\mathrm{i}g}{3}A^\nu A^\kappa A^\lambda\right]. \tag{3.7}$$

One can easily check that

$$\partial_\mu K^\mu = \frac{1}{4}\,\mathrm{Tr}\left[\widetilde{F}_{\mu\nu}F^{\mu\nu}\right]. \tag{3.8}$$

Here we have introduced the dual field strength tensor

$$\widetilde{F}_{\mu\nu} = \frac{1}{2}\epsilon_{\mu\nu\rho\sigma}F^{\rho\sigma}. \tag{3.9}$$

The charge associated with this current, the so called *topological charge* Q, is

$$\begin{aligned} Q &= \frac{g^2}{4\pi^2}\int_{V^4} \mathrm{d}^4x\, \partial_\mu K^\mu \\ &= \frac{g^2}{4\pi^2}\int_{\partial V^4 = \mathcal{S}^3} K_\perp \mathrm{d}^3x, \end{aligned} \tag{3.10}$$

where we have applied Gauß's theorem in order to change from an integration over the Euclidean space-time V^4 to an integration over the surface $\partial V^4 = \mathcal{S}^3$. At the surface of the sphere the gauge field is given by Eq. (3.3), where the current reads as

$$K_\mu = \frac{1}{6g^2}\epsilon_{\mu\nu\kappa\lambda}\,\mathrm{Tr}\left[\left(U^\dagger(x)\partial^\nu U(x)\right)\left(U^\dagger(x)\partial^\kappa U(x)\right)\left(U^\dagger(x)\partial^\lambda U(x)\right)\right] \tag{3.11}$$

Thus we see that the topological charge Q of the current in V^4 corresponds to the winding number n_W of the field on its surface ∂V^4 given by Eq. (3.6).

A physically realised configuration has to fulfil the condition of minimal action, which is satisfied by a self-dual field strength tensor. This can be seen by the following consideration.

$$\int \mathrm{d}^4x\,\mathrm{Tr}\left[F_{\mu\nu} \pm \widetilde{F}_{\mu\nu}\right]^2 \geq 0 \tag{3.12}$$

Using $\left(F_{\mu\nu} \pm \widetilde{F}_{\mu\nu}\right)^2 = 2\left(F_{\mu\nu}F^{\mu\nu} \pm F_{\mu\nu}\widetilde{F}^{\mu\nu}\right)$ we obtain

$$\int \mathrm{d}^4x\,\mathrm{Tr}\left[F_{\mu\nu}F^{\mu\nu}\right] \geq \left|\int \mathrm{d}^4x\,\mathrm{Tr}\left[F_{\mu\nu}\widetilde{F}^{\mu\nu}\right]\right|. \tag{3.13}$$

Equality is thus achieved in the case of (anti-)self-duality,

$$F_{\mu\nu} = \pm\widetilde{F}_{\mu\nu}. \tag{3.14}$$

This implies that the Euclidean action is proportional to the topological charge,

$$S_\mathrm{E} = \frac{1}{2}\int \mathrm{d}^4x\,\mathrm{Tr}\left[F_{\mu\nu}F^{\mu\nu}\right] = \frac{8\pi^2}{g^2}\left|Q\right|. \tag{3.15}$$

Eq. (3.10) tells us, that $F_{\mu\nu}$ cannot be zero over the whole volume V^4, it vanishes only on the boundary $\mathcal{S}^3$. In 1975 Belavin *et al.* [1] found an explicit field configuration, the *instanton* configuration, having all the properties needed,

$$\begin{aligned} A_\mu(x) &= \frac{\mathrm{i}}{g}\frac{\rho^2}{\rho^2+x^2}\left(\partial_\mu U(x)\right)U^\dagger(x) \\ &= -\frac{\mathrm{i}}{g}\frac{1}{\rho^2+x^2}\frac{\sigma_\mu\bar{x}-x\bar{\sigma}_\mu}{2}. \end{aligned} \tag{3.16}$$

$U(x)$ is an element[2] of the gauge group,

$$U(x) = \frac{x_\mu\sigma^\mu}{\sqrt{x^2}} \quad \in SU(2), \tag{3.17}$$

and ρ is some arbitrary scale parameter, usually referred to as the *size* of the instanton. It is straight forward to show that this solution fulfils the condition of Eq. (3.14). Thus in Euclidean space instantons are solutions of the equations of motion with finite action. They are characterised by their topological charge $Q = 1$.

The instanton solution in the form of Eq. (3.16) is written down in so called *regular gauge*. Later on, it will be convenient to work in *singular* gauge which is obtained by the following gauge transformation with $U(x) = x_\mu\sigma^\mu/\sqrt{x^2}$ [26],

$$\begin{aligned} A_\mu(x) \to A_\mu^{\mathrm{sing}}(x) &= UA_\mu U^\dagger + \frac{i}{g}U\partial_\mu U^\dagger \\ &= -\frac{\mathrm{i}}{g}\frac{\rho^2}{x^2\left(\rho^2+x^2\right)}\left[\sigma_\mu x_\nu\bar{\sigma}^\nu - x_\mu\right]. \end{aligned} \tag{3.18}$$

In order to generalise the gauge group to $SU(N_c)$, N_c being the number of colours, one has to embed the $SU(2)$-instanton configuration in an appropriate way into $SU(N_c)$ [34, 35, 36]. The usual way to do this is as follows. One embeds the I-representation into the left upper corner of an $N_c \times N_c$-matrix, such that all entries except those of the instanton are vanishing. Yet the embedding has to guarantee the invariance of the instanton orientation in colour space. Therefore we need to make a general, but constant $SU(N_c)$-gauge transformation of this $N_c \times N_c$-matrix,

$$\begin{aligned} \left(A_\mu^{N_c\times N_c}\right)^i{}_j &= (U)^i{}_k \begin{pmatrix} \left(A_\mu^{2\times2}\right)^\alpha_\beta & 0 & \dots & 0 \\ 0 \quad 0 & 0 & \dots & 0 \\ \vdots \quad \vdots & \vdots & \ddots & \vdots \\ 0 \quad 0 & 0 & \dots & 0 \end{pmatrix}^k_l \left(U^\dagger\right)^l{}_j \\ &= (U)^i{}_\alpha \left(A_\mu^{2\times2}\right)^\alpha{}_\beta \left(U^\dagger\right)^\beta{}_j. \end{aligned} \tag{3.19}$$

[2]For the definition of σ_μ and $\bar{\sigma}_\mu$ in Euclidean space-time see Appendix A.

Here the Greek indices are running from 1 to 2, whereas the Latin indices are running from 1 to the number of colours N_c. The matrices $U^i{}_\alpha$ couple the colour indices $i = 1, 2, \ldots, N_c$ with the spin indices $\alpha = 1, 2$ in a non-trivial way. One needs $4N_c - 5$ parameters [36] to describe these matrices, see also Sect. 5.1. In the main Chapters. 5 and 6 of this work we will deal with $SU(3)$ instantons, since we aim for a comparison of our results with lattice computations that have simulated the $SU(3)$ vacuum.

3.2 The instanton as a tunnelling process

In this section we ask for the physical interpretation of the instanton solution. We will see that in Minkowski space-time it corresponds to a quantum-mechanical tunnelling process between vacuum states with different topological charge [37, 38]. The argumentation follows [38]. In order to show this let us go to yet another gauge[3] - the *temporal* gauge, where the time component ought to be zero,

$$A_0^{\text{temp}}(x) = 0, \tag{3.20}$$

by means of a gauge transformation

$$A_\mu^{\text{temp}}(x) = U^{\text{temp}}(x) A_\mu(x) U^{\text{temp}\,\dagger}(x) + \frac{\mathrm{i}}{g} U^{\text{temp}}(x) \partial_\mu U^{\text{temp}\,\dagger}(x). \tag{3.21}$$

$U^{\text{temp}}(x)$ is now the element of the gauge group necessary to achieve the temporal gauge. As a consequence of this condition we find that

$$\frac{\partial}{\partial x_0} U^{\text{temp}}(x) = -A_0(x) U^{\text{temp}}(x). \tag{3.22}$$

Plugging in the instanton solution of Eq. (3.16) and solving the differential equation yields [29]

$$U^{\text{temp}}(x) = \exp\left\{ \mathrm{i} \frac{\mathbf{x}\cdot\sigma}{\sqrt{\rho^2 + \mathbf{x}^2}} \left[\arctan\left(\frac{x_4}{\sqrt{\rho^2 + \mathbf{x}^2}} \right) + \pi \left(n + \frac{1}{2} \right) \right] \right\}. \tag{3.23}$$

The spatial components of Eq. (3.16) vanish at infinity and thus at $x_0 = \pm\infty$ we are left with

$$A_i^{\text{temp}}(x)\Big|_{x_0 = \pm\infty} = \frac{\mathrm{i}}{g} U^{\text{temp}\,\dagger}(x) \partial_i U^{\text{temp}}(x), \tag{3.24}$$

where

$$U^{\text{temp}}(x_0 = -\infty) = \exp\left[\mathrm{i}\pi \frac{\mathbf{x}\cdot\sigma}{\sqrt{\rho^2 + \mathbf{x}^2}}\, n \right] \tag{3.25}$$

[3] We are still working in Euclidean space at this point.

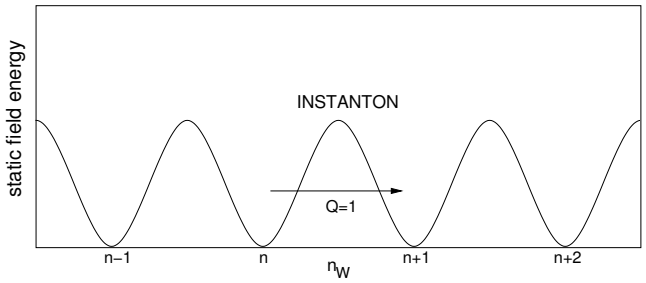

Figure 3.1: The instanton corresponds to a tunnelling process between degenerate vacua with different winding number in Minkowski space-time.

and

$$U^{\text{temp}}(x_0 = \infty) = \exp\left[\mathrm{i}\pi \frac{\mathbf{x}\cdot\sigma}{\sqrt{\rho^2 + \mathbf{x}^2}}\,(n+1)\right]. \tag{3.26}$$

The I-gauge potential $A_i^{(I)}$ at $x_0 = -\infty$ belongs to the vacuum state $|n\rangle$. After evolving in Euclidean time $A_i^{(I)}$ ends up at $x_0 = \infty$ in the vacuum state $|n+1\rangle$. Hence we conclude that the instanton configuration of Eq. (3.16) connects two vacuum states with different winding numbers n and $n+1$, respectively. The two states are separated by an energy barrier, see Fig. 3.1.

This brings us to the physical interpretation of the instanton in Minkowski time: It describes a tunnelling process between two ground states differing by $Q = 1$ (or $Q = -1$ in the case of an anti-instanton). This can be understood by the argumentation below. Classically there exists no path between two vacua with different winding number. But quantum mechanics tells us that tunnelling processes are allowed and they can be described with the help of classical paths in imaginary time. Since it is the minimum of the Euclidean action, the instanton solution does indeed describe such a path. One can calculate the barrier-penetration amplitude with the help of the WKB-method. The leading term of the tunnelling amplitude is given by

$$P \propto \mathrm{e}^{S_{\mathrm{E}}} = \mathrm{e}^{-\frac{8\pi^2}{g^2}|Q|} = \mathrm{e}^{-\frac{8\pi^2}{g^2}}. \tag{3.27}$$

Recapitulating one can say that instantons can be interpreted in two ways: On the one hand they are solutions of the Euclidean equations of motions localised in space and time[4]. On the other hand they are tunnelling *processes* between topologically different ground states in Minkowski space.

[4]This is why 't Hooft named them instantons in analogy to solitons in non-linear mechanics.

3.3 Perturbative vacuum-to-vacuum amplitude

The transition amplitude for an I-induced tunnelling process can be calculated in the framework of I-perturbation theory. A first approximation was already given by the WKB approach, see Eq. (3.27). In order to fix the pre-exponential factor F of the path integral,

$$\mathcal{Z} = F \int \mathcal{D}A_\mu \exp(-S_{\rm E})\Big|_{A^{\rm cl}=A^{(I)}}, \tag{3.28}$$

the fluctuations around the classical path have to taken be into account. Thus one has to compute the one-loop vacuum-vacuum amplitude about a single instanton [6]. The full calculation, being extensive and elaborate, was carried out first by 't Hooft [6]. For reasons of normalisation one needs to divide by the same amplitude about the ordinary vacuum,

$$\langle 0|0\rangle^{(I)} = \frac{\mathcal{Z}^{(I)}}{\mathcal{Z}^{(0)}} = \frac{\int \mathcal{D}A_\mu \exp(-S_{\rm E})|_{A^{\rm cl}=A^{(I)}}}{\int \mathcal{D}A_\mu \exp(-S_{\rm E})|_{A^{\rm cl}=0}}. \tag{3.29}$$

In I-perturbation theory the general gauge potential A_μ is expanded about the classical I-configuration $A_\mu^{(I)}(x,\gamma)$,

$$A_\mu(x,\gamma) = A_\mu^{(I)}(x,\gamma) + A_\mu^{\rm qu}(x), \tag{3.30}$$

where γ denotes the collective coordinates, parameters of the I-configuration, see Sect. 5.1. This expansion is also known as the *background field method*, see [39, 40]. Still the strong coupling constant α_s has to be small just like in conventional pQCD. We make the assumption that instantons are well separated from each other such that no interactions take place. This simplification is called the *dilute-gas approximation* [38]. Plugging in $A_\mu(x,\gamma)$ the action becomes

$$S_{\rm E} = \frac{1}{2}\int {\rm d}^4x\, {\rm Tr}\left[F_{\mu\nu}F^{\mu\nu}\right] = S^{\rm cl} + \frac{1}{2}\int {\rm d}^4x A_\mu^{\rm qu} M_A^{\mu\nu} A_\nu^{\rm qu} + \ldots, \tag{3.31}$$

where $S^{\rm cl}$ is the well-known action of the instanton field $S^{\rm cl} = 8\,\pi^2/g^2$ and "..." contains the remaining fermion and ghost fields not considered here. The term linear in A_μ^{qu} vanishes because the instanton configuration satisfies the equation of motion and minimises the action.

In this work only the the zero mode contribution is recalculated in Sect. 5.3. It will be the central quantity for our symmetry considerations later on. The complete computation requires the use of various techniques such as regularisation of the amplitude and integration over the collective coordinates (detailed discussion of the latter in Sect. 5.1), ending up with

$$\langle 0|0\rangle^{(I)} = \frac{\mathcal{Z}^{(I)}}{\mathcal{Z}^{(0)}} = \int {\rm d}^4z \int {\rm d}U \int {\rm d}\rho\, D(\rho,\mu_{\rm r}), \tag{3.32}$$

where the I-size distribution $D(\rho, \mu_{\rm r})$ depends on the I-size ρ and the renormalisation scale $\mu_{\rm r}$.

The one-loop results of [6, 41] have been improved in [42], now including renormalisation group invariance at two-loop level,

$$\frac{1}{D(\rho,\mu_{\rm r})}\frac{{\rm d}D(\rho,\mu_{\rm r})}{{\rm d}\log\mu_{\rm r}} = \mathcal{O}(\alpha_s^2). \tag{3.33}$$

The result for the I-size distribution is found to be

$$D(\rho,\mu_{\rm r})_{I-{\rm pert.}} = \frac{1}{\rho^5} d \left(\frac{2\pi}{\alpha_s(\mu_{\rm r})}\right)^{2N_c} \exp\left\{-\frac{2\pi}{\alpha_s(\mu_{\rm r})}\right\} (\mu_{\rm r}\rho)^b, \tag{3.34}$$

where [16]

$$b = \beta_0\Delta_1 - \Delta_2, \quad \Delta_1 = 1 + \frac{\beta_1}{\beta_2}\frac{\alpha_s(\mu_{\rm r})}{4\pi}, \quad \Delta_2 = 4\,N_c\,\beta_0\frac{\alpha_s(\mu_{\rm r})}{4\pi} \tag{3.35}$$

and $\alpha_s(\mu_{\rm r})$ is the running coupling constant as function of the renormalisation scale $\mu_{\rm r}$ at 2-loop level,

$$\alpha_s(\mu_{\rm r}) = \frac{4\pi}{\beta_0 \log\left(\frac{\mu_{\rm r}^2}{\Lambda^2}\right)}\left[1 - \frac{\beta_1}{\beta_0^2}\frac{\log\left(\log\left(\frac{\mu_{\rm r}^2}{\Lambda^2}\right)\right)}{\log\left(\frac{\mu_{\rm r}^2}{\Lambda^2}\right)}\right]. \tag{3.36}$$

The parameter Λ is the usual scale of QCD fixed by measuring the coupling constant at a certain scale like the mass of the Z-boson M_Z. As in conventional perturbation theory β_0 and β_1 are the first two coefficients of the β-function:

$$\beta_0 = \frac{11}{3}N_c - \frac{2}{3}N_f, \tag{3.37}$$

$$\beta_1 = \frac{34}{3}N_c^2 - \left(\frac{13}{3}N_c - \frac{1}{N_c}\right)N_f. \tag{3.38}$$

The result of Eq. (3.34) does not correspond to the full two-loop level, since the constant d is known only at one-loop level. In the $\overline{\rm MS}$-scheme it is given by

$$d = \frac{C_1}{(N_c-1)!\,(N_c-2)!}\exp\left\{-N_cC_2 + N_fC_3\right\} \tag{3.39}$$

with the numerical values for the coefficients

$$C_1 = 0.466, \quad C_2 = 1.54 \quad \text{and} \quad C_3 = 0.153. \tag{3.40}$$

However, in the form of Eq. (3.34) the dependence of the size distribution on the renormalisation scale μ_r is considerably reduced. Already at the one-loop level, see also Sect. 5.1, the explicit μ_r-dependence cancels:

$$\begin{aligned} D(\rho)_{1-\mathrm{loop}} &\propto \frac{1}{\rho^5}\left(\frac{2\pi}{\alpha\left(\mu_\mathrm{r}\right)}\right)^{2N_c}(\rho\mu_\mathrm{r})^{\beta_0}\exp\left\{-\frac{2\pi}{\alpha_s(\mu_\mathrm{r})}\right\} \\ &= \frac{1}{\rho^5}\left(\frac{2\pi}{\alpha\left(\mu_\mathrm{r}\right)}\right)^{2N_c}(\rho\mu_\mathrm{r})^{\beta_0}\exp\left\{-\frac{\beta_0}{2}\log\left(\frac{\mu_\mathrm{r}^2}{\Lambda^2}\right)\right\} \\ &= \frac{1}{\rho^5}(\rho\Lambda)^{\beta_0}\left(\frac{2\pi}{\alpha\left(\mu_\mathrm{r}\right)}\right)^{2N_c} \end{aligned} \tag{3.41}$$

Eq. (3.41) shows an explicit dependence only on ρ and Λ at first order. However, the factor $\left(2\pi/\alpha\left(\mu_\mathrm{r}\right)\right)^{2N_c}$ including a strong dependence on μ_r, remains. One can see that the tunnelling amplitude of Eq. (3.32) is divergent in the IR region for larger-size instantons at a fixed value of μ_r which is depicted in Fig. 2.1 in Sect. 2.

3.4 Physical impact of instantons

Obviously the question arises whether it is possible to distinguish the topologically different vacua physically. Sect. 3.4.1 deals with that issue. If this is indeed feasible, one will ask for the physical effects of instantons (in QCD). This will be discussed in Sects. 3.4.2 till 3.4.4.

3.4.1 Instantons and light quarks

If one adds massless quarks[5] to the theory there is indeed a physical observable, the axial charge,

$$Q_5 = \int_{\mathbb{R}^3} \mathrm{d}^3\mathbf{x}\, J_0^5(\mathbf{x},t), \tag{3.42}$$

answering the above question of the distinction between the different vacua. $J_0^5(\mathbf{x},t)$ is the time-component of the axial current defined below. Moreover the issue is related to the mechanism of anomalies. In 1969 Adler, Bell and Jackiw (ABJ) [43, 44] found the so called axial anomaly.

Anomalies arise whenever symmetries are conserved at the classical level, but not at the quantum level. In our case the axial $U(1)_A$ symmetry becomes anomalous under quantisation, therefore the corresponding current, the axial current defined by the operator

$$\hat{J}_\mu^5 = \bar{\psi}\gamma_\mu\gamma_5\psi, \tag{3.43}$$

[5]Of course this is an idealisation. However, since u-, d- and s-quarks are indeed very light quarks, this is a legitimate approximation.

is not conserved. This was found when computing loop diagrams involving external vector and axial-vector currents. They cannot be regulated in such a way that all the currents remain conserved [32]. The anomaly equation reads [45]

$$\partial_\mu J^{5\mu} = N_f \frac{g^2}{16\pi^2} \operatorname{Tr}\left[F^a_{\mu\nu}\widetilde{F}^{\mu\nu}_a\right], \tag{3.44}$$

where N_f is the number of flavours added to the theory. We see that the ABJ-anomaly is related to instantons, since the integrated right hand side of Eq. (3.44) is proportional to the topological charge Q.

One might ask how instantons lead to the non-conservation of the axial charge. The difference in the axial charge is given by the relation

$$\begin{aligned} \Delta Q_5 &= Q_5(t=\infty) - Q_5(t=-\infty) \\ &= \#\ (q+\bar{q})_R - \#\ (q+\bar{q})_L \\ &= \int \mathrm{d}^4x\, \partial_\mu J^{5\mu}. \end{aligned} \tag{3.45}$$

ΔQ_5 counts the difference between the number of left and right handed fermions and anti-fermions, $\#\ (q+\bar{q})_R$ and $\#\ (q+\bar{q})_L$, respectively. The above equation can be expressed by means of the fermion propagator $S(x,x)$,

$$S(x,y) = \langle x|(-\mathrm{i}\not{D})^{-1}|y\rangle. \tag{3.46}$$

By using $J^{5\mu} = \langle\bar{q}|\hat{J}^{5\,\mu}|q\rangle$ and the properties of the trace we find

$$\Delta Q_5 = N_f \int \mathrm{d}^4x\, \partial_\mu \operatorname{Tr}\left[S(x,x)\gamma^\mu\gamma_5\right]. \tag{3.47}$$

We can write the propagator in terms of eigenfunctions $\mathrm{i}\not{D}\psi_\lambda = \lambda\psi_\lambda$ of the Dirac operator,

$$S(x,y) = \sum_\lambda \frac{\psi_\lambda(x)\psi^\dagger_\lambda(y)}{\lambda}. \tag{3.48}$$

Plugging in Eq. (3.48) into Eq. (3.47) gives then

$$\Delta Q_5 = N_f \int \mathrm{d}^4x \operatorname{Tr}\left[\sum_\lambda \frac{\psi_\lambda(x)\psi^\dagger_\lambda(y)}{\lambda} 2\lambda\gamma_5\right]. \tag{3.49}$$

Now for every non-zero λ, $\gamma_5\psi$ is an eigenvector of the Dirac operator with an eigenvalue $-\lambda$. We conclude the contributions from ψ_λ cancele those from $\gamma_5\psi_\lambda$ and so only the zero modes contribute to the axial charge,

$$\Delta Q_5 = 2\,N_f\;(n_R - n_L)\,, \tag{3.50}$$

where n_L and n_R are the number of left and right handed zero modes, respectively.

An important discovery of 't Hooft [7] was, that the Dirac operator has indeed a right-handed zero mode $\kappa^{(I)}(x)$ in the instanton background field,

$$\not{D}\kappa^{(I)}(x) = \left(\not{\partial} - \mathrm{i}\,g\,\not{A}^{(I)}(x)\right)\kappa^{(I)}(x) = 0. \tag{3.51}$$

In an anti-instanton field we obtain a left-handed zero mode $\bar{\phi}^{(\bar{I})}(x)$. In Weyl representation and in singular gauge the right-handed fermionic zero modes in an I-background field are given by [6]

$$\begin{aligned}
\kappa_{\dot{\alpha}}^{(I)k}(x) &= \frac{1}{\pi}\rho^{3/2}\epsilon^{\alpha\beta}\,(U)^k_\beta\,\frac{\bar{x}_{\dot{\alpha}\alpha}}{x^4}\left(\frac{x^2}{\rho^2+x^2}\right)^{3/2}, \\
\bar{\phi}_k^{(I)\dot{\alpha}}(x) &= \frac{1}{\pi}\rho^{3/2}\epsilon_{\beta\alpha}\left(U^\dagger\right)^\beta_k\,\frac{x^{\alpha\dot{\alpha}}}{x^4}\left(\frac{x^2}{\rho^2+x^2}\right)^{3/2}.
\end{aligned} \tag{3.52}$$

The left-handed zero modes can be obtained by conjugation of Eq. (3.52). See Appendix A for a definition of the Weyl spinors.

Thus the ABJ-anomaly is saturated in the following sense[6]. A change in the topological charge due to a tunnelling process goes along with the creation and annihilation of fermions of a given chirality, the fermionic zero modes, violating the conservation of the axial current [7],

$$\Delta Q_5 = 2\,N_f\;(n_R - n_L) = 2\,N_f\,Q. \tag{3.53}$$

Since these fermionic zero modes have a definite chirality, quarks will flip their chirality as they pass an I-region [32]. Therefore instantons induce processes that cannot be found in perturbative QCD. This important characteristic provides an opportunity for measurable processes, see Sect. 3.4.3.

3.4.2 Instantons responsible for chiral symmetry breaking

At this point we are ready to discuss one of the most important effects of instantons in QCD: They are believed to be responsible for spontaneous chiral symmetry breaking (SχSB). After all it is SχSB producing 95% of the mass around us [8, 9, 10, 11, 12, 13].

[6]This is a consequence of the more general Atiyah-Singer index theorem, which relates the topological charge with the difference in the number of left- and right handed zero modes, [46, 47].

The $U(1)_A$ problem

Here the argumentation follows Ref. [48]. The massless QCD Lagrangian allows for the following global symmetries:

$$\begin{aligned} SU\left(N_f\right)_V: &\quad \psi_q \to \exp\left(\mathrm{i}\alpha_a^q \lambda^a/2\right)\psi_q \\ SU\left(N_f\right)_A: &\quad \psi_q \to \exp\left(\mathrm{i}\beta_a^q \gamma_5 \lambda^a/2\right)\psi_q \\ \left(U\left(1\right)_V\right)^{N_f}: &\quad \psi_q \to \exp\left(\mathrm{i}\alpha^q\right)\psi_q \\ \left(U\left(1\right)_A\right)^{N_f}: &\quad \psi_q \to \exp\left(\mathrm{i}\beta^q \gamma_5\right)\psi_q, \end{aligned} \tag{3.54}$$

where ψ_q denotes the quark fields, q = u,d,s,.. . This symmetry, which is called the *chiral* symmetry, is spontaneously broken,

$$SU\left(N_f\right)_V \times SU\left(N_f\right)_A \times U\left(1\right)_V \times U\left(1\right)_A \to SU\left(N_f\right)_V \times U\left(1\right)_V, \tag{3.55}$$

to the subgroup of vector symmetries with dimension N_f^2. The breaking of of $SU\left(N_f\right)_A$ generates a multiplet of $N_f^2 - 1$ pseudoscalar *Goldstone bosons*. For a theory with three flavours these are eight massless pseudoscalar mesons: π^+, π^0, π^-, K^+, K^0, $\bar{K}^0$, K^- and η_8. The *explicit* breaking of chiral symmetry by the QCD quark-mass term generates the experimentally observed masses of these mesons. However, the global group $U\left(1\right)_A$ is not anomaly-free and therefore gives, even in a theory with massless quarks, *no massless* Goldstone boson. For quite a while it was not clear what happened to that Goldstone boson. This is the famous $U(1)_A$ problem.

There exists an important relation, the *Witten-Veneziano relation* [49, 50], which states that the *topological susceptibility* χ_{top}, which is the fluctuation of the topological charge density $Q(x) = \partial_\mu \left(\bar{\psi}(x)\gamma^\mu\gamma^5\psi(x)\right)$, is proportional to the square of the pseudoscalar flavour-singlet mass m_0 and its decay constant f_0,

$$\chi_{\mathrm{top}}^{(N_f=0)} \equiv \int \mathrm{d}^4x \langle Q(x)Q(0)\rangle = 2f_0^2\, m_0^2. \tag{3.56}$$

As a consequence of this relation the mass for the pseudo-scalar meson (η' in $SU(N_f = 3)$) is large compared to the masses of pions and kaons. Thus the $U(1)_A$ problem is solved by the Witten-Veneziano relation, i.e. by means of instantons [6].

Chiral symmetry breaking through instantons

We know from the observation of a huge mass splitting between parity partners, that the chiral symmetry must be broken spontaneously. An example would be the splitting between the vector meson ρ (770 MeV) and the axial vector meson a_1 (1260 MeV) [51], which is about 500 MeV.

Actually this number indicates a very strong breaking, which cannot be explained by the quark-mass terms alone. The quarks are too light. Now it is the fermionic zero modes of Eq. (3.52), that are intimately connected with SχSB [8, 52]. When instantons interact through fermion exchanges, zero modes can form a collective quark condensate. Therefore the quark condensate is the associated order parameter [8],

$$\langle \bar{q}q \rangle = -(250 \text{ MeV})^3. \tag{3.57}$$

One [32, 8] imagines that they form a potential well making the light quarks to form bound states. Under the assumption of instantons being sufficiently randomly distributed in the QCD vacuum, there is a non-zero density of eigenvalues near zero. This leads to a much stronger spontaneous breaking of chiral symmetry than induced by the quark-mass terms and thus generates 95% of the hadron masses.

3.4.3 Measuring instanton-induced processes

Since hadrons are collective excitations, one must have a good knowledge of the groundstate of QCD in order to understand their structure. Thus also in the field of hadron spectroscopy instantons are of extreme importance and their experimental verification, still lacking today, would be a major step towards an understanding of the world of hadrons.

It has been shown by Ringwald and Schrempp [15, 16, 17, 18], that in principle it is possible to discover I-induced processes via deep-inelastic scattering. The particle accelerator HERA offers an excellent opportunity for the experimental search. It was found that both the rate of such processes and the characteristic event signature can be theoretically predicted and moreover the I-induced cross section lies within measurable range. A first analysis of HERA data showed a significant excess of events in case of the H1 collaboration [53] while the corresponding analysis by the ZEUS collaboration did not observe an excess [54]. Due to background, which is difficult to control, a definite answer on that issue, however, was not yet possible.

Since its upgrade HERA II delivers substantially more statistics, so that in the near future instanton search results may be found giving a decisive answer to that issue. There exists also an ongoing project focused on the investigation of the discovery potential for instanton processes at the forthcoming LHC [55, 56].

3.4.4 Instantons in electroweak theory

Instanton-solutions occur in all $SU(N)$ gauge theories, thus also in the electroweak theory, which is a $SU(2)_L \times U(1)$ gauge theory coupled to a Higgs doublet. There the coupling constant is small and the instanton action is large meaning that the semi-classical approximations (e.g. WKB) are

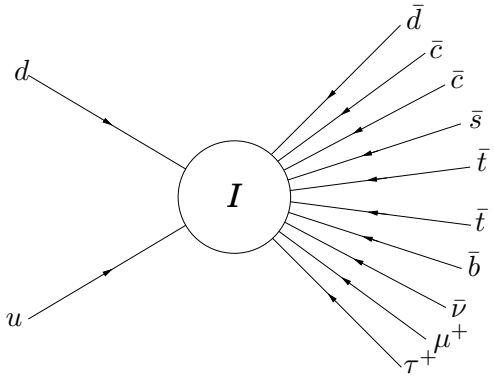

Figure 3.2: Anomalous instanton-induced process in electroweak theory [57, 58].

under control [32]. Electroweak instantons have fermionic zero modes, as well. Their presence also in that case is connected to the axial anomaly [44]. A typical process, as depicted in Fig. 3.2, would be

$$q + q \to 7\bar{q} + 3\bar{l}. \tag{3.58}$$

In particular these processes lead to a violation of the baryon and the lepton number, B and L respectively [7, 6, 14],

$$\Delta B = \Delta L = -n_{\text{gen}} Q, \tag{3.59}$$

where n_{gen} is the number of generations. Unfortunately the tunnelling events are usually very rare. In order to increase the tunnelling rate, scattering processes with collision energies close to the barrier height of the I-field energy were studied, see e.g. [59]. It was hoped that the strong suppression of tunneling events may be overcome at energies of about 10 TeV [57, 58] leading to the dramatic phenomenon of baryon number violation, but most probably this will not be observable [32, 60].

Chapter 4

Suppression of Large Instantons due to Symmetry?

In this chapter we return to our central problem concerning the suppression of large instantons discussed at the beginning in Chapter 2. The following discussion serves as a preparation for the subsequent investigations within our symmetry approach. We start in Sect. 4.1 by giving a more detailed discussion of the lattice data. We address alternative ways to our approach in Sect. 4.2. The last part, Sect. 4.3, gives an overview of conformal transformations and deals with the behaviour of the I-configuration under conformal inversion. It will be the major motivation for the idea investigated here.

4.1 Instantons on the lattice

The most direct and thus very important tool for the investigation of the QCD vacuum consists in numerical simulations on the lattice. The underlying theory, including perturbative and non-perturbative aspects, is numerically simulated essentially without simplifying assumptions[1]. Therefore one can learn something about large size instantons from lattice computations.

The basic idea is to compute the path integral in Euclidean space-time explicitly after having reduced the infinite number of field variables to a finite number. This is done by descretising space and time via the introduction of a hypercubic equally spaced lattice in space and time with coordinates

$$x_\mu \to x(i,j,k,t) = (i\boldsymbol{e_1} + j\boldsymbol{e_2} + k\boldsymbol{e_3} + t\boldsymbol{e_4})\, a, \tag{4.1}$$

[1]Thus interactions of instantons and anti-instantons are fully included.

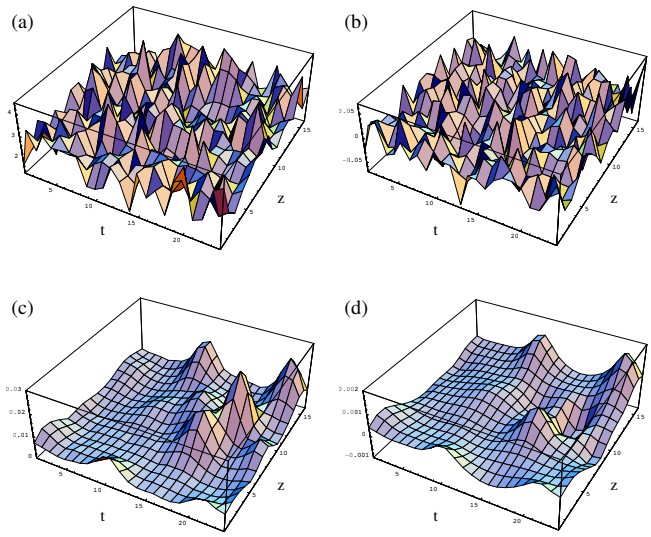

Figure 4.1: A characteristic snapshot of the Lagrange density $\propto F^2$ and the topological charge density $\propto F\widetilde{F}$ before (a,b) and after cooling (c,d) [62]. Three instantons (positive topological charge) and two anti-instantons (negative topological charge) are clearly visible in the cooled samples.

where a is the lattice spacing, the distance between neighbouring points on the lattice, see e.g. [61].

However, simulations of extended topological phenomena on the lattice suffer from difficulties due to perturbative fluctuations on very short scales $\sim a$. This has the effect of covering completely the interesting physics, since topological effects are expected to be of much larger wavelength. To cope with these problems the technique of *cooling* the fields [22] has been invented, where locally[2] the lattice fields over distances much larger than a but still small compared to ρ are smoothed out. In Fig. 4.1 a typical lattice configuration is shown [62]. One clearly sees the differences between uncooled and cooled quantities. This method eliminates quickly the unwanted non-topological quantum fluctuations with short wavelengths. What is left is indeed dominated by instantons [32].

Unfortunately the process of cooling does not leave the topological charge unchanged via two effects. On the one hand instantons, that are too small, will be erased and on the other hand instantons and anti-instantons can annihilate. Thus one tries to minimise the number of cooling

[2]by minimising the plaquette action locally

Table 4.1: "Equivalent" pairs $(\beta, n_{\rm cool})$: The cooling radius is similar [23].

β	$n_{\rm cool}$	$r_{\rm cool}$
6.0	23	0.447(2)
6.2	46	0.460(2)
6.4	80	0459(2)

sweeps $n_{\rm cool}$.

Now we want to discuss the continuum limit for the I-size distribution for this lattice data. This is a bit finical since a cooling sweep is not, in general, a procedure that scales with $\beta = \frac{2N_c}{g(a)^2}$ [63] , the coupling strength on the lattice. However, one can indeed find pairs of the coupling strength and the number of cooling sweeps, for which the size distribution does scale in shape and normalisation. These pairs were found to be $(\beta, n_{\rm cool}) = (6.0, 23), (6.2, 46), (6.4, 80)$ and called "equivalent" in Ref. [22].

The question is whether these pairs have some physical significance. It was shown by Ringwald and Schrempp [23] that they can indeed be interpreted in a physically meaningful way. In order to demonstrate this, an effective "cooling radius" $r_{\rm cool}$ is defined as

$$r_{\rm cool} = \text{const } (\sqrt{n_{\rm cool}})^{1+\delta}\ a, \tag{4.2}$$

where δ is supposed to be small and a is the lattice spacing used for the UKQCD data [22]. By means of a qualitative random walk argument the size of the area, which is cooled after $n_{\rm cool}$ cooling sweeps, is determined by the cooling radius $r_{\rm cool}$. The three "equivalent" pairs $(\beta, n_{\rm cool})$ are found to have a very similar value for the cooling radius $r_{\rm cool}$, see Table 4.1.

With the help of the cooling radius the instanton ensemble on the lattice can be characterised, since, as it was shown in Ref. [23], almost all quantities extracted in Ref. [22] scale with $r_{\rm cool}$. This also holds for the average I-size: If the average I-size $\langle\rho\rangle$ is plotted only as a function of the number of cooling sweeps $n_{\rm cool}$ for fixed values of $\beta = 6.0$, 6.2 and 6.4, respectively, one obtains three widely spread curves, see Fig. 4.2(a). The amazing observation of [23] was that $\langle\rho\rangle$ fits onto one single smooth curve for *all* available values of $(\beta, n_{\rm cool})$ when $\langle\rho\rangle$ is plotted as a function of the cooling radius $r_{\rm cool}$. This can be seen in Fig. 4.2(b). The important characteristic of that curve is the *plateau* which is reached for $\langle\rho\rangle \simeq 0.5$ fm. In Ref. [23] this has been interpreted by in the following way:

By increasing the cooling radius $r_{\rm cool}$ step by step, the ultraviolet fluctuations of short wavelength $\mathcal{O}(a)$ are filtered out first. As a consequence, the effective average I-size $\langle\rho\rangle$ begins to rise. When the cooling radius is further increased most of the unwanted fluctuations smooth

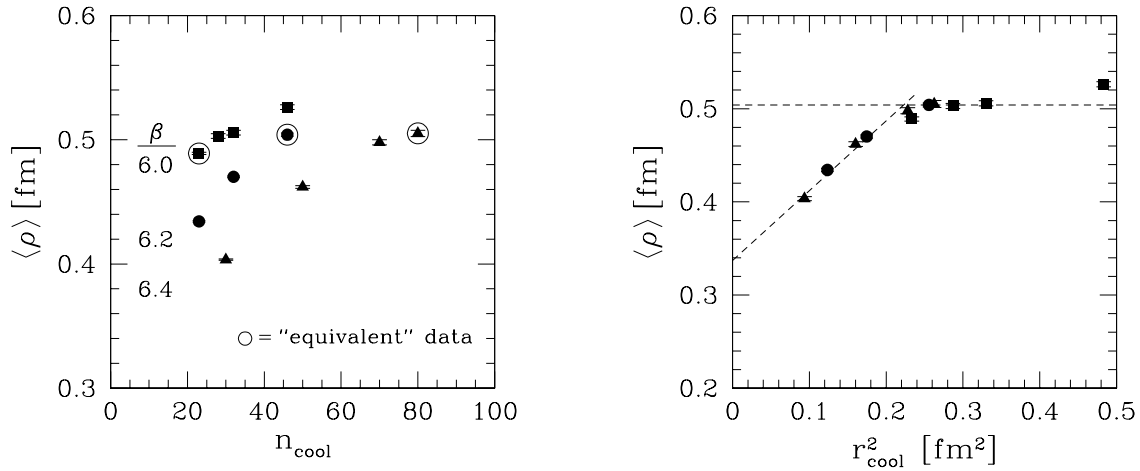

(a) (b)

Figure 4.2: In Fig. (a) The average I-size $\langle\rho\rangle$ for $\beta = 6.0\,[\blacksquare]$, $6.2\,[\bullet]$, $6.4\,[\blacktriangle]$ is depicted as a function of the cooling radius $n_{\rm cool}$. The "equivalent" data [22] are marked by a circle. The dependence on $n_{\rm cool}$ for fixed β is in general strong except for the "equivalent" data. In Fig. (b) The average I-size $\langle\rho\rangle$ is plotted for *all* available values of $n_{\rm cool}$ as a function of the cooling radius $r_{\rm cool}$ of Eq. (4.2). $\langle\rho\rangle$ scales nicely on one smooth curve. There is a clear indication of a *plateau* corresponding to $\langle\rho\rangle \simeq 0.5$ fm [23].

out. We begin to enter the region of a *plateau* in $\langle\rho\rangle$, where the smaller fluctuations have already been eliminated but instantons, having a characteristic extension with physical significance, are not yet strongly affected. The region of the plateau corresponds to $\langle\rho\rangle \simeq 0.5$, which is exactly the peak position of the I-size distribution, see Fig. 2.1. Eventually, also these topological fluctuations will start to be erased and thus the average I-size rises again.

From the above argumentation it can be concluded that the plateau region is the correct regime for the investigation of instanton effects on the lattice, see [23]. The "equivalent" pairs $(\beta, n_{\rm cool})$ of Ref. [22] are found to be precisely situated around the plateau. By using these data sets it is possible to perform the continuum limit for the size-distribution relatively safely, i.e. with only little influence from cooling. In Ref. [23] the remaining dependence on a, already quite

small, of the "equivalent" data for the size distribution was parameterised as,

$$(\rho)^5 \frac{\mathrm{d}\, n_{I+\bar{I}}}{\mathrm{d}^4 x\, \mathrm{d}\rho} = \text{function}\left(\frac{\rho}{\langle \rho\,(a)\rangle}\right). \tag{4.3}$$

The continuum limit[3] $a \to 0$ was then carried out in a quite reliable way by rescaling the arguments

$$\rho \to \frac{\langle\rho(0)\rangle}{\langle\rho(a)\rangle} \cdot \rho. \tag{4.4}$$

The result for the average instanton size [23] was found to be

$$\langle\rho(0)\rangle = 0.518(5)\ \text{fm}, \tag{4.5}$$

which is in agreement with Refs. [19, 64, 20]. The typical size of an instanton is found to be somewhat larger than advocated in Ref. [32, 21]. Investigations on finite volume effects, which become important for large instantons, have been done. They are shown not to have any impact on the results [22].

For the average distance $\bar{R}_{II}$ between two instantons and $\bar{R}_{I\bar{I}}$ between an instanton and an anti-instanton, the UKQCD collaboration [22] found

$$\bar{R}_{II} \sim 0.49\ \text{fm}, \tag{4.6}$$

$$\bar{R}_{I\bar{I}} \sim 0.45\ \text{fm}. \tag{4.7}$$

From the ratio

$$\frac{\langle\rho(0)\rangle}{\bar{R}} \sim 1 \tag{4.8}$$

we conclude that the real vacuum must be dense and instantons, on average (for $\rho \simeq \langle\rho(0)\rangle$), are strongly overlapping. The dilute-gas approximation, however, works almost perfectly for smaller size instantons, i.e. until an instanton size of $\rho \sim 0.35$ fm.

For a quantitative comparison with I-perturbation theory, which was done in [23, 17], the 3-loop form of $\alpha_{\overline{\mathrm{MS}}}$ was used. The 2-loop renormalisation group invariance of $D_{I+\bar{I}}(\rho)$ leads to a virtual independence of the renormalisation scale μ_r. Still it is strongly dependent on $\Lambda_{\overline{\mathrm{MS}}}$. For the investigation of the continuum limit in Ref. [23] accurate lattice results of the ALPHA collaboration [24] for $n_f = 0$, $\Lambda_{\overline{\mathrm{MS}},n_f=0} = (238 \pm 19)$ MeV, were taken. It is worthwhile to mention that the predictions of I-perturbation theory are parameter-free. For this reason the agreement in shape and normalisation with lattice data is striking, see Fig. 4.3. As already pointed out before, these lattice data show some very interesting features.

[3] In [23] $\langle\rho(a)\rangle$ was extrapolated linearly in a^2, i.e. $\langle\rho(a)\rangle = \langle\rho(0)\rangle - \text{const} \cdot a^2$.

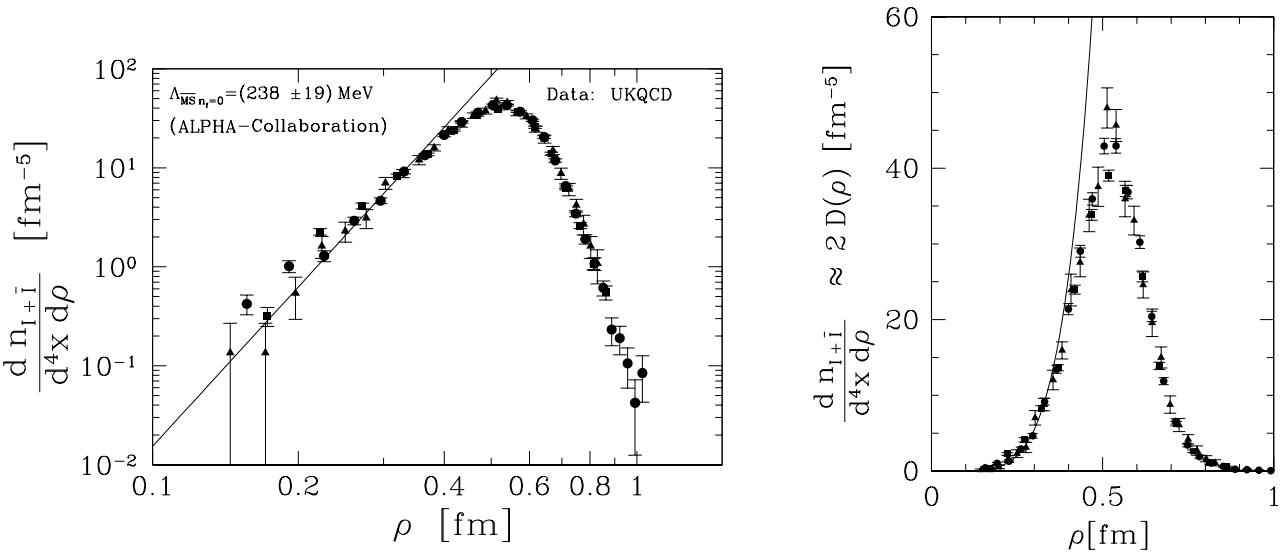

Figure 4.3: Continuum limit [23] of "equivalent" UKQCD data [22] for the $(I+\overline{I})$-size distribution at $(\beta, n_{\rm cools}) = (6.0, 23)$ [■], $(6.2, 46)$ [•], $(6.4, 80)$ [▲]. The solid line corresponds to the predictions from I-perturbation theory [23, 17] at two-loop level of Eq.(3.34). The 3-loop form of $\alpha_{\overline{\rm MS}}$ with $\Lambda_{\overline{\rm MS}\, n_f=0}$ from ALPHA [24] was used. The renormalisation scale is about $\mu_{\rm r} \simeq 1/0.18\,{\rm fm}^{-1}$. (a) The double logarithmic display makes the expected (approximated) power law $\sim \rho^6$ evident. I-perturbation theory is reliable for $\rho \lesssim \rho_{\rm cut} = 0.35$ fm. (b) In the linear display the sharp maximum of the distribution is clearly visible. The agreement in shape and normalisation of I-perturbation theory and lattice data is impressive.

Summarising the discussion of Sect. 2, we have:

- Larger-size instantons are strongly suppressed.
- I-perturbation theory (without any free parameter) is reliable till $\rho \lesssim \rho_{\rm cut} \approx 0.35$ fm, but then breaks down surprisingly rapidly.
- The I-size distribution has a sharp maximum at $\rho_{\rm peak} \simeq 0.52$ fm.
- The size distribution seems to be invariant under an inversion of the I-size,

$$\rho \Leftrightarrow \frac{\rho_{\rm peak}^2}{\rho}.$$

4.2 Alternative approaches to a suppression of larger instantons

There are numerous reasons why instantons are considered to play a crucial role in QCD. But to really pin down their significance, one has to determine the total tunnelling rate in QCD. Unfortunately the dilute-gas approximation in Sect. 3.3 is not able to answer this issue, since the integration of Eq. (3.41) over ρ diverges. Also the integration over the position z yields a divergent factor $V \to \infty$, which, however, can be interpreted as usual by expecting the vacua only to have a finite energy density E/V. There is no such explanation in the case of the instanton size ρ to save the situation.

As mentioned before, this work is devoted to a possible understanding of larger instantons. Over the years this problem has been attacked from various sides. So let us first mention alternative explanations for this break-down as the typical size of an instanton becomes large. The reason for this divergence lies in the collapse of the dilute-gas approximation, which assumes that instantons are well separated such that they do not interact with each other. If instantons are too large, they will start overlapping. This assumption is then clearly violated. That is to say since the average size of the instanton is of the order of the typical separation R between instantons, it is more appropriate to speak of an instanton liquid [32] than of an instanton gas. Thus, next to the tunnelling rate, the size of the average instanton is a very important quantity in the I-sector and plays a key role when describing the characteristics of the QCD vacuum.

In the past one could find two possible explanations for the suppression of larger-size instantons in the literature:

- Higher loop perturbative fluctuations start to grow. However, the two-loop corrections to the semi-classical result are not known so far.

- Non-perturbative effects become important, e.g. multi-instanton effects in the instanton liquid model [32]. This approach is based on Refs. [38, 65]. In that model instantons obtain their finite average size due to interactions among each other.

However, in these models it is not clear why the dilute-gas approximation works perfectly till an I-size of about 0.35 fm and then breaks down so rapidly. The idea of an invariance under conformal space-time inversion,

$$x_\mu \to x'_\mu = \frac{\rho^2_{\text{peak}}}{x^2} x_\mu, \tag{4.9}$$

being behind the strong suppression is a new approach, that would provide an answer to that issue.

4.3 Instantons and conformal inversion

Conformal transformations, conformal inversions in particular, play an essential role in this work. Therefore let us give a short overview of the conformal group and the corresponding transformations in the following section, Sect. 4.3.1. In Sect. 4.3.2 we introduce the transformations laws, which will be used intensively in this work. We address the issue of the behaviour of the I-field under conformal inversion in Sect. 4.3.3.

4.3.1 Conformal transformations

Before giving the actual definition of a conformal transformation let us point out the following aspect. Conformal transformations can be viewed in two different ways, in an *active* and in a *passive* way [66]. In what follows we are dealing with so called *active transformations*, e.g. in a fixed basis the components of a vector change. Active transformations are also known as *point transformations* since they transform points of functions in a given frame of reference.

They have to be sharply distinguished from *passive transformations*, where indeed one does change the frame of reference. In this second formulation not only the components of a vector but also the basis vectors change. The importance of this distinction lies in the different physical interpretation of the two formulations. The purpose of passive coordinate transformations is to describe physics in different frames of reference. Of course, physics should not depend on the coordinate system. In contrast to the passive formulation we want to study what happens to physics under certain active transformations, namely conformal inversions, in a given frame of reference.

A conformal transformation of the coordinates is defined as an invertible mapping $x \to x' = f(x)$, which leaves the line element invariant up to a scale factor $\sigma(x)$ [67, 68],

$$\mathrm{d}s^2 = \sigma(x)\,\mathrm{d}s'^2. \tag{4.10}$$

In our approach conformal transformations are *active* space-time transformations $x \to x' = f(x)$, which have to satisfy the condition [67, 68],

$$g_{\mu\nu}(x)\frac{\partial x^\mu}{\partial x'^\kappa}\frac{\partial x^\nu}{\partial x'^\lambda} = \sigma(x)\; g_{\kappa\lambda}(x'). \tag{4.11}$$

$\sigma(x)$ is sometimes also called *conformal factor*. The epithet *conformal* derives from the fact that the transformations under the corresponding group preserve angles.

The set of conformal transformations in 4 space-time dimensions forms a 15-parameter Lie-group with the Poincaré group as a subgroup. It is made up of inhomogeneous Lorentz trans-

formations $\mathcal{L}_{\text{inh}}$, dilatations $\mathcal{D}$ and special conformal transformations $\mathcal{K}$:

$$\begin{aligned} \mathcal{L}_{\text{inh}}: &\quad x^\mu \to x'^\mu = M^{\mu\nu} x_\nu + a_\mu, \\ \mathcal{D}: &\quad x^\mu \to x'^\mu = \lambda x^\mu, \\ \mathcal{K}: &\quad x^\mu \to x'^\mu = \frac{c^2}{b^2} \frac{x^\mu + \frac{a^\mu}{b^2} x^2}{1 + \frac{2ax}{b^2} + \frac{x^2 a^2}{b^4}} \end{aligned} \tag{4.12}$$

The transformation relevant for our approach is the conformal inversion of space-time,

$$I_{b^2} : x^\mu \to x'^\mu = \frac{b^2}{x^2} x^\mu. \tag{4.13}$$

In principle one could take a factor a, where a is allowed to be positive or negative, instead of b^2. Both, b^2 and $|a|$, are called the radius of the inversion [69, 70]. The inversion has an exceptional role among the conformal transformations, since the set of conformal transformations quoted in Eq. (4.12) can be constructed by means for inhomogeneous Lorentz transformations and inversions only [69, 70].

The special conformal transformation can be composed by an inversion $y^\mu = b^2/x^2 x^\mu$, followed by a translation $T_a : z^\mu = y^\mu + a^\mu$ and another inversion, $x'^\mu = c^2/z^2 z^\mu$:

$$\mathcal{K} = I_{c^2}\, T_a I_{b^2} \tag{4.14}$$

The dilatation can be made up with the help of two inversions having different radii, see also Sect. 6.1,

$$\begin{aligned} I_{b^2}: &\quad x^\mu \to x'^\mu = \frac{b^2}{x^2} x^\mu \\ \mathcal{D}_{a^2/b^2} = I_{a^2}\, I_{b^2}: &\quad x'^\mu \to y^\mu = \frac{a^2}{x'^2} x'^\mu \\ &\qquad\qquad = \frac{a^2}{b^2} \frac{x}{\mu} \\ &\qquad\qquad = \lambda x_\mu. \end{aligned} \tag{4.15}$$

However, the inversion cannot be part of the conformal algebra, since it is a discrete transformation, meaning that it cannot be expressed in terms of an infinitesimal transformation. Thus there exists no generator for the conformal inversion.

In Appendix B a list of relevant scale factors is given in Table B.2, a list of the generators of the conformal group in Table B.1 and also the conformal algebra can be found there.

4.3.2 Transformation laws

Scalar fields transform under conformal transformations as follows [68]

$$\begin{aligned}\phi(x) \to \phi'(x') &= \left|\frac{\partial x'}{\partial x}\right|^{-\Delta/d} \phi(x) \\ &= \sigma(x)^{-\frac{2\Delta}{d}} \phi(x),\end{aligned} \tag{4.16}$$

where d is the dimension of the Euclidean space time and Δ is the *scaling dimension* defined by the behaviour of the scalar function under dilatations $x' = \lambda x$ [71],

$$\phi'(\lambda x) = \lambda^{-\Delta}\phi(x). \tag{4.17}$$

The transformation law for a covariant vector field is given by

$$A'_\mu(x') = \frac{\partial x^\nu}{\partial x'^\mu} A_\nu(x) = \sqrt{\sigma(x)} I_\mu^{\ \nu}(x) A_\nu(x). \tag{4.18}$$

The corresponding contravariant vector field has to transform as [66],

$$A'^\mu(x') = \sigma(x)\frac{\partial x'^\mu}{\partial x^\nu} A^\nu(x) = \sqrt{\sigma(x)} I^\mu_{\ \nu}(x) A^\nu(x), \tag{4.19}$$

where the scale factor $\sigma(x)$ appears when pulling up the index with the help of the metric tensor $g^{\mu\nu}(x')$[4]. We observe that co- and contravariant vector fields transform alike, as expected since we work in Euclidean space. This would not be the case if we considered passive coordinate transformations. Furthermore the length of a vector is not invariant under conformal transformations, in fact it is stretched by the scale factor,

$$A'^\mu(x') A'_\mu(x') = \sigma(x) A^\mu(x) A_\mu(x). \tag{4.20}$$

The generalisation to second order tensors is straight forward:

$$\begin{aligned} F'_{\mu\nu}(x') &= \frac{\partial x^\rho}{\partial x'^\mu}\frac{\partial x^\sigma}{\partial x'^\nu} F_{\rho\sigma}(x), \\ &= \sigma(x) I_\mu^{\ \rho}(x)\, I_\nu^{\ \sigma}(x) F_{\rho\sigma}(x) \\ F'^{\mu\nu}(x') &= \sigma^2(x)\frac{\partial x'^\mu}{\partial x^\rho}\frac{\partial x'^\nu}{\partial x^\sigma} F^{\rho\sigma}(x), \\ &= \sigma(x) I^\mu_{\ \rho}(x)\, I^\nu_{\ \sigma}(x) F^{\rho\sigma}(x), \\ F'^{\mu\nu}(x') F'_{\mu\nu}(x') &= \sigma^2(x) F^{\rho\sigma}(x) F_{\rho\sigma}(x). \end{aligned} \tag{4.21}$$

[4] In the case of a passive transformation this factor would not be included.

4.3.3 Instantons under space-time inversion

Finally we are ready to consider the behaviour of the I-configuration under conformal space-time inversion of radius b. This property was discussed first by Jackiw and Rebbi [26]. Let us compute its behaviour explicitly using the notation of 't Hooft symbols for the $SU(2)$-instanton gauge field, the Pauli matrices are denoted by σ^a, see Appendix A.

$$\begin{aligned} A'_\mu(x',\rho) &= \frac{\partial x^\nu}{\partial x'^\mu} A^{(I)\mathrm{reg}}_\nu(x,\rho) \\ &= \sqrt{\sigma(x)} I_\mu{}^\nu(x) A^{(I)\mathrm{reg}}_\nu(x,\rho) \\ &= \frac{x^2}{b^2}\left(\delta^\nu_\mu - \frac{2x_\mu x^\nu}{x^2}\right)\frac{2}{g}\frac{x^\sigma}{\rho^2+x^2}\eta_{a\nu\sigma}\frac{\sigma^a}{2} \\ &= \frac{2}{g}\frac{\rho'^2}{x'^2}\frac{x'^\sigma}{\rho'^2+x'^2}\eta_{a\mu\sigma}\frac{\sigma^a}{2} \\ &= A^{(\bar I)\mathrm{sing}}_\mu(x',\rho'). \end{aligned} \tag{4.22}$$

As claimed in Sect. 2, we now have checked that under conformal inversion an instanton field in regular gauge of size ρ changes to an *anti*-instanton field in singular gauge of size ρ', where we have defined

$$\rho' \equiv \frac{b^2}{\rho}. \tag{4.23}$$

That means that a coordinate inversion Eq. (4.13) actually has the effect of an inversion of the instantons size, which is the symmetry indicated by the lattice data.

The fact that an instanton changes to an anti-instanton is of no concern, since the size distribution $D_{I+\bar I}(\rho)$ simulated on the lattice is a sum of both, instantons and anti-instantons. The (anti-) instanton contribution to the Lagrange density, since it is gauge-independent, shows the same property [25],

$$\begin{aligned} \mathcal{L}^{(I)}(x,\rho) \to &= \mathcal{L}^{(I)\prime}(x',\rho) \\ &= \mathrm{Tr}\left[F^{(I)\mathrm{reg}\prime}_{\mu\nu}(x',\rho)\, F^{(I)\mathrm{reg}\prime\,\mu\nu}(x',\rho)\right] \\ &= \mathrm{Tr}\left[U(x)\, F^{(\bar I)\mathrm{sing}}_{\mu\nu}(x',\rho')\, U^{-1}(x) U(x) F^{(\bar I)\mathrm{sing}\mu\nu} U^{-1}(x)\,(x',\rho')\right] \\ &= \mathrm{Tr}\left[F^{(\bar I)\mathrm{sing}}_{\mu\nu}(x',\rho')\, F^{(\bar I)\mathrm{sing}\mu\nu}(x',\rho')\right] \\ &= \mathcal{L}^{(\bar I)}(x',\rho') \end{aligned} \tag{4.24}$$

The action is of course invariant[5], since it is independent of the I-size,

$$S_{\mathrm{E}} = \int \mathrm{d}^4x \; \mathcal{L}^{(I)}\left(x,\rho\right) = \int \mathrm{d}^4x' \mathcal{L}^{(\bar{I})}\left(x',\rho'\right) = \frac{8\pi^2}{g^2}. \tag{4.25}$$

As pointed out in Ref. [26], it is possible to put the instanton and anti-instanton solution together by extending the gauge group to $SU(2)_{(I)} \times SU(2)_{(\bar{I})} \sim O(4)$. One obtains a gauge potential of the form

$$A_\mu^{I+\bar{I}}(x) = -\frac{2\mathrm{i}}{\rho^2 + x^2}\Sigma_{\mu\nu}x^\nu, \tag{4.26}$$

where

$$\Sigma_{\mu\nu} = \frac{1}{4\mathrm{i}}\left[\gamma_\mu,\gamma_\nu\right] = \frac{1}{4\mathrm{i}}\begin{pmatrix} \sigma_{\mu\nu} & 0 \\ 0 & \bar{\sigma}_{\mu\nu} \end{pmatrix}. \tag{4.27}$$

We switched back to the notation of the σ-matrices to make it clearly visible what is happening. See Appendix A for a definition of $\sigma^{\mu\nu}$ and the Dirac matrices γ^μ in chiral representation. We notice that the instanton configuration is put into the upper left corner, whereas the anti-instanton can be found in the lower right corner of the matrix representation. The effect of an inversion with a radius equal to the size of the instanton, $b = \rho$, is to produce solutions where, up to a gauge transformation, the upper and lower diagonal matrices are interchanged.

However, this is not what we are up to, since in that case no new scale enters the discussion. The inversion radius we are interested in is $b = \rho_{\mathrm{peak}}$. As already claimed in Chapter 2 we propose that the above relation Eq. (4.22) between smaller- and larger-size instantons is responsible for the rapid breakdown of I-perturbation theory. So far this characteristic of the I-vector potential was only found at the classical level. So obviously one has to ask the following question: Does this symmetry, $\rho \Leftrightarrow \rho'$, survive at the quantum level, that is to say does it show up in the I-size distribution?

[5]Actually the Yang-Mills action is invariant under any conformal transformation.

Chapter 5

Inversion Symmetry at the Quantum Level?

In this chapter we deal with our main issue: The behaviour of the zero mode fraction, a major contribution to the I-size distribution, under a conformal space-time inversion. We start with a detailed discussion of the gauge zero modes and their integration in the functional integral by introducing the method of collective coordinates in Sect. 5.1. It follows a discussion on the importance of the zero mode contributions in Sect. 5.2. We will write down the different types of gauge zero modes explicitely in Sect. 5.3. In the last part of this chapter we will transform the zero mode fraction under conformal inversion and give the results.

5.1 Collective coordinates and zero modes

The question stated at the end of the last section requires a thorough investigation of the behaviour of the I-size distribution $D(\rho)$ at one-loop level under a conformal inversion. In this section we will focus on the importance and evaluation of the zero mode part. Thereafter we consider the behaviour of the zero mode part under an inversion of space-time defined by Eq. (2.3).

In the course of our computations we introduce the method of *collective coordinates* [72, 73], to compute the functional integral near the nontrivial solution of classical equations of motion. Usually this is done in Gaussian approximation. However, there can be directions in functional space along which the solution can be perturbed without changing the action,

$$S[A(x;\gamma)] - S[A(x;\gamma+\delta\gamma)] = 0. \tag{5.1}$$

These directions, which are called *zero modes* χ^0, reflect the symmetries of our system. The name derives from the fact that zero modes are eigenfunctions with zero eigenvalue, $\epsilon_0 = 0$, of the operator M_A, that appears in the expansion of the action to quadratic order about the

classical field[1] in Eq. (3.31):

$$M_A^{\mu\nu}\,\chi_\nu^0 = 0 \tag{5.2}$$

The integration over the zero modes is non-Gaussian and therefore has to be treated carefully.

Zero modes appear whenever the action is invariant under a given transformation, whereas the solution of the equations of motion is not. The parameters γ_i belonging to such transformations are called *collective coordinates*.

In principal for every type of field in the Lagrangian zero modes can occur, thus one speaks of e.g. fermionic, ghost or gauge zero modes. It should be stressed that in what follows we are only dealing with so called *gauge* zero modes, which are the directions of the *gauge potentials* in the functional space not changing the action. This is because we are working in pure Yang-Mills theory. Therefore we will omit the epithet *gauge* when speaking of zero modes. Gauge zero modes must thus be distinguished from the fermionic zero modes of Eq. (3.52), which were eigenfunctions with zero eigenvalue of the *Dirac operator*.

The instanton field is dependent on its size ρ, on its position z_μ and on its orientation in colour space. The action, being constant, does not depend on any of these parameters. For the gauge group $SU(2)$ there would appear three colour zero modes being generated by the Pauli matrices. Since we are considering $SU(3)$ instantons the situation is somewhat different. This problem was addressed first by Bernard [41]. One finds that there appear four additional zero modes coming from the generators λ_4, λ_5, λ_6 and λ_7. The generator λ_8 does not generate a zero mode since it commutes with the generators λ_1, λ_2 and λ_3, i.e. with the instanton field.

Since an instanton of size ρ changes to an anti-instanton of size ρ' under conformal inversion this transformation has the effect of a dilatation. Thus no new zero modes is associated with it. Also the special conformal transformation does not generate a zero mode because it is a composition of two inversions and one translation, see Eq. (4.14).

All in all we have

$$4\ (\text{position})\ +\ 1\ (\text{size})\ +\ (4N_c - 5)\ (\text{orientations}) = 4\ N_c \tag{5.3}$$

collective coordinates parameterising the instanton configuration, see also Sect. 5.3. The 12 collective coordinates of the I-configuration in $SU(3)$ are denoted by γ_i.

[1] In our case this is the classical I-field.

Since the action does not change under a variation of a collective coordinate, we have

$$\begin{aligned} S\left[A^{(I)}(\gamma+\delta\gamma)\right] &= S\left[A^{(I)}(\gamma) + \left.\frac{\partial A^{(I)}}{\partial\gamma}\right|_{\gamma=\delta\gamma}\delta\gamma\right] \\ &= S\left[A^{(I)}\right] + \left.\frac{\delta S}{\delta A^{(I)}}\frac{\partial A^{(I)}}{\partial\gamma}\right|_{\gamma=\delta\gamma}\delta\gamma \\ &\stackrel{!}{=} S\left[A^{(I)}\right], \end{aligned} \tag{5.4}$$

and thus

$$\left.\frac{\delta S}{\delta A^{(I)}}\frac{\partial A^{(I)}}{\partial\gamma}\right|_{\gamma=\delta\gamma}\delta\gamma = 0. \tag{5.5}$$

We find that the directions in functional space, which leave the action invariant, are the derivatives of the gauge fields with respect to the collective coordinates γ,

$$\chi^0_\mu(x) = \frac{\partial A^{(I)}_\mu}{\partial\gamma}. \tag{5.6}$$

At the end of this section we will see that this is an important relation for our symmetry considerations.

Since zero modes are eigenfunctions of M with zero eigenvalue they blow up the functional determinant. Hence we cannot perform a simple Gaussian integration. Instead we replace the integration along the directions of the zero modes with an integration over the collective coordinates. The argumentation given below follows Ref. [41]. We expand the quantum fluctuations A^{qu} in terms of orthogonal eigenfunctions χ_i,

$$A^{qu} = \sum_i \xi_i\chi_i, \tag{5.7}$$

where the eigenfunctions ought to have the norm

$$u_i \equiv \langle\chi_i|\chi_i\rangle. \tag{5.8}$$

Then we can write the measure of the functional integral as

$$\mathcal{D}A = \mathcal{D}A^{qu} = \prod_i \left(\frac{u_i}{2\pi}\right)^{1/2}\mathcal{D}\xi_i. \tag{5.9}$$

Now we perform the Gaussian integration over the non-zero modes. We get

$$\int \mathcal{D}A\, \mathrm{e}^{-S_E} = \int \mathrm{d}\xi_0^{(i)} \left(\frac{u_0^{(i)}}{2\pi}\right)^{1/2} \mathrm{e}^{-S^{cl}} [\det M']^{-1/2}, \tag{5.10}$$

$\det M'$ being the functional determinant of the non-zero eigenvalues and $\xi_0(i)$ being the parameters of the zero modes. By inserting a "Faddeev-Popov unity" for each collective coordinate,

$$1 = u_0^{(i)} \int \mathrm{d}\gamma_i\, \delta\left(\left\langle A^{qu}(\gamma)\, |\chi_0^{(i)}(\gamma)\right\rangle\right) + \dots \tag{5.11}$$

we require the quantum field to be orthogonal to the zero modes. The dots represent terms of higher order which are neglected. Rewriting the Faddeev-Popov unity of Eq. (5.11) gives

$$\begin{aligned} 1 &= u_0^{(i)} \int \mathrm{d}\gamma_i\, \delta\left(\left\langle A^{qu}(\gamma)\, |\chi_0^{(i)}(\gamma)\right\rangle\right) + \dots \\ &= u_0^{(i)} \int \mathrm{d}\gamma_i\, \delta\left(\left\langle \sum_j \xi_j \chi_j \middle| \chi_0^{(i)}(\gamma)\right\rangle\right) + \dots r \\ &= u_0^{(i)} \int \mathrm{d}\gamma_i\, \delta\left(\xi_0^{(i)}\, u_0^{(i)}\right) + \dots \\ &= \int \mathrm{d}\gamma_i\, \delta\left(\xi_0^{(i)}\right) + \dots . \end{aligned} \tag{5.12}$$

After integration over $\xi_0^{(i)}$ we are left with an integration over the collective coordinates and thus avoiding the non-Gaussian directions in functional space.

$$\int \mathcal{D}\, A\mathrm{e}^{-S_E} = \int \mathrm{d}\gamma_i \prod_i \left(\frac{u_0^{(i)}}{2\pi}\right)^{1/2} \mathrm{e}^{-S^{cl}} [\det M']^{-1/2} + \dots \tag{5.13}$$

When dealing with non-Abelian gauge theories it is necessary to fix the gauge. In our case we are working in the background gauge with respect to the the classical field. However, the derivative of the classical field will not, in general, be in the background gauge. Thus we have to add an additional term,

$$\psi_\mu^{(i)} = \frac{\partial A_\mu^{(I)}}{\partial \gamma_i} + D_\mu^{(I)} \Lambda^{(i)}, \tag{5.14}$$

where $D_\mu^{(I)}$ is the gauge-covariant derivative in the instanton field. $\Lambda^{(i)}$ is the gauge transformation we need to bring the (i)th zero mode into the background gauge, i.e.

$$D_\mu^{(I)}\psi^{(i)\mu} = \partial_\mu\psi^{(i)\mu} - \mathrm{i}g\left[A_\mu^{(I)}, \psi^{(i)\mu}\right] = 0. \tag{5.15}$$

Finally we obtain for the one-loop vacuum-vacuum amplitude the following expression

$$\begin{aligned}\langle 0|0\rangle^{(I)} = \frac{\mathcal{Z}^{(I)}}{\mathcal{Z}^{(0)}} &= \int \prod_i \mathrm{d}\gamma_i J\left(\gamma\right) Q\left(\gamma\right) \mathrm{e}^{S^{cl}} \\ &= \int \mathrm{d}^4 z \frac{\mathrm{d}\rho}{\rho^5}\, \mathrm{d}U\, \rho^5 J\left(\gamma\right) Q\left(\gamma\right) \exp\left\{-\frac{8\pi^2}{\alpha_s(\mu_\mathrm{r})}\right\},\end{aligned} \tag{5.16}$$

where $J\left(\gamma\right)$ is the fraction coming from the zero modes. Since in the classical instanton configuration small and large instantons can be connected through conformal inversion, one hopes that this property somehow survives at the one-loop level. This idea is suggested by the relation of Eq. (5.6), since the zero mode contributions, which are a major part of the size distribution $D(\rho)$, are given by the derivatives of the classical fields with respect to γ and by that $D(\rho)$ may inherit the symmetry property of the I-configuration. $Q\left(\gamma\right)$ is the remaining part of non-zero modes,

$$Q\left(\gamma\right) \equiv \frac{\left[\det M_A'(\gamma)\right]^{-1/2}\big|_{A^{cl}=A^{(I)}}}{\left[\det M_A'\right]^{-1/2}\big|_{A^{cl}=0}}. \tag{5.17}$$

By comparison with Eq. (3.32) in Sect. 3.3 we confirm the following relation for the I-size distribution,

$$\begin{aligned}D &= J\left(\gamma\right)\, Q\left(\gamma\right)\, \exp\left\{-\frac{8\pi^2}{\alpha_s(\mu_\mathrm{r})}\right\} \\ &= \frac{\mathrm{d}\left\langle 0|0\right\rangle^{(I)}}{\mathrm{d}\gamma_1 \ldots \mathrm{d}\gamma_{4N_c}} \Leftrightarrow \frac{\mathrm{d}n^I}{\mathrm{d}^4 z\, \mathrm{d}\rho}.\end{aligned} \tag{5.18}$$

5.2 The importance of the zero mode part

In the above section we have seen that there are two main contributions to the I-size distribution, the part coming from the zero modes $J\left(\gamma\right)$ and the non-zero mode fraction $Q\left(\gamma\right)$, which is the ratio of the functional determinants of the path integral,

$$Q\left(\gamma\right) = \frac{\left[\det M_A'(\gamma)\right]^{-1/2}\big|_{A^{cl}=A^{(I)}}}{\left[\det M_A'\right]^{-1/2}\big|_{A^{cl}=0}}. \tag{5.19}$$

It was shown by 't Hooft [6] that

$$Q(\gamma) \sim \left(\frac{1}{\rho\,\mu_{\rm r}}\right)^{\frac{N_c}{3}} \overset{SU(3)}{=} \frac{1}{\rho\,\mu_{\rm r}}. \tag{5.20}$$

The zero mode part is of great importance, especially when considering supersymmetric QCD. There all non-zero mode contributions cancel precisely to any order perturbation theory, see [74, 75]. The size-distribution $D(\rho)$ is entirely given in terms of the zero mode part, as was shown by Shifman, Vainshtein and Zakharov [75].

In case of standard QCD the the size-distribution in the region of the I-size we are interested in, the average I-size $\rho_{\rm peak} \simeq 0.5$ fm, is still dominated by the zero mode part in the following sense, as will be demonstrated in Sect. 5.3:

$$D(\rho)_{1-\rm loop} \propto \rho^{\beta_o} = \rho^{\frac{11}{3}N_c} = \underbrace{\rho^{4\,N_c}}_{\text{ZM part}} \cdot \underbrace{\rho^{-\frac{1}{3}N_c}}_{\text{non-ZM part}} \tag{5.21}$$

In Sect. 5.1 we have shown, that the zero modes correspond to the derivatives of the classical gauge field with respect to the collective coordinates γ,

$$\psi_\mu^{\,0}(x) \sim \frac{\partial A_\mu^{(I)}(x)}{\partial\gamma}. \tag{5.22}$$

Since the instanton field of radius ρ changes under an inversion to an anti-instanton field with radius $\rho' = \frac{\rho_{\rm peak}^2}{\rho}$, it might be possible that the above property of the instanton solution transfers to the zero mode contribution. An investigation of this issue is is the topic of the subsequent sections. In our approach we assume that the non-zero mode part is not affected by inversion. We then might divide it out in the form of a factor $\rho^{-N_c/3}$ [25].

5.3 Zero mode contributions for $SU(3)$

Now we come to our central studies of the dominant part of the size-distribution, the behaviour of the zero modes under space-time inversion. First we have a look on the explicit form of the zero modes. The computations for the gauge group $SU(3)$ were done first by Bernard [41]. In Sect. 5.4, each zero mode will be transformed under an inversion with radius $\rho_{\rm peak}$. Throughout the following computations we will deal with $SU(3)$-instantons in singular gauge. As already mentioned in Sect. 3.1, an $SU(3)$-instanton can be obtained by embedding the $SU(2)$-instanton into the upper-left-hand corner of the fundamental representation of $SU(3)$,

$$A_\mu^{(I)}(x) = \frac{2}{g}\frac{\rho^2}{(x-z)^2\left(\rho^2+(x-z)^2\right)^2}\,U(x)\,\bar\eta_{a\mu\nu}x^\nu\frac{\lambda^a}{2}\,U^\dagger(x) \tag{5.23}$$

where λ^a, $a = 1, 2, 3$ denotes the first three Gell-Mann matrices and z_μ the instanton position. Without loss of generality the the U-matrices[2] describing the colour orientation will be set to unity and the instanton position will be set to zero unless we consider the associated zero modes.

Dilatation Zero Mode

In order to obtain the dilatation zero mode, we have to differentiate the I-gauge field with respect to the I-size ρ:

$$\begin{aligned}\psi_\mu^{(\rho)}(x) &= \frac{\partial A_\mu^{(I)}(x)}{\partial \rho} \\ &= \frac{4}{g}\frac{\rho\,\bar{\eta}_{a\mu\nu}\,x^\nu}{(x^2+\rho^2)^2}\frac{\lambda^a}{2}\end{aligned} \tag{5.24}$$

This zero mode already is in the background gauge, since

$$D_\mu^{(I)}\psi^{(\rho)\,\mu}(x) = \partial_\mu\psi^{(\rho)\,\mu}(x) - \mathrm{i}g\left[A_\mu^{(I)}, \psi^{(\rho)\,\mu}(x)\right] = 0 \tag{5.25}$$

Translation Zero Mode

To obtain the translation zero mode we first must include the translation parameter z_μ, i.e. the instanton position, in the instanton gauge potential. The instanton field is then given by

$$A_\mu^{(I)}(x,z) = \frac{2}{g}\frac{\rho^2\bar{\eta}_{a\mu\nu}(x-z)^\nu}{(x-z)^2((x-z)^2+\rho^2))}\frac{\lambda^a}{2}. \tag{5.26}$$

When differentiating $A_\mu^{(I)}(x,z)$ with respect to z_ν the translation zero mode becomes

$$\begin{aligned}\psi_\mu^{(z)}(\nu,x) &= \frac{\partial A_\mu^{(I)}(x,z)}{\partial z^\nu}\Big|_{z=0} + D_\mu(A_\nu(x)) \\ &= -\partial_\nu A_\mu^{(I)}(x) + \partial_\mu A_\nu^{(I)}(x) + \mathrm{i}g[A_\mu(x), A_\nu(x)] \\ &= -\frac{8}{g}\frac{\rho^2}{(\rho^2+x^2)^2}\left[\frac{x_\mu x^\sigma}{x^2} - \frac{1}{4}\delta_\mu^\sigma\right]\bar{\eta}_{a\nu\sigma} - (\mu \leftrightarrow \nu) \\ &= F_{\mu\nu}(x).\end{aligned} \tag{5.27}$$

The term $D_\mu\left(A_\nu(x)\right)$ is necessary to bring the translation mode into background gauge. It is chosen such that the translation zero mode appears as the *field strength tensor* fulfilling the equations of motion,

$$D_\mu^{(I)}F^{\mu\nu}(x) = 0. \tag{5.28}$$

[2]The internal indices of the U-matrices are supressed in the above equation.

Colour Zero Modes in $SU(3)$

In case of the gauge zero modes the collective coordinates correspond to the parameters of the rotation in the space of the gauge group $SU(3)$. The orientation of an instanton in $SU(3)$ can be described as

$$A_\mu^{(I)}(G) = G^{-1} A_\mu^{(I)} G, \tag{5.29}$$

where G is an element of the group. It is sufficient to consider infinitesimal changes in G with parameters $\mathrm{d}t_i$,

$$G + \delta G = \left(\mathbb{I} - \mathrm{i}\mathrm{d}t^i \lambda_i\right) G, \qquad i = 1, \ldots, 8. \tag{5.30}$$

λ_i are the generators of the gauge group. In our representation they correspond to the eight Gell-Mann matrices. The seven[3] gauge zero modes are then

$$\psi_\mu^{(k)}(x) = \frac{\partial A_\mu^{(I)}[G]}{\partial t^k} = -\mathrm{i}\, G^{-1} \left[A_\mu^{(I)}, \lambda_k\right] G, \tag{5.31}$$

where $k = 1, \ldots, 7$. These modes are not in the background gauge. However, we can bring them into the correct form by adding a term $D_\mu \Lambda^{(k)}$,

$$\psi_\mu^{(k)} = \frac{\partial A^{(I)}[G]_\mu}{\partial t^k} + D_\mu \Lambda^{(k)}, \tag{5.32}$$

with

$$\Lambda^{(k)} = \begin{cases} -\frac{1}{g}\left(\frac{\rho^2}{\rho^2+x^2}\right)\lambda^k, & k = 1,2,3 \\ \frac{1}{g}\left[\left(\frac{x^2}{\rho^2+x^2}\right)^{1/2} - 1\right]\lambda^k, & k = 4,5,6,7 \end{cases} \tag{5.33}$$

As one can see there appear two different kinds of gauge zero modes. This is because the generators λ_i, $i = 1 \ldots 7$, of the gauge group $SU(3)$ form two different kinds of multiplets under the action of $SU(2)$. We will denote the colour zero modes generated by λ_a, where a runs from 1 to 3, as $\psi_\mu^{(a)}(x)$, whereas the colour zero modes generated by λ_α with α running from 4 to 7 will be called $\psi_\mu^{(\alpha)}(x)$. We find for the colour zero modes generated by λ_a

$$\begin{aligned} \psi_\mu^{(a)}(x) &= D_\mu\left(\frac{\lambda^a}{g}\frac{x^2}{x^2+\rho^2}\right) \\ &= \frac{\rho^2}{g(x^2+\rho^2)^2}\Big(2x_\mu\lambda^a - i\,\bar{\eta}_{b\mu\nu}x^\nu\,[\lambda^b, \lambda^a]\Big). \end{aligned} \tag{5.34}$$

[3]The number of colour zero modes is seven instead of eight because the generator λ_8 commutes with λ_1 to λ_3, see Sect. 5.1.

The colour zero modes $\psi_\mu^{(\alpha)}(x)$ are given by

$$\begin{aligned}\psi_\mu^{(\alpha)} &= D_\mu\left(\frac{\lambda_\alpha}{g}\Big(\frac{x^2}{x^2+\rho^2}\Big)^{1/2}\right)\\ &= \frac{\rho^2}{g}\frac{1}{(x^2)^{1/2}(x^2+\rho^2)^{3/2}}\big(x^\mu\lambda_\alpha - i\,\bar\eta_{b\mu\nu}\,x^\nu[\lambda^b,\lambda_\alpha]\big).\end{aligned} \tag{5.35}$$

In the above equations the Latin indices a and b run from 1 to 3 and the Greek indices μ and ν are space-time indices running from 1 to 4, whereas the Greek index α is an internal index running from 4 to 7.

Total zero mode fraction

Now we are ready to compute the total contribution to the functional integral coming from the zero modes. From Eq. (5.13) we know that this is the product of the normalisation integrals of the zero modes[4] [41]:

$$J(\gamma) = \left(\prod_i \frac{1}{\sqrt{2\pi}}\right)(\det U)^{1/2}, \tag{5.36}$$

where

$$U_{ij} = \langle\psi^{(i)},\psi^{(j)}\rangle = 2\int \mathrm{d}^4x\,\mathrm{Tr}\left[\psi_\mu^{(i)}\psi^{(j)\,\mu}\right] \tag{5.37}$$

The computation of the normalisation integrals can be found in the Appendix C. Here only the results are quoted. For the dilatation zero mode we find

$$\|\psi^{(\rho)}(x)\| = \frac{4\pi}{g}. \tag{5.38}$$

Of course we obtain the instanton action for the normalisation integral of the translation zero mode and thus

$$\|\psi^{(z)}(x)\| = \frac{2\sqrt{2}\pi}{g}. \tag{5.39}$$

[4] Actually this is a simplification. However, provided that the gauge transformation Λ, necessary to bring the zero mode into the background gauge, vanishes sufficiently rapidly at large distances, i.e. $\Lambda\psi_\mu < \mathcal{O}\left(1/|x|^3\right)$, the above relation, Eq. (5.36), is correct. This is the case for all our zero modes. See [41] for details.

The normalisation integrals for the colour zero modes $\psi^{(a)}(x)$ and $\psi^{(\alpha)}(x)$ depend on the instanton size ρ:

$$\|\psi^{(a)}(x)\| = \frac{4\pi}{g}\rho \tag{5.40}$$

$$\|\psi^{(\alpha)}(x)\| = \frac{2\sqrt{2}\pi}{g}\rho \tag{5.41}$$

Finally we find for the total zero mode contribution [41]

$$\begin{aligned} J(\gamma) &= \left(\prod_i \frac{1}{\sqrt{2\pi}}\right)(\det U)^{1/2} \\ &= \frac{\|\psi^{(\rho)}\|\,\|\psi^{(z)}\|^4\,\|\psi^{(a)}\|^3\,\|\psi^{(\alpha)}\|^4}{(2\pi)^6} \\ &= \frac{2^{14}\,\pi^6\,\rho^7}{g^{12}}. \end{aligned} \tag{5.42}$$

Generalisation to $SU(N_c)$

The generators of $SU(N_c)$ form one triplet (in the case of $SU(3)$ these were λ_1,λ_2,λ_3) and $2(N-2)$ doublets (realised by λ_4, λ_5,λ_6 and λ_7 in $SU(3)$) under the action of $SU(2)$, whereas all the other generators are singlets, see [41]. Thus there will be $4(N_c-2)$ additional generators of the form Eq. (5.35) to the eight zero modes coming from dilatation, translation and the first three colour zero modes of Eq. (5.34). The total number of colour zero modes corresponds to the $4N_c-5$ parameters [36] of the matrices $U^i_{\ \alpha}$ coupling spin and colour indices in Sect. 3.1. The result for the zero mode contribution in a $SU(N_c)$ gauge theory is then [41]

$$J(\gamma) = \frac{4}{\rho^5}\left(\frac{2\rho\sqrt{\pi}}{g}\right)^{4N_c}. \tag{5.43}$$

From the above equation we can see that the zero mode fraction is indeed a major part. In Eq. (3.41) we wrote down the size distribution including the zero mode and the non-zero mode part:

$$D(\rho)_{1-\text{loop}} \propto \rho^{\beta_o} = \rho^{\frac{11}{3}N_c} = \underbrace{\rho^{4\,N_c}}_{\text{ZM part}} \cdot \underbrace{\rho^{-\frac{1}{3}N_c}}_{\text{non-ZM part}} \tag{5.44}$$

The factor $\rho^{-\frac{1}{3}N_c}$ is small compared to $\rho^{4\,N_c}$ in the region we are interested, which is $\rho_{\text{peak}} \sim 0.5$ fm.

5.4 Results for the zero mode part under inversion

In Sect. 4.3.1 it was seen that the space-time inversion is a conformal transformation. We have to apply the transformation laws of Eq. (4.18) for the dilatation and colour zero modes, since these are clearly vector fields:

$$\begin{aligned}\psi'^{(\rho)}_{\mu}(x') &= \sqrt{\sigma_{\rm inv}(x)} I_{\mu}{}^{\nu}(x) \psi^{(\rho)}_{\nu}(x) \\ &= \frac{2}{g} \frac{\rho'^3}{\rho^2_{\rm peak}} \frac{1}{\left(\rho'^2 + x'^2\right)^2} x'^{\nu} \bar{\eta}_{a\mu\nu} \lambda^a, \end{aligned} \tag{5.45}$$

$$\psi'^{(a)}_{\mu}(x') = \frac{1}{g} \frac{\rho'^2}{\left(\rho'^2 + x'^2\right)^2} \left(-2x'_{\mu} \lambda_a - i\, \bar{\eta}_{b\mu\nu}\, x'^{\nu} \left[\lambda^b, \lambda_a\right] \right), \tag{5.46}$$

$$\psi'^{(\alpha)}_{\mu}(x') = \frac{1}{g} \frac{1}{x'^2} \frac{\rho'}{\left(\rho'^2 + x'^2\right)^{3/2}} \left(-x'_{\mu} \lambda_{\alpha} - i\, \bar{\eta}_{b\mu\nu}\, x'^{\nu} \left[\lambda^b, \lambda_{\alpha}\right] \right). \tag{5.47}$$

In the case of the translation zero modes, having the form of the field strength tensor, the correct choice of the transformation law is a delicate question [76]. We assume that these modes transform not like a tensors (Eq. (4.21)), but rather as *four vector fields* under conformal transformations.

$$\begin{aligned}\psi'^{(z)}_{\mu}(\nu; x') &= \sqrt{\sigma_{\rm inv}(x)} I_{\mu}{}^{\nu}(x) \psi^{(z)}_{\nu}(\nu; x) \\ &= \frac{8}{g} \frac{\rho'^2}{\rho^2_{\rm peak}} \frac{x'^2}{\left(\rho'^2 + x'^2\right)^2} \left(\frac{1}{2} \bar{\eta}_{a\nu\mu} + \frac{x'_{\nu} x'^{\sigma}}{x'^2} \bar{\eta}_{a\mu\sigma} \right) \end{aligned} \tag{5.48}$$

Let us now quote the results for the normalisation integrals of the *inverted* dilatation zero modes $\psi'^{(\rho)}_{\mu}(x')$ and the inverted colour zero mode $\psi'^{(a)}_{\mu}(x')$:

$$\| \psi'^{(\rho)}_{\mu}(x') \| = \frac{4\pi}{g} \frac{\rho^2_{\rm peak}}{\rho^2} = \frac{4\pi}{g} \frac{\rho'}{\rho} \tag{5.49}$$

$$\| \psi'^{(a)}_{\mu}(x') \| = \frac{4\pi}{g} \frac{\rho^2_{\rm peak}}{\rho} = \frac{4\pi}{g} \rho' \tag{5.50}$$

Like in the last section the explicit integrals can be found in Appendix C. Unfortunately there occurs a problem in the case of the inverted translation zero mode $\psi'^{(z)}_{\mu}(x')$ and the inverted

colour zero mode $\psi_\mu'^{(\alpha)}(x')$. They turn out to be *divergent*.

$$\langle \psi_\mu'^{(z)}(x'), \psi_\mu'^{(z)}(x') \rangle = \frac{2\pi^2 \rho_{\text{peak}}^4 \rho^4 48}{g^2} \underbrace{\int_0^\infty \mathrm{d}R \, \frac{1}{R} \frac{1}{(\rho^2 + R^2)^4}}_{\to \infty} \tag{5.51}$$

$$\langle \psi_\mu'^{(\alpha)}(x'), \psi_\mu'^{(\alpha)}(x') \rangle = \frac{2\pi^2 \rho_{\text{peak}}^4 \rho^4 16}{g^2} \underbrace{\int_0^\infty \mathrm{d}R \, \frac{1}{R} \frac{1}{(\rho^2 + R^2)^3}}_{\to \infty} \tag{5.52}$$

The divergence comes from the integration over $1/R$ at the point $R = 0$. This might be due to a mapping of infinity to zero by inversion. In the next chapter we go to a compact space, where one has to integrate over angles instead of the R-integration from 0 to ∞. We will show that by doing so one can solve the problem of these divergent normalisations.

Chapter 6

Introducing a New Scale

Now we come to the main chapter of this work. We start with a motivation for our approach in Sect. 6.1. In Sect. 6.2 we study the I-calculus on the surface of a 4-dimensional sphere. It is followed by the main part of this work, Sect. 6.3 , dealing with the projection of the zero modes onto the $\mathcal{S}_4$ sphere. We finish this chapter with consistency checks for our approach in Sect. 6.4.

6.1 Motivation

The breaking of the dilatation

As pointed out in Sect. 4.3.1, the inversion has an exceptional role within the conformal group, since the inversion together with the translation composes both the special conformal transformation and the dilatation [69, 70],

$$\begin{aligned} \mathcal{D}_{a^2/b^2} = \mathcal{I}_{a^2}\,\mathcal{I}_{b^2}: \quad x^\mu \to x'^\mu \to y^\mu &= \frac{a^2}{x'^2} x'^\mu \\ &= \frac{a^2}{b^2} x^\mu \\ &= \lambda x^\mu \end{aligned} \tag{6.1}$$

The latter is very important in the course of our investigations. In Chapter 2 and Sect. 4.1 we have seen, that the I-size distribution extracted from lattice data shows a sharp maximum at $\rho_{\text{peak}} \simeq 0.5$ fm. The peak position $\rho_{\text{peak}} \simeq 0.5$ corresponds to a characteristic length scale of the I-calculus that has not been present so far. Up to now it is neither understood where this scale comes from nor what is the mechanism behind the rapid break-down of I-perturbation theory. As already pointed out in Sect. 2, in this work we follow the approach of a residual symmetry

under conformal inversion,

$$x_\mu \to x'_\mu = \frac{\rho_{\text{peak}}}{x^2} x_\mu, \tag{6.2}$$

leading to this characteristic shape of the size-distribution. In that context the inversion radius plays a crucial role. Is not to be seen as a continuous parameter of the transformation of Eq. (6.2), but rather as a *fixed* physical value related to the average size of an instanton. The radius of inversion corresponds to the length scale ρ_{peak} indicated by the lattice data.

As a consequence of this new scale the dilatation symmetry clearly must be broken. This can be seen by the following consideration: If the radius of inversion is allowed to take one, physically distinguished, value only, i.e. $a = b = \rho_{\text{peak}}$, then the dilatation parameter λ has to be equal to one. An invariance under dilatations is not possible anymore, the symmetry must be broken. However, a symmetry under special conformal transformations as well as transformations under the Lorentz group might be preserved. It is worthwhile to mention that the above breaking should be distinguished from the well-known breaking of conformal symmetry via the renormalisation procedure which introduces yet another scale, the renormalisation scale μ_{r}.

It should be noted that the this new scale corresponding to the radius of inversion is not present in the conventional I-calculus. Thus one of our main aims is to introduce ρ_{peak} into the theory of instantons. This is what will be done in the following sections.

(Non-)Invariance under $O(5)$

Let us return for a short moment to the problem that occurred at the end of the last chapter. There we have found that the normalisation integral for the zero modes $\psi'^{(z)}(x')$ and $\psi'^{(\alpha)}(x')$, Eq. (5.51) and (5.52), after a conformal space-time inversion are divergent for the integration limit R going to zero. This problem will be solved by projecting the 4-dimensional Euclidean space onto the surface of a sphere embedded in 5-dimensional Euclidean space [77, 78], where an additional "geometry" factor will appear in the normalisation integrals having the effect of a regulator. The reason being that the sphere is a *compact* and curved manifold.

Actually there exists a whole formalism for the $SU(2)$-instanton calculus on a hypersphere developed by Jackiw and Rebbi, see [26]. The motivation for this formalism was the following observation: The combined instanton anti-instanton field of Eq. (4.26) is invariant under $O(5)$ transformations in Euclidean space. This can be seen by the consideration below.

The $I\bar{I}$-solution of Eq. (4.26) is invariant under a combined space and gauge rotation generated by $J^{\mu\nu}$ in 4-dimensional Euclidean space,

$$J^{\mu\nu} = M^{\mu\nu} + \Sigma^{\mu\nu}, \tag{6.3}$$

where $M^{\mu\nu}$ are the generators of rotations and the Σ-matrices are

$$\Sigma^{\mu\nu} = \frac{1}{4\mathrm{i}} \begin{pmatrix} \sigma^{\mu\nu} & 0 \\ 0 & \bar{\sigma}^{\mu\nu} \end{pmatrix}, \tag{6.4}$$

see Eq. (4.27). Moreover the $I\bar{I}$- solution of Eq. (4.26) is invariant under a combination of translation and special conformal transformation generated by $R^\mu = \frac{1}{2}(K^\mu + P^\mu)$ plus an additional gauge transformation,

$$\mathcal{R}^\mu = R^\mu + \Sigma^{\mu\nu} x_\nu. \tag{6.5}$$

It turns out that the commutation relations for these modified generators $J^{\mu\nu}$ and $\mathcal{R}^\mu$ follow that of $M^{\mu\nu}$ and R^μ. This means, that the algebra closes on $O(5)$. Thus the idea of Jackiw and Rebbi was to formulate the theory in an $O(5)$-covariant fashion.

The advantage of this formulation lies e.g. in the much easier computation of the one-loop amplitude [26, 79, 80, 81]. However, an $O(5)$-covariant theory of instantons is only possible if one chooses the radius of the sphere to be equal to the size of the instanton ρ.

In this chapter we will study the $O(5)$ formalism carefully and adopt it to our needs. The crucial difference in our approach lies in the radius of the sphere. In contrast to what has been done in the past, the radius of the sphere we consider corresponds to the average instanton size ρ_{peak}.

The radius of the sphere equals the radius of inversion: $b = \rho_{\text{peak}}$. This new description offers a solution for one of our main tasks: We will achieve the introduction of the *desired scale* ρ_{peak} into the instanton calculus by *taking the radius of the sphere to be equal to the fixed parameter* ρ_{peak}.

The limits $\rho/\rho_{\text{peak}} \to 0$ and ∞, respectively, will be very instructive and thus studied carefully. Due to a ρ/ρ_{peak} scaling, smaller sized instantons on the sphere can be studied by either considering the limit of a sphere with infinite radius, i.e. $\rho_{\text{peak}} \to \infty$, or by investigating $\rho \to 0$ while ρ_{peak} is fixed. By this we can check the consistency of our formulation with respect to the results from Euclidean space. The behaviour of larger instantons on the sphere can be analysed by looking at either a decreasing radius ρ_{peak} or an increasing instanton size ρ.

However, we will not keep $O(5)$-invariance for two reasons. First of all because an $O(5)$-invariance cannot be maintained if the radius of the sphere differs from the radius of the instanton ρ. Secondly we will work with $SU(3)$-instantons for which an $O(5)$-invariant formalism does not exist anyway, since the gauge group $SU(3)$ is too large.

At the end of this chapter we will consider two more cases, which allow for important checks of our approach:

The radius of the sphere equals the instanton size: $b = \rho$. This allows for contact to existing works and consistency tests for our calculations.

The radius of the sphere equals the inverted instanton size: $b = \rho' = \frac{\rho_{\text{peak}}^2}{\rho}$. In that case the connection to the results for the inverted zero mode part can be made.

6.2 The stereographic projection

Let us study first how the instanton calculus can be "lifted" onto the 4-dimensional surface of a 5-dimensional sphere. This is done via *stereographic projection* [77, 78], which is defined by the following active transformation, see Fig. 6.1,

$$\mathcal{P}_b : \quad x_\mu \to r_a = (r_\lambda, r_5)\,, \tag{6.6}$$

where

$$\begin{aligned} r_\lambda &= b\,\frac{2\,b^2\,x_\lambda}{b^2+x^2}, \\ r_5 &= b\,\frac{b^2-x^2}{b^2+x^2}. \end{aligned} \tag{6.7}$$

From now on we will use Latin indices for the 5-dimensional space whereas the Greek indices run as usual from $1\ldots4$.

In Fig. 6.1 a mapping of the two-dimensional Euclidean space onto the surface $\mathcal{S}_2$ of a three-dimensional sphere via stereographic projection is depicted. In the above definition of the stereographic projection the 4-dimensional Euclidean space is placed in the equatorial-plane, $r_5 = 0$, of the 5-dimensional sphere. A point P of the 4d-Euclidean space is projected onto the sphere $\mathcal{S}_4$ by following a straight line g from the south pole S through the point P. The intersection point of the straight line g and the sphere gives the projected point P′.

The radius squared of the sphere is given by

$$r_a\,r^a = b^2, \tag{6.8}$$

which is a constraint on the transformation of Eq. (6.6) necessary to reduce the degrees of freedom to four. At this point b is still an arbitrary scale.

The active transformation of Eq. (6.7) is a conformal transformation,

$$\begin{aligned} g_{\mu\nu}(x) &= \frac{\partial r^a}{\partial x^\mu}\frac{\partial r^b}{\partial x^\nu}\delta_{ab} \\ &= \frac{4b^4}{(b^2+x^2)^2}\delta_{\mu\nu}. \end{aligned} \tag{6.9}$$

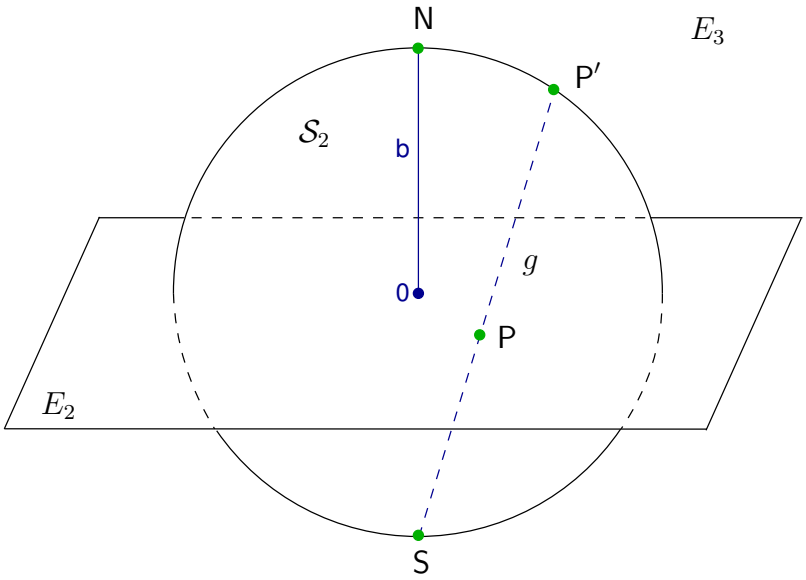

Figure 6.1: Stereographic projection of the two-dimensional Euclidean space onto a two-dimensional sphere $\mathcal{S}_2$ embedded in a 3-dimensional Euclidean space E_3. The Euclidean space E_2 is illustrated via the equatorial-plane. A point P of the Euclidean space E_2 is projected to the point P′ on the sphere $\mathcal{S}_2$ by drawing a straight line g from the south pole S through P subtending the sphere at the point P′.

Its scale factor is

$$\sigma(x)_{\text{sp}} = \frac{(b^2 + x^2)^2}{4b^4}. \tag{6.10}$$

6.2.1 5-dimensional spherical coordinates

In order to compute the relation of the area element on the sphere and the volume element in Euclidean space we have to introduce spherical coordinates,

$$\begin{aligned} r_1 &= b\, \sin\psi \sin\phi \sin\theta \sin\alpha, \\ r_2 &= b\, \sin\psi \sin\phi \sin\theta \cos\alpha, \\ r_3 &= b\, \sin\psi \sin\phi \cos\theta, \\ r_4 &= b\, \sin\psi \cos\phi, \\ r_5 &= b\, \cos\psi, \end{aligned} \tag{6.11}$$

where

$$\begin{aligned} \alpha &\in [0, \pi], \\ \theta &\in [0, \pi], \\ \phi &\in [0, 2\,\pi), \\ \psi &\in [0, \pi]. \end{aligned} \tag{6.12}$$

The volume element is given by

$$\mathrm{d}^5 r = b^4 \, \sin\psi^3 \sin\phi^2 \sin\theta \mathrm{d}b \, \mathrm{d}\psi \, \mathrm{d}\phi \, \mathrm{d}\theta \, \mathrm{d}\alpha. \tag{6.13}$$

Thus we can read of the area element of a sphere with radius b

$$\mathrm{d}A\big|_b = b^4 \, \sin\psi^3 \sin\phi^2 \sin\theta \, \mathrm{d}\psi \, \mathrm{d}\phi \, \mathrm{d}\theta \, \mathrm{d}\alpha. \tag{6.14}$$

The relation between the 4-dimensional Euclidean volume element and the area element on the hypersphere turns out to be quite remarkable:

$$\begin{aligned} \mathrm{d}A\big|_b &= \frac{16\, b^8}{(b^2 + x^2)^4} \mathrm{d}^4 x \\ &= \frac{1}{\sigma(x,b)^2_{\mathrm{sp}}} \mathrm{d}^4 x, \end{aligned} \tag{6.15}$$

where $\sigma(x,b)^2_{\mathrm{sp}}$ plays the role of a geometry factor. The proof is given below. Surprisingly, we find that the factor $\frac{16\, b^8}{(b^2+x^2)^4}$ corresponds to the Lagrange density of the instanton,

$$\mathcal{L} = -\frac{1}{2} \, \mathrm{Tr} \, [F_{\mu\nu} F^{\mu\nu}] = -\frac{8}{g^2} \frac{6\, \rho^4}{(\rho^2 + x^2)^4}, \tag{6.16}$$

in 4-dimensional space for the case of $b = \rho$ apart from a numerical factor.

We have obtained $\mathrm{d}A$ as follows. First we consider the transformation of x_μ to r_μ and compute the volume element.

$$\mathrm{d}^4 r \equiv \mathrm{d}r_1 \, \mathrm{d}r_2 \, \mathrm{d}r_3 \, \mathrm{d}r_4 = \frac{16\, b^8 (b^2 - x^2)}{(b^2 + x^2)^5} \mathrm{d}^4 x \tag{6.17}$$

The relation between $\mathrm{d}r_{(4)}$ and the volume element in spherical coordinates is

$$\begin{aligned} \mathrm{d}^4 r &= b^4 \sin^3\psi \sin^2\phi \sin\theta \cos\psi \, \mathrm{d}A \, \mathrm{d}\theta \, \mathrm{d}\phi \, \mathrm{d}\psi \\ &= \cos\psi \, \mathrm{d}A\big|_b \\ &= \frac{b^2 - x^2}{b^2 + x^2} \, \mathrm{d}A\big|_b. \end{aligned} \tag{6.18}$$

Plugging this into Eq. (6.17) gives the desired result Eq. (6.15).

6.2.2 Projection of vector fields onto the sphere

To project the I-calculus onto the sphere one must know how to "lift" the I-vector potentials to the surface of the sphere. In what follows we will derive the transformation laws for vector fields under stereographic projection in general. This is done by applying the usual rules for conformal transformations of vector fields, see Sect. 4.3.1. Later we will consider the special case of the I-vector potential and, most importantly for our approach, the case of the zero modes in Sect. 6.3.

Let us start with the active transformation law for *contravariant* vector fields.

$$\widehat{A}^a = \sigma(x)_{\rm sp} \frac{\partial r^a}{\partial x^\mu} A^\mu(x), \tag{6.19}$$

with

$$\begin{aligned} \widehat{A}^\lambda(r) &= \frac{b^2+x^2}{2b^2} A^\lambda - \frac{x\cdot A}{b^2} x^\lambda, \\ \widehat{A}^5(r) &= -\frac{x\cdot A}{b}. \end{aligned} \tag{6.20}$$

Comparison of this result with references [26] and [82] shows agreement if the radius of the sphere corresponds to size of instantons, i.e. $b=\rho$.

When it comes to the transformation laws for the *covariant* vector fields one has to be careful. The application of the transformation law of Eq. (4.19) in Sect. 4.3.2 does not work. The reason is that the operator $\frac{\partial}{\partial r^a}$ cannot be naively applied, precisely because the constraint $r_a r^a = b^2$ is not included yet. This problem has not occurred for the contravariant vector fields since the differential operator $\frac{\partial}{\partial x^\mu}$ is well-defined. There no reduction of the degrees of freedom is necessary. Since we want to stay on the surface of the sphere, only the angular derivatives must appear. They are given by the angular momentum operators [77],

$$L_{ab} = -i\left(r_a \frac{\partial}{\partial r^b} - r_b \frac{\partial}{\partial r^a}\right) \tag{6.21}$$

Therefore we have to replace the differential operator $\frac{\partial}{\partial r^a}$ by the operator l_a [82],

$$\begin{aligned} l_a &= i\, r^b L_{ba} \\ &= \frac{\partial}{\partial r^a} - \frac{1}{b^2} r_a \left(r\cdot\partial\right). \end{aligned} \tag{6.22}$$

For the transformation of the covariant vector fields we then obtain

$$\widehat{A}_a(r) = l_a(x^\mu) A_\mu, \tag{6.23}$$

with

$$\begin{aligned}\widehat{A}_\lambda(r) &= \frac{b^2+x^2}{2b^2}A_\lambda - \frac{x\cdot A}{b^2}x_\lambda,\\ \widehat{A}_5(r) &= -\frac{x\cdot A}{b}.\end{aligned} \tag{6.24}$$

We find that co- and contravariant vector fields transform alike as we have expected. For the contraction of the vector fields we get

$$\widehat{A}_a(r)\widehat{A}^a(r) = \sigma(x)_{\rm sp}\, A_\mu(x)A^\mu(x), \tag{6.25}$$

i.e. the length is stretched by the scale factor $\sigma(x)_{\rm sp}$. The equations (6.19) and (6.23) obey the constraint

$$r_a\widehat{A}^a(r) = 0, \tag{6.26}$$

which is necessary to reduce the degrees of freedom from five to four. The stereographic projection is done in such a way that this constraint comes naturally with the transformation rules to ensure that the projected vector fields indeed stay on the sphere.

The instanton field in $O(5)$-covariant fashion

Since we know how to project vector fields, we are able to lift the I-vector potential onto the sphere. In the case of $b=\rho$, i.e. the radius of the sphere is equal to the I-size, it is possible to write the $I\bar{I}$-potential in an $O(5)$ covariant fashion, because the $I\bar{I}$-solution of Eq. (4.26) is invariant under $O(5)$ transformations, see Sect. 6.1. In order to do so, one has to extend the matrix representation of the gauge group $O(4)$, defined by Eq. (4.27), to $O(5)$ by defining the matrix $\Sigma_{\mu 5}$

$$\Sigma_{\mu 5} = \frac{\gamma_\mu}{2}, \tag{6.27}$$

where γ_μ are the Dirac matrices in the chiral representation, see Appendix A. Then the antisymmetric representation $\Sigma_{ab} = -\Sigma_{ba}$ is isomorphic to the infinitesimal generators of the gauge group $O(5)$ [26]. After a rather lengthy but straight forward gauge transformation,

$$\widehat{A}'^{(I)}_a(r) \overset{b=\rho}{=} U^{-1}\widehat{A}^{(I)}_a(r)U + U^{-1}\mathrm{i}r^b L_{ab}U, \tag{6.28}$$

where

$$U(r) = \frac{\rho - 2\Sigma_{\mu 5}x^\mu}{(\rho^2+x^2)^{1/2}}, \tag{6.29}$$

we end up with the required form for the $I\bar{I}$-solution,

$$\widehat{A}'^{(I)}_a(r) = \frac{1}{g}\,\Sigma_{ab} r^b, \tag{6.30}$$

in agreement with [26]. The $I\bar{I}$-configuration of Eq. (6.30) looks indeed very simple. The dependence on the collective coordinates is not visible. The whole dynamics seems to be put into the area element $\mathrm{d}A$ which includes the geometry factor $\sigma(x)_{\mathrm{sp}}$. Let us stress again that this is only possible in the case of $\rho = b$, i.e. when no new scale is introduced.

6.2.3 Projection of second-order tensor fields onto the sphere

The transformation law for a general second order *contravariant* tensor under an active conformal transformation is straight forward:

$$\widehat{F}^{ab}(r) = \sigma^2(x)_{\mathrm{sp}}\,\frac{\partial r^a}{\partial x^\mu}\frac{\partial r^b}{\partial x^\nu}F^{\mu\nu}(x) \tag{6.31}$$

The individual components of the tensor are here

$$\left(\widehat{F}\right)^{ab} = \begin{pmatrix} \left(\widehat{F}\right)^{\lambda\sigma} & \left(\widehat{F}\right)^{\lambda 5} \\ \left(\widehat{F}\right)^{5\sigma} & \left(\widehat{F}\right)^{55} \end{pmatrix}. \tag{6.32}$$

Since we are mainly interested in the field strength tensor later on, we will restrict ourselves from now on to antisymmetric second-order tensors, i.e. $F^{ab} = -F^{ba}$ with

$$\begin{aligned}
\widehat{F}^{\lambda\sigma}(r) &= \sigma(x)^2_{\mathrm{sp}}\frac{\partial r^\lambda}{\partial x^\mu}\frac{\partial r^\sigma}{\partial x^\nu}F^{\mu\nu}(x) \\
&= \sigma(x)_{\mathrm{sp}}\left[F^{\rho\sigma}(x) - \frac{1}{\sqrt{\sigma(x)_{\mathrm{sp}}}}\frac{x^\rho}{b^2}x_\mu F^{\mu\sigma} - \frac{1}{\sqrt{\sigma(x)_{\mathrm{sp}}}}\frac{x^\sigma}{b^2}x_\nu F^{\lambda\nu}\right], \\
\widehat{F}^{\lambda 5}(r) &= \sigma(x)^2_{\mathrm{sp}}\frac{\partial r^\lambda}{\partial x^\mu}\frac{\partial r^5}{\partial x^\nu}F^{\mu\nu}(x) \\
&= -\sqrt{\sigma(x)_{\mathrm{sp}}}\frac{x_\nu}{b}F^{\lambda\nu}(x) = -\widehat{F}^{5\lambda}(r), \\
\widehat{F}^{55}(r) &= \sigma(x)^2_{\mathrm{sp}}\frac{\partial r^5}{\partial x^\mu}\frac{\partial r^5}{\partial x^\nu}F^{\mu\nu}(x) = 0.
\end{aligned} \tag{6.33}$$

Therefore we get

$$F^{\lambda\sigma}(x) = \frac{1}{\sigma(x)_{\mathrm{sp}}}\left[\widehat{F}^{\lambda\sigma}(r) - \frac{x^\rho}{b}\widehat{F}^{5\sigma} - \frac{x^\sigma}{b}\widehat{F}^{\lambda 5}(r)\right]. \tag{6.34}$$

Eq. (6.34) agrees with Ref. [77].

An active transformation of a second order *covariant* tensor is done as follows. We replace the operator $\frac{\partial}{\partial r^a}$ by $l_a = \mathrm{i} r^b L_{ba}$. We find

$$\widehat{F}_{ab}(r) = l_a(x^\mu)\; l_b(x^\nu) F_{\mu\nu}(x) \tag{6.35}$$

with

$$\begin{aligned}
\widehat{F}_{\lambda\sigma}(r) &= \sigma(x)_{\mathrm{sp}} \left[F_{\lambda\sigma}(x) - \frac{1}{\sqrt{\sigma(x)_{\mathrm{sp}}}} \frac{x_\lambda}{b^2} x^\mu F_{\mu\sigma}(x) - \frac{1}{\sqrt{\sigma(x)_{\mathrm{sp}}}} \frac{x_\sigma}{b^2} x^\nu F_{\lambda\nu}(x) \right], \\
\widehat{F}_{\lambda 5}(r) &= -\sqrt{\sigma(x)_{\mathrm{sp}}} \frac{x^\nu}{b} F_{\lambda\nu} = -\widehat{F}_{5\lambda}(r), \\
\widehat{F}_{55}(r) &= 0.
\end{aligned} \tag{6.36}$$

Again co- and contravariant components transform alike. The contracted tensors are stretched by a factor $\sigma(x)^2_{\mathrm{sp}}$.

In analogy to the case of vector fields (Eq.(6.26) also antisymmetric second-order tensors fulfil a constraint. It is

$$r_a \widehat{F}^{ab} = 0. \tag{6.37}$$

Thus the number of free parameters for $F_{ab}(r)$ is ten which is equivalent to the number of degrees of freedom of $F_{\mu\nu}(x)$.

The above relations are valid for general antisymmetric second-order tensors on the sphere. It is worthwhile to mention that it is not clear whether the field strength tensor of the Euclidean space $F_{\mu\nu}(x)$ keeps its tensor-property when projected onto a sphere with a radius that differs from the I-size, i.e. $b \neq \rho$. Due to the breaking of dilatation in that case also the tensor-characteristics might be lost, which means that $F_{\mu\nu}(x)$ would transform as four vector fields under a stereographic projection of Eq. (6.6). Invariance of the action under that transformation would not be guaranteed anymore:

$$\begin{aligned}
S_{\mathcal{S}_4} &= \frac{1}{2} \int \mathrm{d}A\big|_b \,\mathrm{Tr}\left[F^{(I)}_{ab}(r) F^{ab\,(I)}(r) \right] \\
&= \frac{1}{2} \int \mathrm{d}^4x \frac{1}{\sigma^2(x)_{\mathrm{sp}}} \,\sigma(x)_{\mathrm{sp}}\, \mathrm{Tr}\left[F^{(I)}_{\mu\nu}(x) F^{\mu\nu\,(I)}(x) \right] \\
&= \frac{1}{2} \int \mathrm{d}^4x \frac{1}{\sigma(x)_{\mathrm{sp}}} \,\mathrm{Tr}\left[F^{(I)}_{\mu\nu}(x) F^{\mu\nu\,(I)}(x) \right] \\
&\neq S_{\mathrm{E}}.
\end{aligned} \tag{6.38}$$

The field strength tensor in $O(5)$-covariant fashion

It is possible to write the field strength tensor in $O(5)$-covariant form being then a totally antisymmetric rank-three tensor [77, 26] in case of a sphere with radius equal to the size of instantons, i.e. $b = \rho$,

$$F^{(I)}_{abc}(r) = \frac{1}{\rho}\left(\mathrm{i}\, L_{ab}\widehat{A}^{(I)}_c + r_a\left[\widehat{A}^{(I)}_b, \widehat{A}^{(I)}_c\right]\right) \quad + \text{cyclic permutations of } a, b, c. \tag{6.39}$$

After a gauge transformation $\widehat{F}'^{(I)}_{abc}(r) = U^{-1}(r)\, F^{(I)}_{abc}(r)\, U(r)$ with

$$U(r) = \frac{\rho - 2\Sigma_{\mu 5}x^\mu}{(\rho^2 + x^2)^{1/2}}, \tag{6.40}$$

the field strength tensor gets the simple form [82]

$$\widehat{F}'^{(I)}_{abc}(r) = \frac{\mathrm{i}}{\rho}\left(r_a\Sigma_{bc} + r_c\Sigma_{ab} + r_b\Sigma_{ca}\right), \tag{6.41}$$

which is dual to the rank-two tensor [77],

$$\widehat{F}^{(I)}_{ab} = \frac{1}{6}\epsilon_{abcde}F^{cde\,(I)}. \tag{6.42}$$

The I-action in that case is invariant since the conformal scale factor cancels with the factor coming from the Jacobian of the stereographic projection,

$$\begin{aligned} S_{\mathcal{S}_4} &= \frac{1}{2}\int \mathrm{d}A\big|_\rho \,\mathrm{Tr}\left[F^{(I)}_{ab}(r)F^{ab\,(I)}(r)\right] \\ &= \frac{1}{2}\int \mathrm{d}^4x \frac{1}{\sigma^2(x,\rho)_{\mathrm{sp}}}\,\sigma^2(x,\rho)_{\mathrm{sp}}\,\mathrm{Tr}\left[F^{(I)}_{\mu\nu}(x)F^{\mu\nu\,(I)}(x)\right] \\ &= \frac{1}{2}\int \mathrm{d}^4x\,\mathrm{Tr}\left[F^{(I)}_{\mu\nu}(x)F^{\mu\nu\,(I)}(x)\right] \\ &= S_{\mathrm{E}}. \end{aligned} \tag{6.43}$$

6.2.4 Normalisation integrals on the sphere

The purpose of this section is to prepare the necessary transformation rules for vector fields and their normalisation integrals transformed under an inversion in Euclidean space followed by a stereographic projection. This sequence of transformations will be used extensively in the next section for various special radii of the sphere, thus we give the general transformation rules at

this point. We start with quoting the behaviour of the conformal factor of the stereographic projection and of the area elements under conformal inversion in Euclidean space first. Throughout this section the radius of inversion is denoted by b,

$$\mathcal{I}_{b^2}: \quad x_\mu \to x'_\mu = \frac{b^2}{x^2} x_\mu \tag{6.44}$$

whereas d indicates the radius of the sphere,

$$\mathcal{P}_d: \quad x_\mu \to \begin{cases} r_\mu = d\,\frac{d^2-x^2}{d^2+x^2} \\ r_5 = d\,\frac{d^2-x^2}{d^2+x^2} \end{cases} . \tag{6.45}$$

Fields transformed under a stereographic projection of Eq. (6.45) are denoted by hats, the prime marks a quantity transformed under an inversion of Eq. (6.44).

The relation between the conformal factor of the stereographic projection at the point x_μ and the point $x'_\mu = \frac{b^2}{x^2} x_\mu$ is as follows

$$\begin{aligned} \sigma_{\rm sp}\,(x', d) &= \frac{\left(d^2 + x'^{\,2}\right)^2}{4\,d^4} \\ &= \frac{d'^{\,4}}{x^4} \frac{\left(d'^{\,2} + x^2\right)^2}{4\,d'^{\,4}} \\ &= \frac{d'^{\,4}}{b^4} \sigma^{-1}_{\rm inv}\,(b, x)\ \sigma_{\rm sp}\,(x, d')\,, \end{aligned} \tag{6.46}$$

where $d' = \frac{b^2}{d}$. Thus the area element defined in Eq. (6.14) of Sect. 6.2.1 transforms under a conformal inversion in Euclidean space as

$$\begin{aligned} \mathrm{d}A'\big|_d &\equiv \mathrm{d}^4x' \sigma^{-2}_{\rm sp}(d, x') \\ &= \frac{b^8}{d'^{\,8}} \mathrm{d}^4x \sigma^{-2}_{\rm sp}(d', x) \\ &= \frac{b^8}{d'^{\,8}} \mathrm{d}A\big|_{d'}. \end{aligned} \tag{6.47}$$

If the radius of inversion is equal to the radius of the five-dimensional sphere, i.e. $b = d = d'$, the area element is invariant,

$$\mathrm{d}A'\big|_b = \mathrm{d}A\big|_b. \tag{6.48}$$

For the radius of the sphere at the point x'_μ being equal to the instanton size ρ we find the following relation for the area element,

$$\mathrm{d}A'\big|_\rho = \frac{b^8}{\rho'^{\,8}} \mathrm{d}A\big|_{\rho'}, \quad \text{implying immediately} \quad \mathrm{d}A'\big|_{\rho'} = \frac{b^8}{\rho^8} \mathrm{d}A\big|_\rho. \tag{6.49}$$

Let us study normalisation integrals for vector fields $\widehat{B}(r)$, which are projected onto a sphere with radius d. They are defined by

$$\begin{aligned}\int \mathrm{d}A\big|_d \widehat{B}_a\,(r)\,\widehat{B}^a\,(r) &\equiv \int \mathrm{d}^4x\,\sigma_{\mathrm{sp}}^{-1}\,(x,d)\;B_\mu(x)B^\mu(x)\\ &= \int \mathrm{d}^4x\,\frac{4\,d^4}{\left(d^2+x^2\right)^2}B_\mu(x)B^\mu(x).\end{aligned} \tag{6.50}$$

We see that in the normalisation integral an additional conformal factor coming from the stereographic projection appears, which has the effect of a regulator. We will return to that issue in the next section.

We transform the vector field $B_\mu(x)$ in Euclidean space under a conformal inversion, see also Eq. (4.19),

$$B'^{\,\mu}(x') = \sqrt{\sigma(x,b)_{\mathrm{inv}}}\frac{\partial x'^\mu}{\partial x^\lambda}B^\lambda(x), \tag{6.51}$$

and project it onto a sphere with radius d by applying Eq. (6.19),

$$\widehat{B}'^{\,a}\,(r') = \sqrt{\sigma(x',d)_{\mathrm{sp}}}\frac{\partial r'^{\,a}}{\partial x^\mu}B'^{\,\mu}(x'). \tag{6.52}$$

The normalisation integral for $\widehat{B}'^{\,a}\,(r')$ is then given by

$$\begin{aligned}\int \mathrm{d}A'\big|_d\,\widehat{B}'_a\,(r')\,\widehat{B}'^{\,a}\,(r') &= \int \mathrm{d}A'\big|_d\;\sigma_{\mathrm{sp}}\,(x',d)\;B'_\mu(x')B'^{\,\mu}(x')\\ &= \frac{b^8}{d'^{\,8}}\frac{d'^{\,4}}{b^4}\int \mathrm{d}A\big|_{d'}\,\sigma(b,x)_{\mathrm{inv}}^{-1}\;\sigma_{\mathrm{sp}}\,(x,d')\;\sigma(b,x)_{\mathrm{inv}}\,B_\mu(x)B^\mu(x)\\ &= \frac{b^4}{d'^{\,4}}\int \mathrm{d}A\big|_{d'}\,\sigma_{\mathrm{sp}}\,(x,d')\;B_\mu(x)B^\mu(x)\\ &= \frac{b^4}{d'^{\,4}}\int \mathrm{d}A\big|_{d'}\widehat{B}_a\,(r)\,\widehat{B}^a\,(r)\,.\end{aligned} \tag{6.53}$$

Again we find invariance in case of equal radii for inversion and stereographic projection, i.e. $b = d = d'$.

6.3 Introduction of the new scale

We now come to the main part of this work. Let us begin with a summary of the important "corner stones" of our symmetry approach so far and give an outline on our forthcoming strategy.

We have shown in Sect. 4.3.3 that the instanton solution with radius ρ changes under an inversion in Euclidean space to an anti-instanton solution with radius ρ'. The idea of our symmetry approach is that this property might be "inherited" by the quantum level, i.e. by the I-size distribution $D(\rho)$. The reason being that a very important contribution to $D(\rho)$ comes from zero modes, which correspond precisely to the derivatives of the classical instanton field, showing the desired behaviour, with respect to the collective coordinates.

As we have pointed out in Sect. 5.2, in supersymmetric QCD the size distribution is determined by zero mode contributions only, the non-zero mode part cancels exactly to any order perturbation theory [74, 75]. In case of conventional QCD these contributions still form the dominant part, see Eq. (5.21) in Sect. 5.2. Thus our investigations focus on the zero mode part.

The lattice data, however, show the full instanton size distribution including both the zero mode contribution $J(\gamma)$ and the non-zero mode part $Q(\gamma)$. For a reasonable comparison of our calculations with these data, we have to pay attention to $Q(\gamma)$, as well. The non-zero mode part is given by the ratio of the functional determinants and is proportional to [6]

$$Q(\gamma) \sim \frac{1}{\rho \mu_{\mathrm{r}}}. \tag{6.54}$$

In our approach we assume that the non-zero mode part is not affected by a conformal inversion. We then might either divide it out by the factor $(\rho_{\mathrm{peak}}/\rho)^{(N_c/3)}$ in the lattice data [25] or include it in our considerations by multiplying with $(\rho_{\mathrm{peak}}/\rho)^{(N_c/3)}$.

However, when we were studying the behaviour of the zero mode contribution under inversion in Euclidean space we found that the normalisation integrals were divergent, see also Eqs. (5.51) and (5.52) in Sect. 5.4,

$$\begin{aligned}
\langle \psi_\mu'^{(z)}(x'), \psi_\mu'^{(z)}(x') \rangle &= \frac{2\pi^2 \rho_{\mathrm{peak}}^4 \rho^4 48}{g^2} \underbrace{\int_0^\infty \mathrm{d}R \, \frac{1}{R} \frac{1}{(\rho^2 + R^2)^4}}_{\to \infty} \\
\langle \psi_\mu'^{(\alpha)}(x'), \psi_\mu'^{(\alpha)}(x') \rangle &= \frac{2\pi^2 \rho_{\mathrm{peak}}^4 \rho^4 16}{g^2} \underbrace{\int_0^\infty \mathrm{d}R \, \frac{1}{R} \frac{1}{(\rho^2 + R^2)^3}}_{\to \infty},
\end{aligned} \tag{6.55}$$

due to the integration over $1/R$ at $R = 0$. Thus we need some kind of regulator mechanism.

Our solution to that issue is as follows. We compute the zero modes in Euclidean space first and then lift them by means of stereographic projection to a sphere with radius ρ_{peak}. In the last

section we have given the normalisation integrals for vector fields projected onto such a sphere. These integrals include a conformal factor $\sigma_{sp}(x)$, which has precisely the effect of a regulator as we will see later on. This is because the sphere is a compact manifold. Thus we can determine the zero mode part projected to the sphere and study its properties under conformal inversion.

Most importantly, the process of projection allows for the introduction of the new scale ρ_{peak}, which is indicated by the lattice data, into the theory. The average instanton size ρ_{peak} appears as the radius of the sphere. The radius of inversion equals then the radius of the sphere of stereographic projection.

The crucial question will be whether eventual symmetries under a space-time inversion turn into symmetries under an inversion of the I-size. After all this is the symmetry the lattice data seem to obey. In order to compare our results on the sphere with the lattice data we multiply the zero mode fraction on the sphere with ρ_{peak}/ρ in analogy to $1/(\rho\mu_{\text{r}})$ in Euclidean space coming from the non-zero mode part Q.

As before fields transformed under a stereographic projection are denoted by hats, e.g. $\widehat{\psi}(r)$, the prime labels quantities transformed under an inversion in Euclidean space, e.g. $\psi'(x')$.

Projection of the zero modes

The procedure described above is done straight forward in the case of the dilatation zero mode $\psi_\mu^{(\rho)}(x)$, and the colour zero modes $\psi_\mu^{(a)}(x)$ and $\psi_\mu^{(\alpha)}(x)$, since these are clearly vector fields.

In case of the translation zero mode $\psi_\mu^{(z)}(x)$ this is a more delicate affair, since so far it is not clear, whether these zero modes transform as four vector fields under the stereographic projection of Eq. (6.7) or as one tensor field. We assume, that they transform vector-field like.

For the normalisation integrals of the zero modes projected on the sphere we have to evaluate the following expression applying Eq.(6.50):

$$\begin{aligned}\left\langle \widehat{\psi}\left(r\right), \widehat{\psi}\left(r\right)\right\rangle_{\rho_{\text{peak}}} &\equiv \int \mathrm{d}A\big|_{\rho_{\text{peak}}} \operatorname{Tr}\left[\widehat{\psi}_a(r)\widehat{\psi}^a(r)\right] \\ &= \int \mathrm{d}^4x\, \sigma_{\text{sp}}^{-1}\left(\rho_{\text{peak}}, x\right) \operatorname{Tr}\left[\psi_\mu(x)\psi^\mu(x)\right] \\ &= \int \mathrm{d}^4x\, \frac{4\,\rho_{\text{peak}}^4}{\left(\rho_{\text{peak}}^2 + x^2\right)^2} \operatorname{Tr}\left[\psi_\mu(x)\psi^\mu(x)\right]\end{aligned} \tag{6.56}$$

Notice the additional conformal factor $\sigma_{\text{sp}}\left(\rho_{\text{peak}}, x\right)$, which was not included in the normalisation integrals in Euclidean space, which were given by

$$\langle \psi_\mu(x), \psi^\mu(x)\rangle = \int \mathrm{d}^4x \operatorname{Tr}\left[\psi_\mu(x)\psi^\mu(x)\right]. \tag{6.57}$$

We compare Eq. (6.56) to the normalisation integral of the inverted zero modes $\widehat{\psi'}(r')$ projected onto a sphere with radius ρ_{peak},

$$\begin{aligned}
\left\langle \widehat{\psi'}\left(r'\right), \widehat{\psi'}\left(r'\right)\right\rangle_{\rho_{\text{peak}}} &= \int \mathrm{d}A'\big|_{\rho_{\text{peak}}} \operatorname{Tr}\left[\widehat{\psi'}_a(r')\widehat{\psi'}^a(r')\right] \\
&= \int \mathrm{d}^4x' \, \frac{4\,\rho_{\text{peak}}^4}{\left(\rho_{\text{peak}}^2 + x'^2\right)^2} \operatorname{Tr}\left[\psi'_\mu(x')\psi'^\mu(x')\right] \\
&= \int \mathrm{d}^4x \, \sigma_{\text{inv}}^{-2}(b,x) \, \frac{4\,\rho_{\text{peak}}^4 \sigma_{\text{inv}}(b,x)}{\left(\rho_{\text{peak}}^2 + x^2\right)^2} \sigma_{\text{inv}}(b,x) \operatorname{Tr}\left[\psi_\mu(x)\psi^\mu(x)\right] \\
&= \int \mathrm{d}^4x \, \frac{4\,\rho_{\text{peak}}^4}{\left(\rho_{\text{peak}}^2 + x^2\right)^2} \operatorname{Tr}\left[\psi_\mu(x)\psi^\mu(x)\right] \\
&= \int \mathrm{d}A\big|_{\rho_{\text{peak}}} \operatorname{Tr}\left[\widehat{\psi}_a(r)\widehat{\psi}^a(r)\right] \\
&= \left\langle \widehat{\psi}\left(r\right), \widehat{\psi}\left(r\right)\right\rangle_{\rho_{\text{peak}}} .
\end{aligned} \tag{6.58}$$

Since the radius of the sphere and the radius of inversion are equal, we find that *they are invariant!* There is *no difference* between the normalisation integrals of the projected zero modes, $\widehat{\psi}_a(r)$, and of the projected and an additionally inverted zero modes, $\widehat{\psi'}_a(r')$. As a consequence the troublesome zero modes inverted in Euclidean space, the translation zero mode $\psi'^{(z)}(x')$ and the colour zero mode $\psi'^{(\alpha)}(x')$ turn out to be *finite* after an inversion.

The invariance is due the factor $\sigma_{\text{inv}}(x)$ coming from the transformation of the conformal factor of stereographic projection,

$$\frac{4\,\rho_{\text{peak}}^4}{\left(\rho_{\text{peak}}^2 + x'^2\right)^2} = \frac{4\,\rho_{\text{peak}}^4}{\left(\rho_{\text{peak}}^2 + x^2\right)^2} \sigma_{\text{inv}}(x). \tag{6.59}$$

This leads to a cancellation of all factors $\sigma_{\text{inv}}(x)$ in Eq. (6.58). We see immediately, that this behaviour could not be found for the projection of tensor fields, since we would get an additional factor $\sigma_{\text{inv}}(x)$, see Sect. 4.3.2.

In Table 6.1 the normalisation integrals for all types of zero modes are listed. The results of the integration, somewhat complicated functions, are given in Appendix E. All normalisation integrals can be written as functions of κ,

$$\kappa \equiv \frac{\rho}{\rho_{\text{peak}}}. \tag{6.60}$$

Table 6.1: Normalisation integrals $\langle\widehat{\psi},\widehat{\psi}\rangle_{\rho_{\rm peak}}$ of Eq. (6.58) for zero modes projected on a sphere with radius $b=\rho_{\rm peak}$. The results of the integration, somewhat complicated functions, are given in Appendix E. In the limit of small instantons on the sphere we obtain the results from Euclidean space stretched by a factor of 2. The zero mode normalisations in Euclidean space are denoted by $\|\psi\|_{\rm E}$, the ones on the sphere by $\|\widehat{\psi}\|$.

Kind of zero mode	Normalisation integral on the sphere $\langle\widehat{\psi},\widehat{\psi}\rangle_{\rho_{\rm peak}}$	Limit for small instantons on sphere $\kappa\to 0$
Dilatation $\widehat{\psi}^{(\rho)}$	$\frac{4\cdot 48}{g^2}\rho'^6\int {\rm d}^4x\frac{x^2}{(\rho_{\rm peak}^2+x^2)^2(\rho'^2+x^2)^4}$	$\|\widehat{\psi}^{(\rho)}\|\simeq\frac{8\pi}{g}=2\|\psi^{(\rho)}\|_{\rm E}$
Translation $\widehat{\psi}^{(z)}$	$\frac{4\cdot 48}{g^2}\rho_{\rm peak}^4\rho'^4\int {\rm d}^4x\frac{1}{(\rho_{\rm peak}^2+x^2)^2(\rho'^2+x^2)^4}$	$\|\widehat{\psi}^{(z)}\|\simeq\frac{4\sqrt{2}\pi}{g}=2\|\psi^{(z)}\|_{\rm E}$
Colour ZM $\widehat{\psi}^{(a)}$	$\frac{4\cdot 48}{g^2}\rho_{\rm peak}^4\rho'^4\int {\rm d}^4x\frac{x^2}{(\rho_{\rm peak}^2+x^2)^2(\rho'^2+x^2)^4}$	$\|\widehat{\psi}^{(a)}\|\simeq\frac{8\pi}{g}\rho=2\|\psi^{(a)}\|_{\rm E}$
Colour ZM $\widehat{\psi}^{(\alpha)}$	$\frac{4\cdot 16}{g^2}\rho_{\rm peak}^4\rho'^2\int {\rm d}^4x\frac{x^2}{(\rho_{\rm peak}^2+x^2)^2(\rho'^2+x^2)^3}$	$\|\widehat{\psi}^{(\alpha)}\|\simeq\frac{4\sqrt{2}\pi}{g}\rho=2\|\psi^{(\alpha)}\|_{\rm E}$

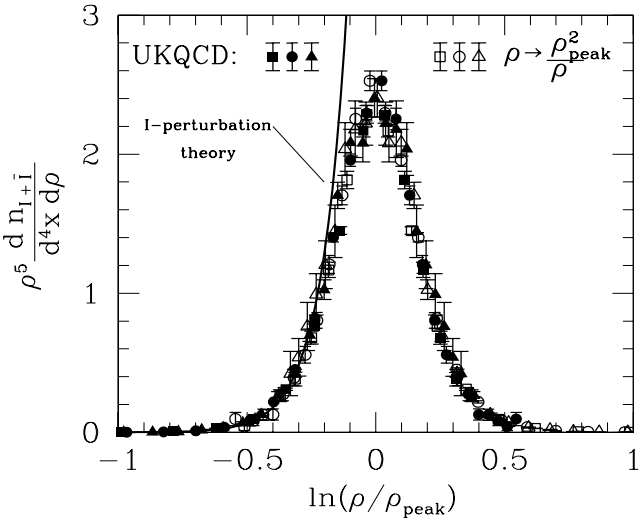

Figure 6.2: UKQCD lattice data [22, 23] for the instanton-size distribution $D(\rho)\,\rho^5$. $D(\rho)\,\rho^5$, a dimensionless quantity, seems to be symmetric under $\rho \leftrightarrow \rho' = \rho^2_{\rm peak}/\rho$.

From Eq. (6.58) we conclude that the dominant part of the I-size distribution $D(\rho)$ on the sphere is invariant under conformal space-time inversion of radius $\rho_{\rm peak}$ in Euclidean space. Now we come to the crucial question: Does the invariance of the total zero mode fraction under space-time inversion imply an invariance under inversion of the instanton size ρ? For it is precisely this behaviour the lattice data indicate, see Fig. 6.2, and which is suggested by our symmetry approach. That is to say we are interested in whether the total zero mode contribution

$$\widehat{J}(\kappa) = \frac{1}{(2\pi)^6} \|\widehat{\psi}_a^{(\rho)}\| \times \|\widehat{\psi}_a^{(z)}\|^4 \times \|\widehat{\psi}_a^{(a)}\|^3 \times \|\widehat{\psi}_a^{(\alpha)}\|^4 \tag{6.61}$$

on the sphere is invariant under the following transformation:

$$\rho \leftrightarrow \rho' = \rho^2_{\rm peak}/\rho. \tag{6.62}$$

In order to answer this question, we consider first the various types of zero mode contribution individually. In Figs. 6.3 - 6.6 the normalisation integrals of the four different types of zero modes are plotted against $\ln(\kappa)$. It is visible at first sight, that, except for the colour zero mode $\psi_a^{(a)}(r)$ shown in Fig. 6.5, the individual normalisations are *not invariant* under the required transformation

$$\rho \to \rho' \quad \Leftrightarrow \quad \kappa \to \frac{1}{\kappa} \quad \Leftrightarrow \quad \ln(\kappa) \to -\ln(\kappa). \tag{6.63}$$

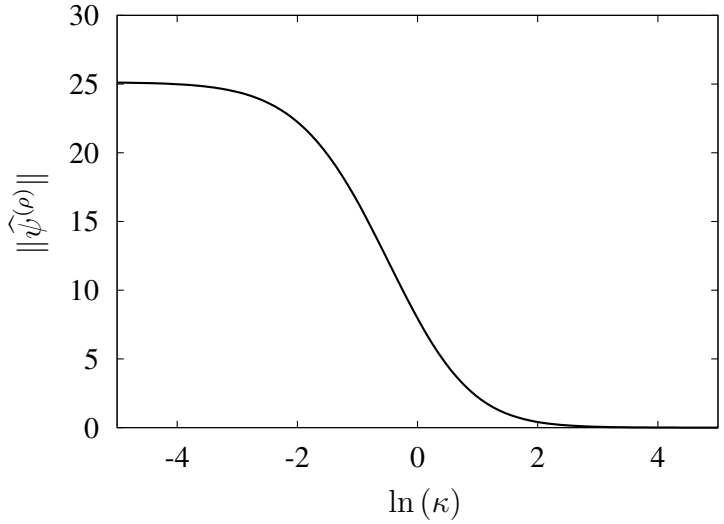

Figure 6.3: Normalisation $\|\widehat{\psi}^{(\rho)}\|$ of the dilatation zero mode $\widehat{\psi}^{(\rho)}$ on the sphere.

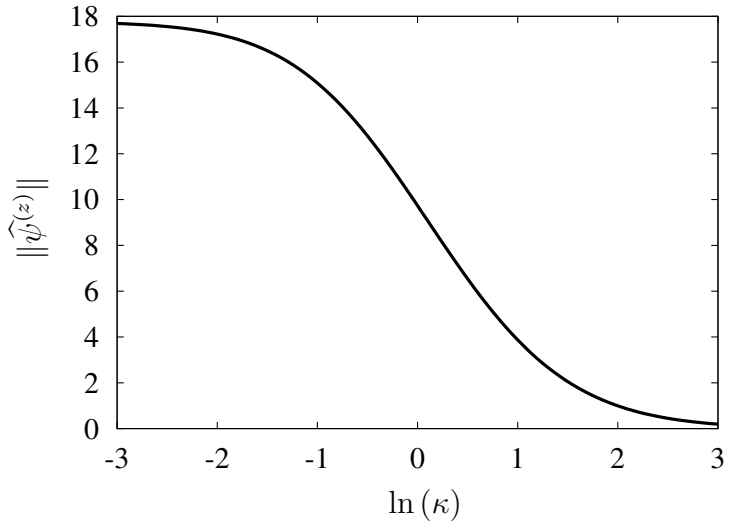

Figure 6.4: Normalisation $\|\widehat{\psi}^{(z)}\|$ of the translation zero mode $\widehat{\psi}^{(z)}$ on the sphere.

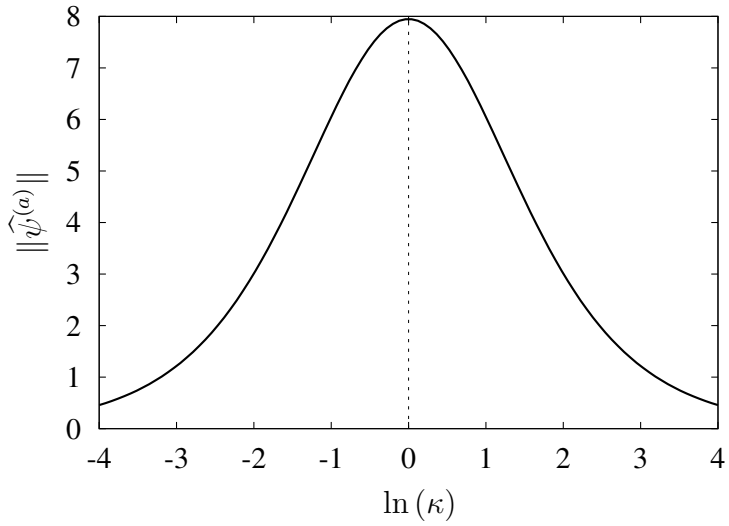

Figure 6.5: Normalisation $\|\widehat{\psi}^{(a)}\|$ of the colour zero mode $\widehat{\psi}^{(a)}$ on the sphere. $\|\widehat{\psi}^{(a)}\|$ is perfectly symmetric under an inversion of the I-size.

.

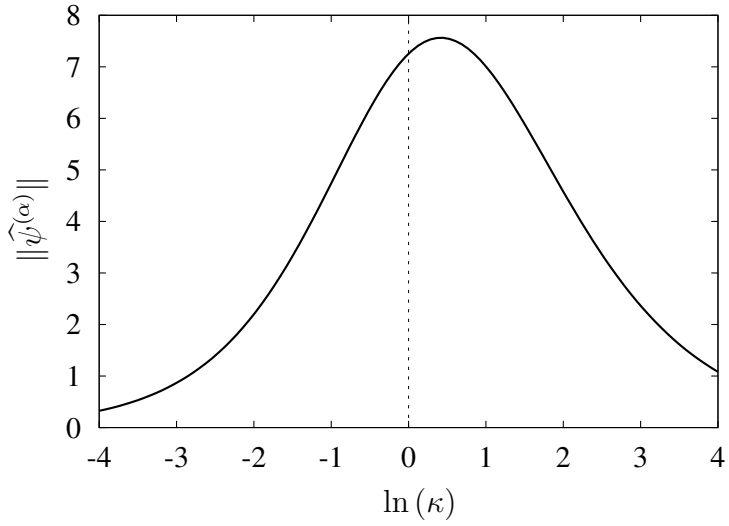

Figure 6.6: Normalisation $\|\widehat{\psi}^{(\alpha)}\|$ of the colour zero mode $\widehat{\psi}^{(\alpha)}$ on the sphere.

However, when we look at the total zero mode fraction $\widehat{J}(\kappa)$, we find the following, very promising results depicted in Fig. 6.7:

- Larger sized instantons are strongly suppressed.
- Despite the fact that three of the four types of zero mode contributions are asymmetric under
$$\kappa \leftrightarrow 1/\kappa, \tag{6.64}$$
the total zero mode fraction times κ^5, $\widehat{J}(\kappa)\,\kappa^5$, is nonetheless approximately invariant under this transformation![1] The peak position is shifted from the centre only by a value of $\ln(\kappa_{\max}) = 0.34$ corresponding to $\kappa_{\max} = 1.414 \sim \sqrt{2}$.

Following our approach, which assumes that the non-zero mode part $Q(\kappa)$ is not affected by an inversion, we include $Q(\kappa)$ by multiplying a factor[2] $1/\kappa$. The peak position of $\widehat{J}(\kappa)\,\kappa^4$ is now at a value of $\ln(\kappa_{\max}) = 0.1812$ with $\kappa_{\max} \simeq 1.19$. If we then make the following substitution in the total zero mode fraction,
$$\kappa \to 1.19\kappa, \tag{6.65}$$
we can move the peak position to the center as can be seen in Fig. 6.8. *The symmetry is virtually perfect*! Fig. 6.9 shows that the size distribution on the sphere and the inverted distribution are visually almost indistinguishable over thirteen orders of magnitude.

Two possibilities are near at hand for explaining such a shift:

- The shift could be the effect of the renormalisation procedure. The invariance under space-time inversion eventually transfers best to an invariance under an inversion of the instanton size, when working in an appropriate renormalisation scheme. A good candidate for such a scheme would be the "instanton renormalisation-scheme" introduced by Ringwald and Schrempp [23].
- The radius of the sphere can be redefined. In Euclidean space the peak position $\rho_{\text{peak}} \simeq 0.6$ fm of the dimensionless quantity $D(\rho)\,\rho^5$ is about $1.19\,\tilde{\rho}_{\text{peak}}$ with $\tilde{\rho}_{\text{peak}} \simeq 0.5$ fm being the peak position of the actual size distribution $D(\rho)$. A priori the radius of the sphere does not need to correspond to the peak position of the size distribution on the sphere $\widehat{J}(\kappa)\ 1/\kappa$ but might also be associated with the peak position of $\kappa^4\,\widehat{J}(\kappa)$.

[1] In Euclidean space the factor $(\rho\mu_{\text{r}})^5$ is often multiplied to the instanton size distribution of dimension $[\text{fm}]^{-5}$ in order to obtain a dimensionless quantity. In analogy to that we multiply the zero mode fraction on the sphere with κ^5.

[2] The corresponding non-zero mode fraction in Euclidean space is proportional to $1/(\rho\mu_{\text{r}})$.

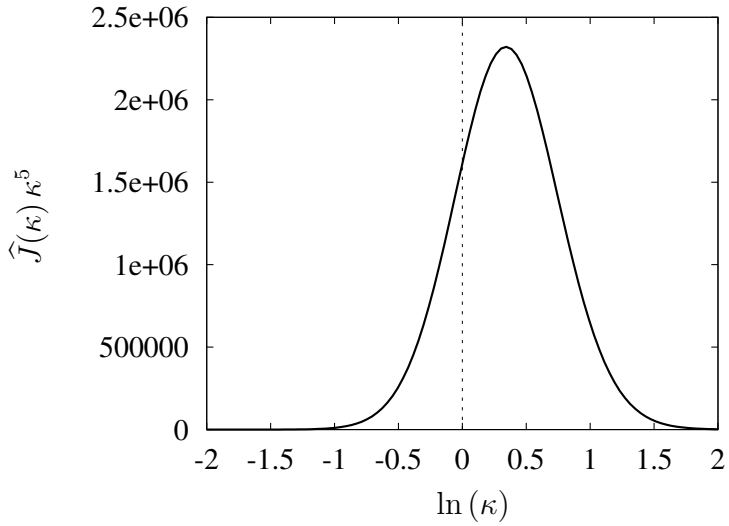

Figure 6.7: Total zero mode contribution $\widehat{J}(\kappa)$ times κ^5 on the sphere. The factor κ^5, which allows for a comparison with the lattice data, leads to a better symmetry. The peak is shifted from the center by a value of 0.34.

Let us discuss next some important *analytical* properties of the total zero mode part $\widehat{J}(\kappa)$. Since $\widehat{J}(\kappa)$ is dependent only on κ, which is the ratio of the I-size ρ over the radius of the sphere ρ_{peak}, the following limits are identical:

$$\kappa \to 0: \quad \begin{cases} \text{The radius of the sphere } \rho_{\text{peak}} \text{ goes to infinity while the instanton size } \rho \text{ is fixed.} \\ \text{The instanton size } \rho \text{ goes to zero while the radius of the sphere } \rho_{\text{peak}} \text{ is fixed.} \end{cases}$$

We have a look on the limits in detail:

Limit of small instantons on the sphere:

$$\kappa \to 0 \;\Leftrightarrow\; \rho_{\text{peak}} \to \infty \;\Leftrightarrow\; \rho \to 0 \tag{6.66}$$

If the radius of the sphere goes to infinity we obtain the same values for the normalisation as in Euclidean space, see Table 6.1 and compare to the ones in Sect. 5.3, except for an additional factor of 2 for every zero mode normalisation. It comes from the conformal factor of the stereographic projection:

$$\widehat{\psi}_a \widehat{\psi}^a = \frac{4\,\rho_{\text{peak}}^4}{\left(\rho_{\text{peak}}^2 + x^2\right)^2} \psi_\mu \psi^\mu \overset{\rho_{\text{peak}} \to \infty}{=} 4\,\psi_\mu \psi^\mu \tag{6.67}$$

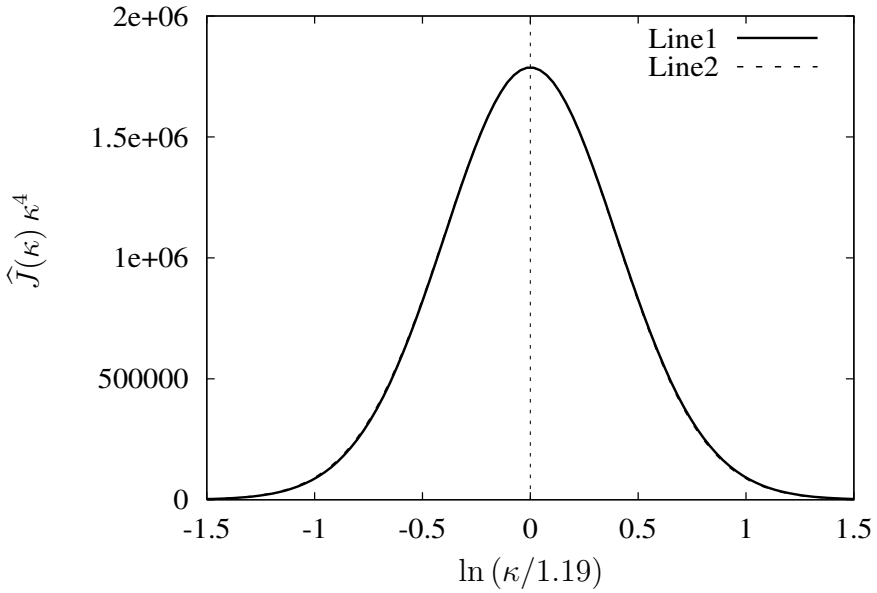

Figure 6.8: Centered total zero mode fraction $\widehat{J}(\kappa)$ times κ^4 on the sphere: Line1 shows the total zero mode fraction plotted against $\ln(\kappa/1.19)$. Line2 shows the zero mode fraction plotted against an inverted I-size, i.e. $-\ln(\kappa/1.19)$. The factor κ^4 includes the non-zero mode fraction proportional to $1/\kappa$ and a factor κ^5 in analogy to the factor ρ^5 in Euclidean space. The symmetry under $\kappa \leftrightarrow 1/\kappa$ is indeed startling.

The zero mode part $\widehat{J}(\kappa)$ rises with $\mathcal{O}(\rho^7)$ for small instantons as we expect from I-perturbation theory.

Limit of large instantons on the sphere:

$$\kappa \to \infty \;\Leftrightarrow\; \rho_{\text{peak}} \to 0 \;\Leftrightarrow\; \rho \to \infty \tag{6.68}$$

The behaviour for large instantons is even more interesting. We find that $\widehat{J}(\kappa)$ is of $\mathcal{O}(1/\rho^7)$, i.e. it drops with the the same power!

Limit for $\kappa = 1$:

This corresponds to the case of $\rho_{\text{peak}} = \rho$, which will be studied in detail in the next section. The expansion of $\widehat{J}(\kappa)$ about $\kappa = 1$ gives, as expected, the results of Sect. 6.4.1.

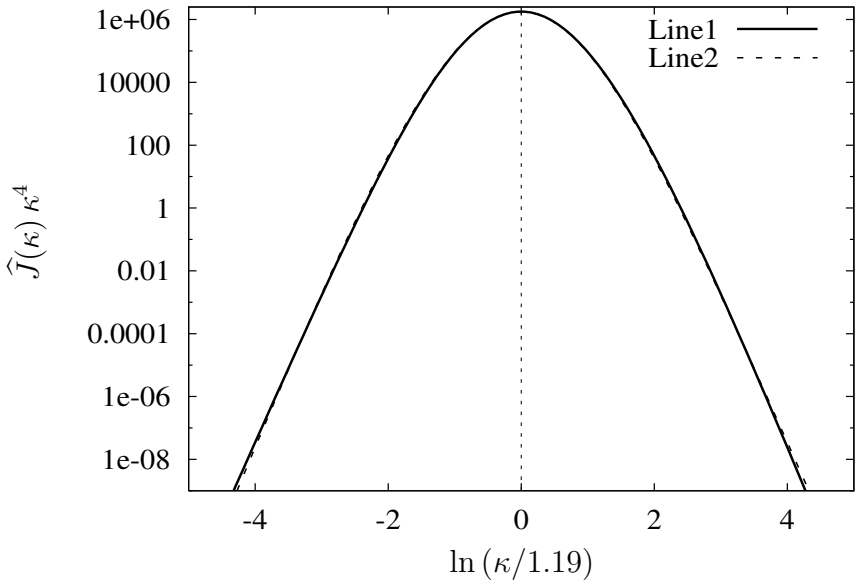

Figure 6.9: Centered size distribution on the sphere: Line1 shows the total zero mode fraction plotted against $\ln(\kappa/1.19)$. Line2 shows the zero mode fraction plotted against an inverted I-size, i.e. $-\ln(\kappa/1.19)$. The symmetry under $\kappa \leftrightarrow 1/\kappa$ is visually hardly distinguishable over thirteen orders of magnitude.

All in all we find a *correct description of the I-size distribution at qualitative level*. The zero mode fraction on the sphere is not only approximately invariant under an inversion of the I-size. Moreover we find that it raises and falls off with the correct power of the I-size ρ!

We must stress that this is only true if the translation zero modes transform as four vector fields under conformal transformations. This result cannot be achieved if they transform as a second-order tensor either under conformal inversion or conformal stereographic projection or both.

6.4 Consistency checks

The projection of the zero modes on a sphere with radius $b = \rho$, which will be addressed in the subsequent section, enables us to establish contact to existing work. This sphere corresponds to the one of Rebbi and Jackiw [26], no new scale is introduced. However, our method differs from [26] when it comes to the order of computation steps. We determine the zero modes in Euclidean space first and project them onto the sphere thereafter, whereas in Ref. [26] this was done the other way round.

In this section we study the differences of the normalisation integrals between our approach and the one in Ref. [26]. We begin with a discussion of our results for the "conventional" projection $b = \rho$. Thereafter we make contact to the results for the inverted zero modes in Euclidean space, which were missing so far. We make a rather lengthy digression in Sect. 6.4.3, where we determine the generators for the zero modes on the sphere. In that course we explain the disadvantages of the approach of Ref. [26]. In Appendix D we discuss the identification of the zero modes on the sphere and their normalisation integrals.

6.4.1 The conventional projection: $b = \rho$

In this section we repeat the procedure of the last section. The difference lies in the radius of the sphere which corresponds now to the size of the instanton, i.e. $b = \rho$.

$$\left\langle \widehat{\psi}\,(r)\,,\widehat{\psi}\,(r)\right\rangle_{\rho} = \int \mathrm{d}A\big|_{\rho}\ \mathrm{Tr}\left[\widehat{\psi}_a(r)\widehat{\psi}^a(r)\right] \tag{6.69}$$

In Table 6.2 the results for the normalisations of the zero modes on the sphere are given. The total zero mode fraction is

$$\begin{aligned} J(\gamma) &= \frac{1}{(2\pi)^6}\|\widehat{\psi}^{(\rho)}(x)\| \times \|\widehat{\psi}^{(z)}(x)\|^4 \times \|\widehat{\psi}^{(a)}(x)\|^3 \times \|\widehat{\psi}^{(\alpha)}(x)\|^4 \\ &= \frac{1}{(2\pi)^6}\left[\sqrt{\frac{2}{5}}\frac{4\pi}{g}\right]\left[\sqrt{\frac{6}{5}}\frac{2\sqrt{2}\pi}{g}\right]^4\left[\sqrt{\frac{2}{5}}\frac{4\pi\rho}{g}\right]^3\left[\sqrt{\frac{2}{3}}\frac{2\sqrt{2}\pi\rho}{g}\right]^4 \\ &= \frac{1}{(2\pi)^6}\left(\frac{2\sqrt{2}}{5}\right)^4\frac{2^{20}\,\pi^{12}\,\rho^7}{g^{12}}. \end{aligned} \tag{6.70}$$

We find the following results. The zero mode fraction projected on the hypersphere shows the same dependence on ρ as in Euclidean space, see Eq. (5.42) in Sect. 5.3. The different pre-factor $\left(2\sqrt{2}/5\right)^4$ in the normalisation comes from the process of projection. Its origin is a pure geometrical one, see also Sect. 6.4.2.

Table 6.2: Normalisations of zero modes projected on a hypersphere with radius $b = \rho$ given by Eq. (6.69). The normalisation integrals on the sphere agree with the ones in Euclidean space, denoted by $\|\psi_\mu^{(\rho)}(x)\|_{\mathrm{E}}$, apart from a different normalisation pre-factor, which has a geometrical origin.

Kind of zero mode	Normalisation integral $\langle\widehat{\psi},\widehat{\psi}\rangle_\rho$	Normalisation $\langle\widehat{\psi},\widehat{\psi}\rangle_\rho^{1/2}$
Dilatation $\widehat{\psi}^{(\rho)}(r)$	$\frac{4\cdot 48}{g^2}\rho^2\int \mathrm{d}^4x \frac{x^2}{(\rho^2+x^2)^6}$	$\sqrt{\frac{2}{5}}\frac{4\pi}{g} = \sqrt{\frac{2}{5}}\|\psi_\mu^{(\rho)}(x)\|_{\mathrm{E}}$
Translation $\widehat{\psi}^{(z)}(r)$	$\frac{4\cdot 48}{g^2}\rho^4\int \mathrm{d}^4x \frac{1}{(\rho^2+x^2)^6}$	$\sqrt{\frac{6}{5}}\frac{2\sqrt{2}\pi}{g} = \sqrt{\frac{6}{5}}\|\psi_\mu^{(z)}(x)\|_{\mathrm{E}}$
Colour ZM $\widehat{\psi}^{(a)}(r)$	$\frac{4\cdot 48}{g^2}\rho^4\int \mathrm{d}^4x \frac{x^2}{(\rho^2+x^2)^6}$	$\sqrt{\frac{2}{5}}\frac{4\pi}{g}\rho = \sqrt{\frac{2}{5}}\|\psi_\mu^{(a)}(x)\|_{\mathrm{E}}$
Colour ZM $\widehat{\psi}^{(\alpha)}(r)$	$\frac{4\cdot 16}{g^2}\rho^4\int \mathrm{d}^4x \frac{1}{(\rho^2+x^2)^5}$	$\sqrt{\frac{2}{3}}\frac{2\sqrt{2}\pi}{g}\rho = \sqrt{\frac{2}{3}}\|\psi_\mu^{(\alpha)}(x)\|_{\mathrm{E}}$

When comparing our results for the normalisations of dilatation and translation zero modes[3] to the ones of Refs. [79] and [80], we find that they deviate only by a factor $2^4/3^4$. This is due our different approach, where we compute the zero modes in Euclidean space first and then project them onto the, whereas in Refs. [79] and [80] this was done the other way round. The procedure is not commutable. In Section 6.4.3 we will deal with that issue.

As the last point of this section we address the behaviour of these projected zero modes under

[3]Only this comparison is possible, since the colour zero modes on the hypersphere are not considered in Refs. [79, 80].

inversion in Euclidean space. We find after a straight forward computation

$$\begin{aligned}\left\langle \widehat{\psi}'\left(r'\right), \widehat{\psi}'\left(r'\right)\right\rangle_{\rho} &= \int \mathrm{d}A'\big|_{\rho} \,\mathrm{Tr}\left[\widehat{\psi}'_{a}\left(r'\right)\widehat{\psi}'^{\,a}\left(r'\right)\right] \\ &= \frac{b_{\mathrm{inv}}^{4}}{\rho'^{\,4}} \int \mathrm{d}A\big|_{\rho'} \,\mathrm{Tr}\left[\widehat{\psi}_{a}(r)\widehat{\psi}^{a}(r)\right] \\ &= \frac{b_{\mathrm{inv}}^{4}}{\rho'^{\,4}} \left\langle \widehat{\psi}\left(r\right), \widehat{\psi}\left(r\right)\right\rangle_{\rho'},\end{aligned} \tag{6.71}$$

where b_{inv} is the radius of inversion and $\rho' = b_{\mathrm{inv}}^{2}/\rho$ the inverted instanton size. The normalisation integrals of the inverted zero modes projected onto a sphere with radius equal to the instanton size ρ correspond to those of the uninverted ones projected onto a sphere with radius equal to the inverted instanton size ρ' times a factor $\rho^{4}/b_{\mathrm{inv}}^{4}$. For a reasonable comparison with the uninverted zero modes projected onto a sphere with radius ρ we have to project the inverted zero modes onto a sphere with a radius that equals also the inverted instanton size. This will be done in the next section.

6.4.2 Inverted zero modes and stereographic projection: $b = \rho'$

Since an inversion changes an I-configuration of size ρ to an $\bar{I}$-configuration of size ρ', one has to project the zero modes $\psi'(x')$ transformed under inversion of radius ρ_{peak} onto a sphere of radius $\rho' = \rho_{\mathrm{peak}}^{2}/\rho$. This allows for a contact to the results for the normalisation integrals of the inverted zero modes in Euclidean space, which have been lacking so far.

$$\begin{aligned}\left\langle \widehat{\psi}'\left(r'\right), \widehat{\psi}'\left(r'\right)\right\rangle_{\rho'} &= \int \mathrm{d}A'\big|_{\rho'} \,\mathrm{Tr}\left[\widehat{\psi}'_{a}\left(r'\right)\widehat{\psi}'^{a}\left(r'\right)\right] \\ &= \frac{b^{4}}{\rho^{4}} \int \mathrm{d}A\big|_{\rho} \,\mathrm{Tr}\left[\widehat{\psi}_{a}\left(r\right)\widehat{\psi}^{a}\left(r\right)\right] \\ &= \frac{b^{4}}{\rho^{4}} \left\langle \widehat{\psi}\left(r\right), \widehat{\psi}\left(r\right)\right\rangle_{\rho} \\ &= \frac{\rho'^{\,2}}{\rho^{2}} \left\langle \widehat{\psi}\left(r\right), \widehat{\psi}\left(r\right)\right\rangle_{\rho}.\end{aligned} \tag{6.72}$$

Most importantly we find a *finite normalisation* for the translation zero mode $\widehat{\psi}'^{(z)}_{a}$ and the colour zero mode $\widehat{\psi}'^{(\alpha)}_{a}$ due to the compactness of the sphere. The additional conformal factor $\sigma(x)_{\mathrm{sp}}(x',\rho')$ has, as mentioned in Sect. 6.3, the effect of a regulator. These zero modes were divergent before in the Euclidean space, see Sect. 5.4. Moreover we see that the powers of ρ' for the dilatation $\widehat{\psi}'^{(\rho)}(x')$ and the colour zero mode $\widehat{\psi}'^{(a)}(x')$ correspond to our former results

of Euclidean space, see Eq. (5.49) and (5.50). The contribution of these zero modes is then in total,

$$\begin{aligned} J(\gamma_{inv}) &= \frac{1}{(2\pi)^6}\|\widehat{\psi}'^{(\rho)}(x')\| \times \|\widehat{\psi}'^{(z)}(x')\|^4 \times \|\widehat{\psi}'^{(a)}(x')\|^3 \times \|\widehat{\psi}'^{(\alpha)}(x')\|^4 \\ &= \frac{1}{(2\pi)^6}\left[\sqrt{\frac{2}{5}}\frac{4\pi}{g}\frac{\rho'}{\rho}\right]\left[\sqrt{\frac{6}{5}}\frac{2\sqrt{2}\pi}{g}\frac{\rho'}{\rho}\right]^4\left[\sqrt{\frac{2}{5}}\frac{4\pi\rho'}{g}\right]^3\left[\sqrt{\frac{2}{3}}\frac{2\sqrt{2}\pi\rho'}{g}\right]^4 \\ &= \frac{1}{(2\pi)^6}\left(\frac{2\sqrt{2}}{5}\right)^4\frac{2^{20}\,\pi^{12}\,\rho'^{7}}{g^{12}}\frac{\rho'^{5}}{\rho^5}. \end{aligned} \tag{6.73}$$

It should be noticed that the same new pre-factor $\left(2\sqrt{2}/5\right)^4$ for the normalisation on the sphere appears as for the projection with radius $b = \rho$. This means that it is a pure geometrical factor.

The results for the inverted zero modes on the sphere with radius ρ' are quite intriguing though not as perfectly invariant as in case of $b = \rho_{\text{peak}}$, when the radius of the sphere equaled the radius of inversion. They show a dependence on ρ' which corresponds to the same power as the zero mode fraction before inversion but with inverted I-size and multiplied by an additional ratio $\frac{\rho'^5}{\rho^5}$.

6.4.3 Generators of conformal transformations on the hypersphere

In this section we make a rather lengthy digression. The purpose of this "deviation" from the straight line of argumentation is to show why our strategy later on differs very much from what has been done in the past. In order to do this we consider the appearance of the conformal transformations and their generators in terms of the r-coordinates on the hypersphere. We will see that there is a way to combine three generators to form the $O(5)$ generators S_a, that will be responsible for the dilatation and translation zero modes on the hypersphere. Thus one can calculate the corresponding zero mode contributions on the sphere.

Dilatation

A dilatation in 4-dimensional space with the parameter λ is done as follows,

$$\mathcal{D}_\lambda: \quad x_\mu \to x'_\mu = \lambda x_\mu. \tag{6.74}$$

We consider the coordinates r_μ and r_5 separately, when stating the appearance of the above transformation in terms of the r-coordinates:

$$\mathcal{D}_\lambda^{(5)}: \quad \begin{cases} r_\mu \to r'_\mu = \lambda \frac{\frac{b^2}{\lambda^2} 2x_\mu}{\frac{b^2}{\lambda^2}+x^2} \\ \\ r_5 \to r'_5 = b\, \frac{\frac{b^2}{\lambda^2}-x^2}{\frac{b^2}{\lambda^2}+x^2} \end{cases} \tag{6.75}$$

We have to expand the transformation in terms of λ close to one, $\lambda \sim 1$,

$$r'_\mu = (1+\epsilon)\, \frac{\frac{b^2}{(1+\epsilon)^2} 2x_\mu}{\frac{b^2}{(1+\epsilon)^2}+x^2}, \tag{6.76}$$

where ϵ is arbitrarily small and dimensionless. Terms of the order $\mathcal{O}(\epsilon^2)$ are neglected. For the expansion in ϵ one obtains

$$\begin{aligned} r'_\mu &= r_\mu + \epsilon\, \frac{r_5}{b}\, r_\mu + \mathcal{O}\left(\epsilon^2\right), \\ r'_5 &= r_5 - \frac{\epsilon}{b}\left(b^2 - r_5^2\right) + \mathcal{O}\left(\epsilon^2\right). \end{aligned} \tag{6.77}$$

Hence the change in r_a is

$$\delta r_\mu = \epsilon\, \frac{r_5}{b}\, r_\mu \quad \text{and} \qquad\qquad \delta r_5 = -\epsilon\, \frac{1}{b}(b^2 - r_5^2). \tag{6.78}$$

Now we can determine the generator of the dilatation on the hypersphere by considering the change of a scalar field $\phi(r)$ under the required transformation,

$$\begin{aligned} \phi(r') &= \phi(r) + \frac{\partial \phi(r)}{\partial r^a} \delta r^a \\ &= \left(1 + \frac{\epsilon}{b}\left(r_5 r_\mu \frac{\partial}{\partial r^\mu} - \left(b^2 - r_5^2\right) \frac{\partial}{\partial r^5}\right)\right) \phi(r) \\ &\equiv \left(1 + \mathrm{i}\, D\, \frac{\epsilon}{b}\right) \phi(r). \end{aligned} \tag{6.79}$$

We can read off the generator from Eq. (6.79),

$$D = -\mathrm{i}\left(r_5\, r_\mu\, \partial^\mu - (b^2 - r_5^2)\partial^5\right). \tag{6.80}$$

Translation

Although the translation in Euclidean space is simple,

$$T_a: \quad x_\mu \to x'_\mu = x_\mu + z_\mu, \tag{6.81}$$

this is not the case for the corresponding transformation on the $O(5)$-sphere, see Ref. [77]:

$$T_a^{(5)}: \quad \begin{cases} r_\mu \to r'_\mu & = \frac{1}{N}\left(r_\mu + \frac{1}{b}(b+r_5)z_\mu\right), \\ r_5 \to r'_5 & = \frac{1}{N}\left(r_5 - \frac{1}{b^2}\frac{z^2}{2}(b+r_5) - \frac{1}{b}r_\nu z^\nu\right), \end{cases} \tag{6.82}$$

where

$$N = 1 + \frac{1}{b^3}\frac{z^2}{2}(b+r_5) + \frac{1}{b^2}r_\mu z^\mu \quad \text{and} \quad z^2 = z_\nu z^\nu. \tag{6.83}$$

It should be noticed that this transformation law is nonlinear already at the order $\mathcal{O}(a)$. Again we make an expansion, this time in terms of small z_μ.

$$\begin{aligned} \frac{1}{N} &= 1 - \frac{1}{b^2}r_\nu z^\nu + \mathcal{O}\left(z^2\right) \\ r'_\mu &= r_\mu + \frac{1}{b}\left(\left(b+r_5\right)z_\mu - \frac{1}{b}r_\nu z^\nu r_\mu\right) + \mathcal{O}\left(z^2\right) \\ r'_5 &= r_5 - \frac{1}{b^2}r_\nu z^\nu\ \left(b+r_5\right) + \mathcal{O}\left(z^2\right) \end{aligned} \tag{6.84}$$

Therefore

$$\delta\, r_\mu = \frac{1}{b}\left(\left(b+r_5\right)z_\mu - \frac{r_\nu z^\nu}{b}r_\mu\right), \qquad \delta\, r_5 = -\frac{r_\nu z^\nu}{b^2}\left(b+r_5\right). \tag{6.85}$$

Once more we consider changes of a scalar field to pin down the generator of the translation on the hypersphere,

$$\phi(r') = \left[1 + \frac{1}{b}\left(\left(b+r_5\right)z_\mu - \frac{r_\nu z^\nu}{b}r_\mu\right)\partial^\mu - \frac{1}{b^2}r_\nu z^\nu(b+r_5)\partial^5\right]\phi(r). \tag{6.86}$$

We find for the generator of translation on the sphere

$$P_\mu = -\mathrm{i}\left(\left(b+r_5\right)g_{\mu\nu} - \frac{r_\mu r_\nu}{b}\right)\partial^\nu + \mathrm{i}\frac{1}{b}\left(b+r_5\right)r\mu\,\partial^5. \tag{6.87}$$

Special Conformal Transformation

We already know that the SCT is a composition of an inversion, a translation and another inversion. To make life easier we consider here only the special case of equal radii for inversion and the $\mathcal{S}_4$ sphere. This simplification will not affect our investigations of the behaviour of the zero mode contribution under conformal inversion later on. In that particular case the coordinate inversion on the sphere turns out to be very simple. The space-time inversion in Euclidean space,

$$\mathcal{I}^{(4)}_{b^2}: \quad x_\mu \to x'_\mu = \frac{b^2}{x^2} x_\mu, \tag{6.88}$$

corresponds to the following transformation on the hypersphere

$$\mathcal{I}^{(5)}_{b^2}: \quad \begin{cases} r_\mu \to r'_\mu & = \frac{2\,b^2\,x'_\mu}{b^2+x'^2} = \frac{2\,b^2\,x_\rho}{b^2+x^2} = r_\mu, \\ r_5 \to r'_5 & = b\,\frac{b^2-x'^2}{b^2+x'^2} = b\,\frac{x^2-b^2}{b^2+x^2} = -r_5. \end{cases} \tag{6.89}$$

The connection between space-time inversion in Euclidean space and its appearance under stereographic projection is depicted in Fig. 6.10, where a stereographic projection of a line onto a one-dimensional surface of a two-dimensional sphere is depicted. The two points P and Q defining the two distances x and x', respectively are related by the condition of inversion with radius b in Euclidean space,

$$\frac{x}{b} = \frac{b}{x'}. \tag{6.90}$$

In Fig. 6.10 we see that the projected points P′ and Q′ differ only in the sign of the coordinate r_5. An inversion in Euclidean space corresponds to an exchange of the northern and southern hemisphere of $\mathcal{S}_4$. This means that the effect of an inversion can also be achieved by changing the source point of the stereographic projection from the south to the north pole. The generalisation to 5 dimensions is straight forward.

As a consequence of the simple form of Eq. (6.89) the SCT does not differ much from translation on the hypersphere,

$$\mathcal{K}^{(5)}: \quad \begin{cases} r_\mu \to r'_\mu & = \frac{1}{N'}\left(r_\mu + \frac{1}{b}(b-r_5)z_\mu\right), \\ r_5 \to r'_5 & = \frac{1}{N'}\left(r_5 + \frac{1}{b^2}\frac{z^2}{2}(b-r_5) - \frac{1}{b}r_\nu z^\nu\right), \end{cases} \tag{6.91}$$

where $N' = 1 + \frac{1}{b^3}\frac{z^2}{2}(b-r_5) + \frac{1}{b^2}r_\nu z^\nu$. After an expansion in small z_μ we have

$$\delta r_\mu = \frac{1}{b}\left((b-r_5)\,a_\mu - \frac{r_\nu a^\nu}{b} r_\mu\right) \quad \text{and} \quad \delta r_5 = \frac{r_\nu a^\nu}{b^2}\,(b-r_5)\,. \tag{6.92}$$

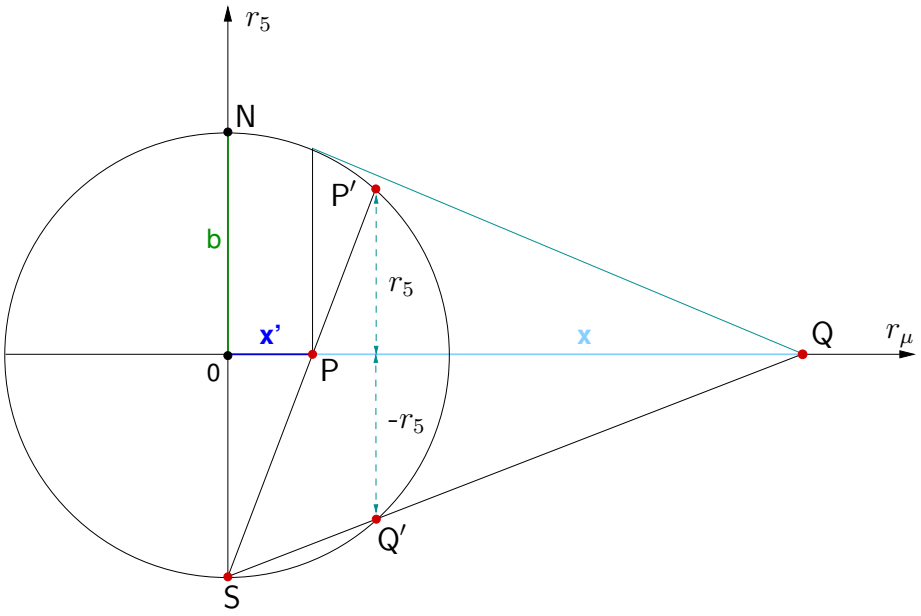

Figure 6.10: Relation between inversion and stereographic projection: The points P and Q define the two distances x and x'. x and x' are related by the condition of inversion. As a consequence the projected points P′ and Q′ differ only in the sign of the coordinate r_5. An inversion leads to an exchange of the northern and southern hemisphere.

Applying the same techniques as above we find for the generators of the SCT,

$$K_\mu = -\mathrm{i}\left((b - r_5)\, g_{\mu\nu} - r_\mu r_\nu\right)\partial^\nu - \mathrm{i}\frac{1}{b}\,(b - r_5)\, r_\mu\, \partial^5. \tag{6.93}$$

$O(5)$ generators S_a

As pointed out in Ref. [26], it is possible to combine the generators P_μ, K_μ and D together such that they form $O(5)$ generators S_a. These are now exactly the generators creating the dilatation and translation zero modes in the $O(5)$-formalism. This is because the $I\bar{I}$-field in the $O(5)$-formalism is invariant under the transformations $J_{\mu\nu}$ and $\mathcal{R}_\mu$. Thus it must be these remaining five generators S_a producing these zero modes.

The construction of S_a is done as follows:

$$\begin{aligned} \mathrm{i}P_\mu \frac{C^\mu}{b} + \mathrm{i}\, D\frac{C^5}{b^2} &= -\partial_a C^a + \frac{1}{b^2} r_b C^b r_a \partial^a \\ &\quad + \frac{1}{b}\left(r_\mu C^\mu \partial_5 - r_5 C^\mu \partial_\mu\right), \end{aligned} \tag{6.94}$$

where the parameters of translation z^μ are now replaced by C^μ and the parameter of dilatation λ by C^5/b. The new parameters C^μ and C^5 combine to the 5-dimensional vector C^a which has the dimension of a length. Compare the above equation to

$$\begin{aligned} -\mathrm{i}K_\mu \frac{C^\mu}{b} + \mathrm{i}\, D\frac{C^5}{b^2} &= -\partial_a C^a + \frac{1}{b^2} r_b C^b r_a \partial^a \\ &\quad - \frac{1}{b}\left(r_\mu C^\mu \partial_5 - r_5 C^\mu \partial_\mu\right). \end{aligned} \tag{6.95}$$

Thus we find the following generator,

$$\begin{aligned} S_a &= -\mathrm{i}\,\left(\frac{1}{2}\left(P_\mu - K_\mu\right), D\right) \\ &= -\mathrm{i}\,\left(\partial_a + r_a r_b \partial^b\right) \end{aligned} \tag{6.96}$$

with the corresponding coordinate transformation,

$$r_a \to r'_a \simeq r_a + \frac{1}{b^2} r_a r_b C^b + C_a. \tag{6.97}$$

It should be mentioned that this transformation is *not* conformal. In Appendix D the derivation of the translation and dilatation zero modes in the $O(5)$-covariant formalism and their normalisation integrals can be found. Comparison to the normalisation integrals of Refs. [79, 80] shows agreement. However when it comes to our actual subject, the behaviour of the zero mode fraction under conformal inversion, there occur two problems when working with these zero modes:

- First of all the zero modes generated by S_a can only be written down in a useful way for equal values of the I-size and the radius of the sphere, $b = \rho$. This is not what we want since in that case no new scale can be introduced.
- Secondly, a definition of colour zero modes in the $O(5)$ formalism could be done for $SU(2)$-instantons only, since it is not possible to lift the $SU(3)$-instantons onto the $O(5)$-sphere. So far we have only derived the translation and dilatation zero modes. It is not so clear how to write down the colour zero modes in the $O(5)$-formalism.

Since we are interested in $SU(3)$-instantons primarily we have embarked on another strategy, by computing the zero modes in Euclidean space first and lifting them to the hypersphere of stereographic projection thereafter.

Chapter 7

Conclusion and Outlook

Being topological fluctuations of the gluon field, instantons represent an essential part of non-perturbative QCD. The average I-size is one of the crucial quantities when characterising the structure of the QCD vacuum. However, within the framework of I-perturbation theory it it impossible to predict its numerical value since the integration over the I-size distribution $D(\rho)$ is divergent. Luckily enough lattice simulation show a physically reasonable behaviour of $D(\rho)$ indicating a sharp peak at an average I-size of $\rho_{\text{peak}} \simeq 0.5$ fm and by that a *sudden* deviation from one-loop analytical calculations. In this work the approach of a symmetry being responsible for the rapid breakdown of I-perturbation theory was explored. For that purpose a thorough investigation of the behaviour of the I-size distribution at one-loop level under conformal inversion was made. The idea is that the regarded symmetry, a conformal inversion of space-time, appears as an inversion of the I-size. Summarising the above results we can say the following.

- The dominant part of the I-size distribution $D(\rho)$ is divergent under a conformal inversion since two out of four zero mode normalisation integrals are infinite.
- This problem can be cured by lifting the I-calculus on the 4-dimensional surface of a 5-dimensional sphere via stereographic projection. The integration over the sphere, which is a compact and curved manifold, leads to a finite result.
- In the case of equal radii for the sphere and the conformal inversion, i.e. $b = \rho_{\text{peak}}$, we find a zero mode contribution on the sphere which agrees surprisingly well with the lattice data at qualitative level: $\widehat{J}(\rho)$ raises with a power of ρ^7 and decreases with $1/\rho^7$.
- Moreover we obtain a zero mode contribution on the sphere with $b = \rho_{\text{peak}}$, which is perfectly invariant under a space-time inversion. As a consequence, the size distribution on the sphere is almost symmetric when it comes to an inversion of the instanton size.

- After a substitution of the ration ρ/ρ_{peak} with $1.19\,\rho/\rho_{\text{peak}}$ the symmetry under an inversion of the instanton size of the size distribution on the sphere is nearly perfect over thirteen orders of magnitude.

- In the limit of small instantons on the sphere we find the same zero mode contribution as in Euclidean space times a factor two coming from the conformal factor of stereographic projection. The same results are found in the limit of an infinite radius of the sphere while the instanton size is fixed.

- We achieve the introduction of the new scale ρ_{peak} into the I-calculus by means of the above projection. It appears as the radius of the sphere.

- If we chose the radius of the sphere to equal the instanton size, i.e. $b = \rho$, we can make contact to existing work. The values for the normalisations depend weakly on the sequence of the projection procedure.

Concluding we can say that the dominating part of the size-distribution, the zero mode fraction, on a 4d-sphere with radius $b = \rho_{\text{peak}}$ shows perfect invariance under conformal inversion of the coordinates x_μ and as a consequence turns into an almost perfect invariance under inversion of the I-size ρ. Naturally there are many open questions which call for our attention:

- First of all the behaviour of the translation zero mode under conformal transformations should be resolved, since our successful approach depends on the assumption of a vector field-like transformation law.

- A further investigation of the physical meaning of the sphere and in particular its radius ρ_{peak} would be of great interest. This is related to the question of where the scales of the strong interactions, e.g. the scale of confinement Λ_{conf}, the scale of chiral symmetry breaking $\Lambda_{\chi\text{SB}}$ or the scale of saturation Q_s, come from which can be found nowhere in the QCD Lagrangian.

- The introduction of the inversion scale ρ_{peak} should lead to a breaking of dilatation symmetry. So far it is not clear, how this breaking takes place. However, it is indicated by the non-vanishing trace of the energy-momentum tensor since this goes along with the breaking of that symmetry. A further investigation of the following relation could bring some insight to this topic: $\rho_{\text{peak}} \propto \langle 0 \left| \frac{\alpha_s}{\pi} G^{a\,2}_{\mu\nu} \right| \rangle^{-1/4} \propto \left(-\theta^\mu_\mu\right)^{-1/4}$ [25].

- Last but not least it would be worthwhile to continue the search for conformal invariance in the I-sector and in QCD in general.

Appendix A

Notations and Conventions

We define the Euclidean Dirac γ-matrices as

$$\gamma_\mu = \begin{pmatrix} 0 & \bar{\sigma}_\mu \\ \sigma_\mu & 0 \end{pmatrix}, \quad \gamma^5 = \begin{pmatrix} -1 & 0 \\ 0 & 1 \end{pmatrix}. \tag{A.1}$$

They satisfy the Clifford algebra,

$$\{\gamma_\mu, \gamma_\nu\} = 2\delta_{\mu\nu}. \tag{A.2}$$

As usual, the dot over an index distinguishes the left- and right-handed $SU(2)$ representations. The σ-matrices are given as

$$(\sigma_\mu)^{\alpha\dot{\beta}} = (-\mathrm{i}\sigma_a, 1)^{\alpha\dot{\beta}}, \quad (\bar{\sigma}_\mu)_{\dot{\alpha}\beta} = (\mathrm{i}\sigma_a, 1)_{\dot{\alpha}\beta}, \tag{A.3}$$

with the Pauli matrices in the standard notation,

$$\sigma^1 = \begin{pmatrix} 0 & 1 \\ 1 & 0 \end{pmatrix}, \quad \sigma^2 = \begin{pmatrix} 0 & -\mathrm{i} \\ \mathrm{i} & 0 \end{pmatrix}, \quad \sigma^3 = \begin{pmatrix} 1 & 0 \\ 0 & -1 \end{pmatrix}. \tag{A.4}$$

They obey the algebraic relation

$$\sigma_\mu \bar{\sigma}_\nu + \sigma_\nu \bar{\sigma}_\mu = 2\delta_{\mu\nu}. \tag{A.5}$$

Furthermore we define

$$\sigma_\mu \bar{\sigma}_\nu - \sigma_\nu \bar{\sigma}_\mu \equiv \bar{\sigma}_{\mu\nu}. \tag{A.6}$$

Euclidean Dirac spinors are decomposed in the Weyl basis according to

$$\psi = \begin{pmatrix} \kappa_{\dot{\alpha}} \\ \phi^\alpha \end{pmatrix}, \qquad \bar{\psi} = \begin{pmatrix} \bar{\phi}^{\dot{\alpha}}, & \kappa_\alpha \end{pmatrix}. \tag{A.7}$$

The conjugate spinor $\bar{\psi}$ is defined as

$$\bar{\psi} \equiv \psi^\dagger \gamma^0. \tag{A.8}$$

Wick rotation

The connection between Euclidean space and Minkowski space, where the metric tensor is defined as $g^{\mu\nu} = \mathrm{diag}\,(1,-1,-1,-1)$, is obtained by means of analytical continuation. One replaces the Euclidean Dirac γ-matrices according to

$$(\gamma_4)_{\mathrm{E}} = \left(\gamma^0\right)_{\mathrm{M}}, \quad (\gamma_m)_{\mathrm{E}} = -\mathrm{i}\,(\gamma^m)_{\mathrm{M}}, \quad \left(\gamma^5\right)_{\mathrm{E}} = -\left(\gamma^5\right)_{\mathrm{M}}, \tag{A.9}$$

and obtains the Dirac γ-matrices in Minkowski space-time in chiral representation:

$$\gamma^0 = \begin{pmatrix} 0 & 1 \\ 1 & 0 \end{pmatrix}, \quad \gamma^m = \begin{pmatrix} 0 & \sigma^m \\ -\sigma^m & 0 \end{pmatrix}, \quad \gamma^5 = \begin{pmatrix} 1 & 0 \\ 0 & -1 \end{pmatrix}. \tag{A.10}$$

For coordinate vectors x_μ and their conjugate momenta p_μ we have the general replacements

$$\begin{aligned} x_4 &= \mathrm{i}x^0, & (x_m)_{\mathrm{E}} &= +\,(x^m)_{\mathrm{M}}, \\ p_4 &= -\mathrm{i}p^0, & (p_m)_{\mathrm{E}} &= -\,(p^m)_{\mathrm{M}}. \end{aligned} \tag{A.11}$$

Applying these prescriptions, the volume elements change as

$$\left(\mathrm{d}^4x\right)_{\mathrm{E}} = \mathrm{i}\left(\mathrm{d}^4x\right)_{\mathrm{M}}, \qquad \left(\mathrm{d}^4p\right)_{\mathrm{E}} = -\mathrm{i}\left(\mathrm{d}^4p\right)_{\mathrm{M}}, \tag{A.12}$$

and the action is replaced by

$$S_{\mathrm{M}} = \mathrm{i}\,S_{\mathrm{E}}. \tag{A.13}$$

't Hooft symbols

The 't Hoof symbols are defined as [6]

$$\eta_{a\mu\nu} = \begin{cases} \epsilon_{a\mu\nu}, & \mu,\nu = 1,2,3, \\ -\delta_{a\nu}, & \mu = 4, \\ \delta_{a\mu}, & \nu = 4, \\ 0, & \mu = \nu = 4. \end{cases} \tag{A.14}$$

The symbols $\bar{\eta}_{a\mu\nu}$ differ from $\eta_{a\mu\nu}$ by a change in the sign of the Kronecker deltas. The 't Hooft symbols obey the following relations:

$$\begin{aligned} 3\eta_{a\mu\nu} &= -\eta_{a\nu\mu}, & \eta_{a\mu\nu}\eta_b^{\mu\nu} &= 4\delta_{ab}, \\ \eta_{a\mu\nu}\eta^{a\mu\lambda} &= 3\delta_\nu^\lambda, & \eta_{a\mu\nu}\eta^{a\mu\nu} &= 12, \\ \eta_{a\mu\nu}\bar{\eta}^{b\mu\nu} &= 0, & \eta_{a\gamma\mu}\bar{\eta}^{b\gamma\lambda} &= \eta_{a\gamma\lambda}\bar{\eta}^{b\gamma\mu}, \\ \eta_{a\mu\nu} &= \frac{1}{2}\epsilon_{\mu\nu\alpha\beta}\eta_a^{\alpha\beta}, & \eta_{a\mu\nu}\eta^{a\gamma\lambda} &= \delta_\mu^\gamma\delta_\nu^\lambda - \delta_\mu^\lambda\delta_\nu^\gamma + \epsilon_{\mu\nu}^{\gamma\lambda}, \\ \epsilon_{\mu\nu\lambda\sigma}\eta_a^{\gamma\sigma} &= \delta_\mu^\gamma\eta_{a\nu\lambda} - \delta_\nu^\gamma\eta_{a\mu\lambda} + \delta_\lambda^\gamma\eta_{a\mu\nu}, & \eta_{a\mu\nu}\eta_b^{\mu\lambda} &= \delta_{ab}\delta_\nu^\lambda + \epsilon_{abc}\eta_\nu^{c\lambda}, \\ \epsilon_{abc}\eta^{b\mu\nu}\eta^{c\gamma\lambda} &= \delta^{\mu\gamma}\eta_a^{\nu\lambda} - \delta^{\mu\lambda}\eta_a^{\nu\gamma} + \delta^{\nu\lambda}\eta_a^{\mu\gamma}. \end{aligned} \tag{A.15}$$

Furthermore the relation to the σ-matrices is

$$\begin{aligned} \bar{\sigma}_\mu \sigma_\nu &= \delta_{\mu\nu} + \mathrm{i}\eta_{a\mu\nu}\sigma^a, \\ \sigma_\mu \bar{\sigma}_\nu &= \delta_{\mu\nu} + \mathrm{i}\bar{\eta}_{a\mu\nu}\sigma^a. \end{aligned} \tag{A.16}$$

Writing the singular gauge instanton field in terms of the 't Hooft symbols gives

$$\begin{aligned} A_\mu(x) &= -\frac{\mathrm{i}}{g}\frac{\rho^2}{x^2\left(\rho^2 + x^2\right)}\left[\sigma_\mu \bar{x} - x_\mu\right] \\ &= \frac{1}{g}\frac{\rho^2}{x^2\left(\rho^2 + x^2\right)}\bar{\eta}_{a\mu\nu}x^\nu\sigma^a. \end{aligned} \tag{A.17}$$

Appendix B

The Conformal Group

Table B.1: Generators of the conformal group

Translation	$P_\mu = -\mathrm{i}\partial_\mu$
Dilatation	$D = -\mathrm{i}x^\mu\partial_\mu$
Rotation	$L_{\mu\nu} = \mathrm{i}\left(x_\mu\partial_\nu - x_\nu\partial_\mu\right)$
SCT	$K_\mu = -\mathrm{i}\left(2x_\mu x^\nu\partial_\nu - x^2\partial_\mu\right)$

The conformal algebra is specified by the following commutation relations:

$$
\begin{aligned}
[D, P_\mu] &= \mathrm{i}P_\mu, & [D, K_\mu] &= -\mathrm{i}K_\mu, \\
[K_\mu, P_\nu] &= 2\mathrm{i}\left(g_{\mu\nu}D - L_{\mu\nu}\right), & [K_\rho, L_{\mu\nu}] &= \mathrm{i}\left(g_{\rho\mu}K_\nu - g_{\rho\nu}K_\mu\right), \\
[P_\rho, L_{\mu\nu}] &= \mathrm{i}\left(g_{\rho\mu}P_\nu - g_{\rho\nu}P_\mu\right), & [K_\mu, K_\nu] &= 0, \\
[L_{\mu\nu}, L_{\rho\sigma}] &= \mathrm{i}\left(g_{\nu\rho}L_{\mu\sigma} + g_{\mu\sigma}L_{\nu\rho} - g_{\mu\rho}L_{\nu\sigma} - g_{\nu\sigma}L_{\nu\rho}\right). & & \qquad \text{(B.1)}
\end{aligned}
$$

Table B.2: Scale factors of important conformal transformations

Inh. Lorentz transformation	$\sigma(x)_{\mathrm{L}} = 1$
Dilatation	$\sigma(x)_{\mathrm{dil}} = \frac{1}{\lambda^2}$
Inversion	$\sigma(x)_{\mathrm{inv}} = \frac{x^4}{b^4}$
SCT	$\sigma(x)_{\mathrm{sct}} = \frac{b^4}{c^4}\left(1 + \frac{2ax}{b^2} + \frac{a^2x^2}{b^4}\right)^2$
Stereographic projection	$\sigma(x)_{\mathrm{sp}} = \frac{\left(b^2+x^2\right)^2}{4b^4}$

Appendix C

Normalisation Integrals of Zero Modes

Dilatation

$$\begin{aligned}\langle\psi^{(\rho)}(x),\psi^{(\rho)}(x)\rangle &= \int \mathrm{d}^4x \frac{8}{g^2}\,\mathrm{Tr}(\lambda_a\lambda^a)\;\bar{\eta}^{a\mu\nu}\;\bar{\eta}_{a\mu\tau}\frac{x_\nu x^\tau\rho^2}{(x^2+\rho^2)^4}\\ &= \frac{16\pi^2}{g^2}\end{aligned} \tag{C.1}$$

$$\begin{aligned}\langle\psi'^{(\rho)}(x'),\psi'^{(\rho)}(x')\rangle &= \int \mathrm{d}^4x \frac{\rho_{\mathrm{peak}}^8}{x^8}\frac{8}{\rho_{\mathrm{peak}}^4\,g^2}\bar{\eta}^{a\mu\tau}\;\bar{\eta}_{a\mu\sigma}\;x_\tau x^\sigma\frac{x^4\rho^2}{(x^2+\rho^2)^4}\,\mathrm{Tr}\,(\lambda_a\lambda^a)\\ &= \frac{2\pi^2\rho_{\mathrm{peak}}^4\rho^2 48}{g^2}\overbrace{\int_0^\infty \mathrm{d}R\,\frac{R}{(R^2+\rho^2)^4}}^{=1/(6\rho^6)}\\ &= \frac{16\pi^2}{g^2}\frac{\rho_{\mathrm{peak}}^4}{\rho^4}\end{aligned} \tag{C.2}$$

Translation

$$\langle\psi^{(z)}(x),\psi^{(z)}(x)\rangle = \int \mathrm{d}^4x\,\frac{1}{2}\,\mathrm{Tr}\,[F_{\mu\nu}(x)F^{\mu\nu}(x)] = S_{\mathrm{cl}} = \frac{8\pi^2}{g^2} \tag{C.3}$$

$$\begin{aligned}\langle \psi'^{(z)}_{\mu}(x'), \psi'^{(z)\,\mu}(x')\rangle &= \int \mathrm{d}^4x\, \frac{\rho^8_{\mathrm{peak}}}{x^8}\frac{x^4}{\rho^4_{\mathrm{peak}}}\frac{1}{2}\,\mathrm{Tr}\,[F_{\mu\nu}(x)F^{\mu\nu}(x)] \\ &= \int \mathrm{d}^4x\, \frac{\rho^4_{\mathrm{peak}}}{x^4}\frac{48}{g^2}\frac{\rho^2}{(\rho^2+x^2)^4} \\ &= \frac{2\pi^2\rho^4_{\mathrm{peak}}\rho^4 48}{g^2}\underbrace{\int_0^\infty \mathrm{d}R\,\frac{1}{R}\frac{1}{(\rho^2+R^2)^4}}_{\to\infty}\end{aligned} \tag{C.4}$$

Colour zero modes $\psi^{(a)}_{\mu}(x)$

$$\begin{aligned}\langle \psi^{(a)}(x), \psi^{(a)}(x)\rangle &= \int \mathrm{d}^4x \frac{\rho^4}{g^2(x^2+\rho^2)^4}\big(8x^2\,\mathrm{Tr}\,(\lambda_a\lambda^a) \\ &\quad - 2\,\bar\eta^{b\mu\rho}\,\bar\eta_{c\mu\sigma}\,x_\rho x^\sigma\,\mathrm{Tr}\,([\lambda_b,\lambda_a][\lambda_c,\lambda^a])\,\big) \\ &= \frac{16\pi^2\rho^2}{g^2}\end{aligned} \tag{C.5}$$

Here we have used the following relation

$$\begin{aligned}2\bar\eta_{b\mu\alpha}\bar\eta_{c\mu\nu}x^\alpha x^\nu\,\mathrm{Tr}\left([\lambda^b,\lambda_a][\lambda^c,\lambda^a]\right) &= 2x^2\,\delta_{bc}\,\mathrm{Tr}\left([\lambda^b,\lambda_a][\lambda^c,\lambda^a]\right) \\ &= -8x^2\,\mathrm{Tr}\left(\epsilon_{bac}\epsilon^{bad}\lambda^c\lambda_d\right) \\ &= -32\,x^2.\end{aligned} \tag{C.6}$$

$$\begin{aligned}\langle \psi'^{(a)}(x'), \psi'^{(a)}(x')\rangle &= \int \mathrm{d}^4x \frac{\rho^8_{\mathrm{peak}}}{x^8}\frac{\rho^4\,x^4}{g^2\,\rho^4_{\mathrm{peak}}\,(x^2+\rho^2)^4} \\ &\quad\times\left(16x^2 - 2\,\bar\eta^{b\mu\rho}\,\bar\eta_{c\mu\sigma}\,x_\rho x^\sigma\,\mathrm{Tr}\,([\lambda_b,\lambda_a][\lambda^c,\lambda^a])\right) \\ &= \frac{2\pi^2\,48\,\rho^4_{\mathrm{peak}}\,\rho^4}{g^2}\overbrace{\int \mathrm{d}R\frac{R}{(R^2+\rho^2)^4}}^{=1/(6\rho^6)} \\ &= \frac{16\pi^2}{g^2}\frac{\rho^4_{\mathrm{peak}}}{\rho^2}\end{aligned} \tag{C.7}$$

Colour zero modes $\psi_\mu^{(\alpha)}(x)$

We make use of

$$\begin{aligned}\bar{\eta}^{a\mu\rho}\ \bar{\eta}_{b\mu\sigma}\ x_\rho x^\sigma\ \mathrm{Tr}\left([\lambda^a,\lambda_l][\lambda^b,\lambda^l]\right) &= x_\rho x_\sigma\left(\delta^a_b\delta^{\rho\sigma}-\epsilon^a_{bc}\bar{\eta}^{c\rho\sigma}\right)\\ &\quad\times\left(-4f_{alm}f^{bln}\,\mathrm{Tr}\left[\lambda^m\lambda_n\right]\right)\\ &= -4\,x^2 f^{alm}f_{aln}\,\mathrm{Tr}\left(\lambda_m\lambda^n\right)\\ \mathrm{Tr}(\lambda_m\lambda_n) &= 2\,\delta_{mn},\end{aligned} \tag{C.8}$$

where $a,b=1\ldots3$ and $l,m,n=4\ldots7$. The Greek indices run from $1\ldots4$. The structure constants of $SU(3)$ are denoted by f_{alm}. Now we can calculate the normalisation integral,

$$\begin{aligned}\langle\psi^{(\alpha)}(x),\psi^{(\alpha)}(x)\rangle &= \int \mathrm{d}^4x\,\frac{\rho^4}{g^2}\frac{4x^2-2\,\bar{\eta}^{a\mu\rho}\bar{\eta}_{b\mu\sigma}x_\rho x^\sigma\,\mathrm{Tr}\left[[\lambda_a,\lambda_l][\lambda^b,\lambda^l]\right]}{x^2(x^2+\rho^2)^3}\\ &= \frac{8\pi^2\rho^2}{g^2}.\end{aligned} \tag{C.9}$$

$$\begin{aligned}\langle\psi'^{(\alpha)}(x'),\psi'^{(\alpha)}(x')\rangle &= \int \mathrm{d}^4x\,\frac{\rho^8_{\mathrm{peak}}}{x^8}\frac{\rho^4}{g^2\rho^4_{\mathrm{peak}}}\frac{x^2}{(x^2+\rho^2)^3}\times\\ &\qquad\left(4x^2-\overbrace{2\,\bar{\eta}^{a\mu\beta}\bar{\eta}_{b\mu\gamma}x_\beta x^\gamma\,\mathrm{Tr}\left([\lambda_a,\lambda_l]\left[\lambda^b,\lambda^l\right]\right)}^{=-12x^2}\right)\\ &= \frac{2\pi^2\rho^4_{\mathrm{peak}}\rho^4 16}{g^2}\underbrace{\int_0^\infty \mathrm{d}R\,\frac{1}{R(R^2+\rho^2)^3}}_{\to\infty}\end{aligned} \tag{C.10}$$

Appendix D

Zero Modes in the $O(5)$-covariant formalism

The $O(5)$ covariant instanton,

$$A^a(r) = -i\,\Sigma^{ab} r_b, \tag{D.1}$$

is not invariant under transformations of the form

$$r'_a = r_a + \frac{1}{s^2} r_a r_b C^b + C_a. \tag{D.2}$$

Thus we can act with the transformation law given above on the instanton gauge field in order to obtain an $I\bar{I}$-field which depends now on new collective coordinates C_a. One need to check whether the transformation law has to obey certain conditions, which are necessary to stay on the surface of the hypersphere: The first constraint tells you that the norm of r'_a has to be s,

$$r'_a r'^a = s^2 + C^2 + 4 r_i C^i + \frac{3}{s^2}\big(r_i C^i\big)^2 \stackrel{!}{=} s^2. \tag{D.3}$$

We get a quadratic equation in $r_i C^i$,

$$r_i C^i = -\frac{2}{3} s^2 \pm \sqrt{\frac{4}{9} - \frac{1}{3} s^2 C^2}. \tag{D.4}$$

The second constraint is the following:

$$\begin{aligned} r'_a A'^a &\stackrel{!}{=} 0 \\ &= -i\Big[\Sigma^{am} C_a r_m \Big(2 + \frac{3}{s^2} r_i C^i\Big)\Big] \end{aligned} \tag{D.5}$$

Together with the first constraint we obtain two conditions in terms of s^2:

$$\begin{aligned} r_i C^i &= -\frac{2}{3}s^2 \\ C^2 &= \frac{4}{3}s^2 \end{aligned} \tag{D.6}$$

Eliminating s^2 gives a descriptive geometrical interpretation

$$\big(C + r\big)^2 = r^2. \tag{D.7}$$

This is the condition for the parameter C_a to ensure that we stay on the surface of the hypersphere when performing the transformation of Eq. (D.2). Now we find a simple inverse transformation and furthermore we can apply the constraints to the transformed gauge field.

$$\begin{aligned} r_a &= 3\big(r'_a - C_a\big) \\ A'^a(r') &= -i\Big[\frac{1}{3}\Sigma^{am} r_m + \frac{1}{s^2} r^a \Sigma^{mn} C_m r_c\Big] \\ &= -i\Big[\Sigma^{am}\big(r'_m - C_m\big) + \frac{9}{s^2}\big(r'^a - C^a\big)\Sigma^{mn} C_m r'_n\Big] \end{aligned} \tag{D.8}$$

Finally we are ready to compute the zero modes by differentiating with respect to C_a.

$$\begin{aligned} \psi^{ab}(r') &= \frac{\partial A'^a}{\partial C^b} \\ &= -i\Big[-\Sigma^{ab} + \frac{9}{s^2}\Sigma^{bm} r'_m\big(r'^a - C^a\big) - \frac{9}{s^2}\delta^{ab}\Sigma^{mn} C_m r'_n\Big] \end{aligned} \tag{D.9}$$

The computation of the norm $\|\psi^{ab}(r')\|$ is rather lengthy.

$$\begin{aligned} \psi_{ab}(r')\psi^{ab}(r') &= -\overbrace{\Sigma_{ab}\Sigma^{ab}}^{\text{(I)}} + \frac{27}{s^2}\overbrace{\Sigma_{bm}\Sigma^{bn} r'^m r'_n}^{\text{(II)}} + \frac{9}{s^2}\overbrace{\Sigma_{bm}\Sigma^{nb}\big(r'^m C_n + C^m r'_n\big)}^{\text{(III)}} \\ &\quad + 2\frac{81}{s^4}\overbrace{\big(\Sigma_{mn} C^m r'^n\big)^2}^{\text{(IV)}} \\ &= \mathbb{I}_{4\times4}\Big(-5 + \frac{27}{s^2} r'^2 - \frac{9}{s^2} 2\big(r' \cdot C\big) + \frac{81}{s^4}\, 2\, \frac{2}{81} s^4\Big) \\ &= 6\ \mathbb{I}_{4\times4} \end{aligned} \tag{D.10}$$

The relation for the Σ-matrices are:

$$
\begin{aligned}
(\mathsf{I}): &\quad \Sigma_{ab}\Sigma^{ab} = 5\,\mathbb{I}_{4\times4} \\
(\mathsf{II}): &\quad r_b r^a \Sigma_{ca}\Sigma^{bc} = b^2\,\mathbb{I}_{4\times4} \\
(\mathsf{III}): &\quad \Sigma_{bm}\Sigma^{nb}\,(r^m C_n + C^m r_n) = -2\,r_a C^a\,\mathbb{I}_{4\times4} = \frac{b^2}{3}\,\mathbb{I}_{4\times4} \\
(\mathsf{IV}): &\quad \Sigma_{mn}C^m r^n\;\Sigma_{pq}c^p r^q = \frac{2}{81}\,b^4
\end{aligned}
\tag{D.11}
$$

$$
\begin{aligned}
\|\psi^{ab}(r')\|^2 &= \frac{1}{2}\int \mathrm{d}A\,\mathrm{Tr}\left[\psi_{ab}(r')\psi^{ab}(r')\right] \\
&= 12\int \frac{16\rho^4}{(\rho^2+x^2)^4}\mathrm{d}^4x \\
&= 2^5\pi^2
\end{aligned}
\tag{D.12}
$$

This result was found by various other authors before by means of different techniques, see [79, 80].

Appendix E

Normalisation integrals on the sphere

Here the results for the normalisation integrals stated in Table 6.1 are given. All integrals are expressed in terms of the ration

$$\kappa = \frac{\rho}{\rho_{\text{peak}}}. \tag{E.1}$$

Dilatation

$$\begin{aligned}\langle \widehat{\psi}'^{(\rho)}, \widehat{\psi}'^{(\rho)} \rangle &= \frac{4 \cdot 48}{g^2} \rho'^6 \int \mathrm{d}^4 x \frac{x^2}{(\rho_{\text{peak}}^2 + x^2)^2 (\rho'^2 + x^2)^4} \\ &= -\frac{768\pi^2 \kappa^2 (1+\kappa^2) \ln(\kappa)}{g^2 (\kappa^2-1)^5 (\kappa^2+1)^5} + \frac{64\pi^2 (\kappa^4 + 10\kappa^2 + 1)}{g^2 (\kappa^2-1)^4 (\kappa^2+1)^4}\end{aligned} \tag{E.2}$$

Translation

$$\begin{aligned}\langle \widehat{\psi}'^{(z)}, \widehat{\psi}'^{(z)} \rangle &= \frac{4 \cdot 48}{g^2} \rho_{\text{peak}}^4 \rho'^4 \int \mathrm{d}^4 x \frac{1}{(\rho_{\text{peak}}^2 + x^2)^2 (\rho'^2 + x^2)^4} \\ &= \frac{384\pi^2 \kappa^4 (\kappa^2+3) \ln(\kappa)}{g^2 (\kappa^2-1)^5 (\kappa^2+1)^5} - \frac{32\pi^2 (17\kappa^4 + 8\kappa^2 - 1)}{g^2 (\kappa-1)^4 (1+\kappa)^4}\end{aligned} \tag{E.3}$$

Colour zero modes $\widehat{\psi}'^{(a)}(r')$

$$\begin{aligned}\langle\widehat{\psi}'^{(a)},\widehat{\psi}'^{(a)}\rangle &= \frac{4\cdot 48}{g^2}\rho_{\text{peak}}^4\rho'^4\int \mathrm{d}^4x\frac{x^2}{(\rho_{\text{peak}}^2+x^2)^2(\rho'^2+x^2)^4}\\ &= \rho_{\text{peak}}^2\left[-\frac{768\pi^2\kappa^4\left(1+\kappa^2\right)\ln(\kappa)}{g^2\left(\kappa-1\right)^5\left(\kappa+1\right)^5}+\frac{64\pi^2\kappa^2\left(\kappa^4+10\kappa^2+1\right)}{g^2\left(\kappa^2-1\right)^2\left(\kappa^2+1\right)^2}\right]\end{aligned} \tag{E.4}$$

Colour zero modes $\widehat{\psi}'^{(\alpha)}(r')$

$$\begin{aligned}\langle\widehat{\psi}'^{(\alpha)},\widehat{\psi}'^{(\alpha)}\rangle &= \frac{4\cdot 16}{g^2}\rho_{\text{peak}}^4\rho'^2\int \mathrm{d}^4x\frac{x^2}{(\rho_{\text{peak}}^2+x^2)^2(\rho'^2+x^2)^3}\\ &= \rho_{\text{peak}}^2\left[\frac{128\pi^2\kappa^4\left(2+\kappa^2\right)\ln(\kappa)}{g^2\left(\kappa-1\right)^4\left(1+\kappa\right)^4}-\frac{32\pi^2\kappa^2\left(1+5\kappa^2\right)}{g^2\left(\kappa-1\right)^3\left(1+\kappa\right)^3}\right]\end{aligned} \tag{E.5}$$

Danksagung

An erster Stelle möchte ich mich herzlichst bei meinem Betreuer Dr. Fridger Schrempp bedanken, der mir diese Diplomarbeit am Deutschen Elektronen Synchrotron in Hamburg ermöglicht hat. Vielen Dank insbesondere für die Vergabe der physikalisch interessanten Fragestellung. Durch zahlreiche Diskussionen und Anregungen habe ich in diesem Jahr mit Sicherheit vieles über Physik gelernt. Weiters möchte ich mich bei Prof. Harald Grosse für die Unterstüzung seitens der Universität Wien bedanken. Großer Dank gebührt auch Maik Petermann, der durch sein akkurates Korrekturlesen und durch seine konstruktive Kritik dieser Arbeit zu wesentlich mehr Reife verholfen hat.

Meinen Bürokollegen Daniela, Tania und Wolfgang möchte ich für die quantitativ hochwertige Unterhaltung und die angenehme Atmosphäre (mit aber eher ohne Blumen) danken. Bei den Mitgliedern der theoretischen Abteilung bedanke ich mich für Kuchenspenden, Wissensspenden und für ein insgesamt wunderbares Jahr. Danke für die netten und gemütlichen Besuche in meinem Wiener Zuhause, Carina!

Michał, dziękuję za wszystko! Vor allem für deine gute Laune und deine Geduld.

Meinen Eltern Maria und Alfred danke ich für Ihre ständige Unterstüzung, Ihre Liebe und dafür, dass meine Schwestern und ich es nicht besser hätten haben können.

"Danke, es war sehr schön, es hat mich sehr gefreut!"

Bibliography

[1] A. A. Belavin, Alexander M. Polyakov, A. S. Shvarts, and Yu. S. Tyupkin. Pseudoparticle solutions of the yang-mills equations. *Phys. Lett.*, B59:85–87, 1975.

[2] V. de Alfaro, S. Fubini, and G. Furlan. A new classical solution of the yang-mills field equations. *Phys. Lett.*, B65:163, 1976.

[3] G. 't Hooft. Magnetic monopoles in unified gauge theories. *Nucl. Phys.*, B79:276–284, 1974.

[4] G. 't Hooft. On the phase transition towards permanent quark confinement. *Nucl. Phys.*, B138:1, 1978.

[5] Mikhail A. Shifman, A. I. Vainshtein, and Valentin I. Zakharov. Qcd and resonance physics. sum rules. *Nucl. Phys.*, B147:385–447, 1979.

[6] G. 't Hooft. Computation of the quantum effects due to a four- dimensional pseudoparticle. *Phys. Rev.*, D14:3432–3450, 1976.

[7] G. 't Hooft. Symmetry breaking through bell-jackiw anomalies. *Phys. Rev. Lett.*, 37:8–11, 1976.

[8] D. Diakonov. Instantons at work. *Prog. Part. Nucl. Phys.*, 51:173–222, 2003.

[9] Dmitri Diakonov. Chiral-symmetry breaking by instantons. 1995.

[10] Dmitri Diakonov and V. Yu. Petrov. Chiral condensate in the instanton vacuum. *Phys. Lett.*, B147:351–356, 1984.

[11] Dmitri Diakonov and V. Yu. Petrov. A theory of light quarks in the instanton vacuum. *Nucl. Phys.*, B272:457, 1986.

[12] Dmitri Diakonov and V. Yu. Petrov. Spontaneous breaking of chiral symmetry in the instanton vacuum. LENINGRAD-86-1153.

[13] P. V. Pobylitsa. The quark propagator and correlation functions in the instanton vacuum. *Phys. Lett.*, B226:387–392, 1989.

[14] A. Ringwald. From qcd instantons at hera to electroweak b+l violation at vlhc. 2003.

[15] S. Moch, A. Ringwald, and F. Schrempp. Instantons in deep-inelastic scattering: The simplest process. *Nucl. Phys.*, B507:134–156, 1997.

[16] A. Ringwald and F. Schrempp. Instanton-induced cross-sections in deep-inelastic scattering. *Phys. Lett.*, B438:217–228, 1998.

[17] F. Schrempp A. Ringwald. Zooming-in on instantons at hera. *Phys. Lett. B*, 503:331–340, 2001.

[18] A. Ringwald and F. Schrempp. Qcdins 2.0: A monte carlo generator for instanton-induced processes in deep-inelastic scattering. *Comput. Phys. Commun.*, 132:267–305, 2000.

[19] Philippe de Forcrand, Margarita Garcia Perez, James E. Hetrick, and Ion-Olimpiu Stamatescu. Topology of full qcd. *Nucl. Phys. Proc. Suppl.*, 63:549–551, 1998.

[20] Margarita Garcia Perez, Owe Philipsen, and Ion-Olimpiu Stamatescu. Cooling, physical scales and topology. *Nucl. Phys.*, B551:293–313, 1999.

[21] Anna Hasenfratz and Chet Nieter. Instanton content of the su(3) vacuum. *Phys. Lett.*, B439:366–372, 1998.

[22] Douglas A. Smith and Michael J. Teper. Topological structure of the su(3) vacuum. *Phys. Rev.*, D58:014505, 1998.

[23] A. Ringwald and F. Schrempp. Confronting instanton perturbation theory with qcd lattice results. *Phys. Lett.*, B459:249–258, 1999.

[24] Stefano Capitani, Martin Luscher, Rainer Sommer, and Hartmut Wittig. Non-perturbative quark mass renormalization in quenched lattice qcd. *Nucl. Phys.*, B544:669–698, 1999.

[25] F. Schrempp. Tracking qcd-instantons. *J. Phys.*, G28:915–926, 2002.

[26] R. Jackiw and C. Rebbi. Conformal properties of a yang-mills pseudoparticle. *Phys. Rev.*, D14:517, 1976.

[27] R. Jackiw, C. Nohl, and C. Rebbi. Conformal properties of pseudoparticle configurations. *Phys. Rev.*, D15:1642, 1977.

[28] L.H. Ryder. *Quantum Field Theory*. Cambridge University Press, 1985.

[29] T.P. Cheng and L.F. Li. *Gauge Theory Of Elementary Particle Physics*. Oxford Science Publications, 1984.

[30] S. Coleman. *Aspects of Symmetry*. Cambridge University Press, 1985.

[31] A. I. Vainshtein, Valentin I. Zakharov, V. A. Novikov, and Mikhail A. Shifman. *ABC of instantons*, volume 1. Singapore, World Scientific, 1999.

[32] Thomas Schafer and Edward V. Shuryak. Instantons in qcd. *Rev. Mod. Phys.*, 70:323–426, 1998.

[33] R. Bott. An application of morse theory to the topology of lie groups. *Bull. Soc. Math. Fr.*, 84:251–281, 1956.

[34] M. F. Atiyah, Nigel J. Hitchin, V. G. Drinfeld, and Yu. I. Manin. Construction of instantons. *Phys. Lett.*, A65:185–187, 1978.

[35] Andre Utermann. Qcd-instantons and saturation at small bjorken-x. (in german). DESY-THESIS-2003-029.

[36] Claude W. Bernard, Norman H. Christ, Alan H. Guth, and Erick J. Weinberg. Pseudoparticle parameters for arbitrary gauge groups. *Phys. Rev.*, D16:2967, 1977.

[37] R. Jackiw and C. Rebbi. Vacuum periodicity in a yang-mills quantum theory. *Phys. Rev. Lett.*, 37:172–175, 1976.

[38] Jr. Callan, Curtis G., Roger F. Dashen, and David J. Gross. Toward a theory of the strong interactions. *Phys. Rev.*, D17:2717, 1978.

[39] M.E. Peskin and D.V. Schroeder. *An Introduction to Quantum Field Theory*. Perseus Books Publishing, L.L.C., 1984.

[40] L. F. Abbott. The background field method beyond one loop. *Nucl. Phys.*, B185:189, 1981.

[41] C. Bernard. Gauge zero modes, instanton determinants, and quantum-chromodynamic calculations. *Phys. Rev. D*, 19:3013, 1979.

[42] T. R. Morris, D. A. Ross, and Christopher T. Sachrajda. Higher order quantum corrections in the presence of an instanton background field. *Nucl. Phys.*, B255:115, 1985.

[43] Stephen L. Adler S. Axial vector vertex in spinor electrodynamics. *Phys. Rev.*, 177:2426–2438, 1969.

[44] J. S. Bell and R. Jackiw. A pcac puzzle: pi0 → gamma gamma in the sigma model. *Nuovo Cim.*, A60:47–61, 1969.

[45] Gerard 't Hooft. Monopoles, instantons and confinement. 1999.

[46] M. F. Atiyah and I. M. Singer. The index of elliptic operators. 1. *Annals Math.*, 87:484–530, 1968.

[47] M. F. Atiyah and I. M. Singer. The index of elliptic operators. 4. *Annals Math.*, 93:119–138, 1971.

[48] M. Bohm, A. Denner, and H. Joos. *Gauge theories of the strong and electroweak interaction*. Stuttgart, Germany: Teubner, 784 p, 2001.

[49] Edward Witten. Current algebra theorems for the u(1) 'goldstone boson'. *Nucl. Phys.*, B156:269, 1979.

[50] G. Veneziano. U(1) without instantons. *Nucl. Phys.*, B159:213–224, 1979.

[51] S. Eidelman et al. Review of particle physics. *Phys. Lett.*, B592:1, 2004.

[52] Edward V. Shuryak. *The QCD vacuum, hadrons and superdense matter*, volume 71. World Sci. Lect. Notes Phys., 2004.

[53] C. Adloff et al. Search for qcd instanton-induced processes in deep- inelastic scattering at hera. *Eur. Phys. J.*, C25:495–509, 2002.

[54] S. Chekanov et al. Search for qcd-instanton induced events in deep inelastic e p scattering at hera. *Eur. Phys. J.*, C34:255–265, 2004.

[55] M. Petermann and F. Schrempp. in preparation.

[56] F. Schrempp. Instanton-induced processes: An overview. 2005.

[57] A. Ringwald. High-energy breakdown of perturbation theory in the electroweak instanton sector. *Nucl. Phys.*, B330:1, 1990.

[58] A. Ringwald, F. Schrempp, and C. Wetterich. Phenomenology of geometrical flavor interactions at tev energies. *Nucl. Phys.*, B365:3–23, 1991.

[59] Hideaki Aoyama et al. Recent developments of the theory of tunneling. *Prog. Theor. Phys. Suppl.*, 127:1–92, 1997.

[60] F. Bezrukov, D. Levkov, C. Rebbi, V. A. Rubakov, and P. Tinyakov. Semiclassical study of baryon and lepton number violation in high-energy electroweak collisions. *Phys. Rev.*, D68:036005, 2003.

[61] W. Greiner, S. Schramm, and E. Stein. *Quantum chromodynamics*. Berlin, Germany: Springer 551 p, 2002.

[62] M. C. Chu, J. M. Grandy, S. Huang, and J. W. Negele. Evidence for the role of instantons in hadron structure from lattice qcd. *Phys. Rev.*, D49:6039–6050, 1994.

[63] I. Montvay and G. Munster. *Quantum fields on a lattice*. Cambridge, UK: Univ. Pr. (1994) 491 p. (Cambridge monographs on mathematical physics).

[64] Philippe de Forcrand, Margarita Garcia Perez, and Ion-Olimpiu Stamatescu. Topology of the su(2) vacuum: A lattice study using improved cooling. *Nucl. Phys.*, B499:409–449, 1997.

[65] Jr. Callan, Curtis G., Roger F. Dashen, and David J. Gross. A theory of hadronic structure. *Phys. Rev.*, D19:1826, 1979.

[66] T. Fulton, F. Rohrlich, and L. Witten. Conformal invariance in physics. *Rev. Mod. Phys.*, 34:442–457, 1962.

[67] V. De Alfaro, S. Fubini, G. Furlan, and C. Rossetti. *Currents in Hadron Physics*. North-Holland Publishing Company, 1973.

[68] P. Di Francesco, P. Mathieu, and Sénéchal. *Conformal Field Theory*. Springer, 1997.

[69] M. Shintani. Space-time inversion as the origin of scale and special conformal transformations: Starting from the space-time inversion. RRK 80-11.

[70] M. Shintani. Invariant systems under the space-time inversion - existence of two kinds of inversion. *Nuovo Cim.*, 71, 1982. RRK-82-2.

[71] V. M. Braun, G. P. Korchemsky, and Dieter Mueller. The uses of conformal symmetry in qcd. *Prog. Part. Nucl. Phys.*, 51:311–398, 2003.

[72] Jean-Loup Gervais and B. Sakita. Extended particles in quantum field theories. *Phys. Rev.*, D11:2943, 1975.

[73] A.V. Yung I.I. Balitsky. Collective-coordinate method for quasizero modes. *Phys. Lett. B*, 168:113, 1986.

[74] D. Amati, K. Konishi, Y. Meurice, G. C. Rossi, and G. Veneziano. Nonperturbative aspects in supersymmetric gauge theories. *Phys. Rept.*, 162:169–248, 1988.

[75] V. A. Novikov, Mikhail A. Shifman, A. I. Vainshtein, and Valentin I. Zakharov. Exact gell-mann-low function of supersymmetric yang-mills theories from instanton calculus. *Nucl. Phys.*, B229:381, 1983.

[76] G. 't Hooft. (private communication).

[77] Stephen L. Adler. Massless, euclidean quantum electrodynamics on the five- dimensional unit hypersphere. *Phys. Rev.*, D6:3445, 1972. FERMILAB-PUB-72-058-T.

[78] Stephen L. Adler. Massless electrodynamics on the five-dimensional unit hypersphere: An amplitude - integral formulation. *Phys. Rev.*, D8:2400–2418, 1973.

[79] Jr. Ore, F. R. How to compute determinants compactly. *Phys. Rev.*, D16:2577, 1977.

[80] S. Chadha, P. Di Vecchia, A. D'Adda, and F. Nicodemi. zeta function regularization of the quantum fluctuations around the yang-mills pseudoparticle. *Phys. Lett.*, B72:103, 1977.

[81] A. A. Belavin and Alexander M. Polyakov. Quantum fluctuations of pseudoparticles. *Nucl. Phys.*, B123:429, 1977.

[82] Jr. Ore, F. R. Quantum field theory about a yang-mills pseudoparticle. *Phys. Rev.*, D15:470, 1977.